Article

Frozen-Density Embedding Strategy for Multilevel Simulations of Electronic Structure

WESOLOWSKI, Tomasz Adam, SHEDGE, Sapana, ZHOU, Xiuwen

CHEMICAL REVIEWS

Review

pubs.acs.org/CR

Frozen-Density Embedding Strategy for Multilevel Simulations of Electronic Structure

Tomasz A. Wesolowski,* Sapana Shedge, and Xiuwen Zhou

Department of Physical Chemistry, University of Geneva, CH-1211 Geneva 4, Switzerland

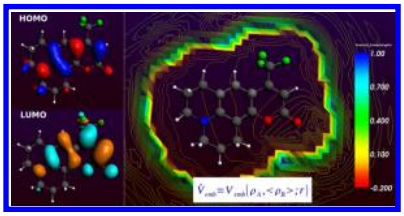

CONTENTS

Special Issue: Calculations on Large Systems

Received: September 12, 2014
Published: April 29, 2015

DOI: 10.1021/cr500502v
Chem. Rev. 2015, 115, 5891−5928

1. INTRODUCTION

Modeling properties of chemical species and chemical reactions requires usually the quantum-mechanical level of description. Approximated methods to solve the electronic Schrödinger equation are indispensable for obtaining data concerning electronic states. Methods from the ever-growing toolbox of quantum chemistry[1,2] are used for this purpose. Due to unfavorable scaling of quantum chemistry methods, a compromise must be made between the accuracy of the numerical results and the size of the system described at the wavefunction level. Chemistry rarely concerns small molecules in vacuum, i.e., systems for which the first-principles based quantum chemistry methods are capable to predict molecular properties with accuracy matching that of experimental measurements. The size of systems, for which experiments are made (liquid phase, surfaces, solids, biomolecules, supramolecular complexes, etc.), excludes usually the straightforward use of the high-accuracy quantum chemistry methods (see refs 3 and 4 for instance). Frequently, it is known in advance that the properties of the investigated system are mainly determined by a small part of the whole system. The explicit quantum mechanical descriptors are, therefore, needed only for the relevant part, whereas the rest of the real system is considered as the source of a small perturbation. It has been long recognized that it is inefficient to apply quantum mechanical descriptors for the entire systems in such cases. Alternatives to the use of wavefunction level of description to the whole large systems have been developed over the years. They are known under such names as QM/MM, hybrid methods, embedding methods, etc. For an overview of such methods in various fields, see the specialized reviews in the present issue or past reviews such as the ones in refs 5−11. In such methods, the environment is represented by means of system specific parameters (electric charges, polarizabilities, atomic potentials) or a polarizable continuum dielectric (PCM[12] and COSMO[13]). Embedding methods are especially successful in simulations of biomolecular systems as evidenced by the 2013 Nobel Prize in Chemistry for Martin Karplus, Michel Levitt, and Arieh Warshel.

The key element in the embedding methods is the embedding operator generated by the environment which affects the embedded wavefunction. It provides coupling between the quantum-mechanical descriptors (embedded orbitals or embedded wavefunction, for instance) and the environment. This operator comprises usually the classical component, i.e., the electrostatic potential generated by the environment, and a component due to the Fermion nature of electrons which has the form of a nonlocal operator. In the pseudopotential theory by Phillips and Kleinman,[14] formulated originally for separating core and valence electrons, the exact pseudopotential is constructed using projector operators assuring orthogonality between frozen and nonfrozen orbitals. The same strategy can be extended for separating molecular fragments or molecules. Nonlocal embedding operators based on either transferrable pseudopotentials or frozen orbitals obtained from localization procedures have been developed in many groups.[15−32] Molecular nonlocal pseudopotentials are frequently further approximated by means of local potentials. The simplest approximation is to neglect the nonelectrostatic component of the embedding potential entirely. It is a common strategy in QM/MM simulations for both molecular[33] and solid state systems[34] especially if the localized basis sets are used for the embedded systems. The nonelectrostatic contributions to the energy of the total system due to the environment are frequently added a posteriori. This approximation breaks entirely with the increase of the range of the used basis sets.[34−37] The local embedding potentials comprising also the nonelectrostatic contributions are introduced based on various guiding principles (see refs 35 and 38−43 for instance). Local embedding potentials are usually interpreted as approximations to the more accurate embedding operator which is a nonlocal pseudopotential. The essential feature of all such local potentials is that they comprise a component which takes into account the intermolecular Pauli repulsion. In the absence of such component, the embedding operator is reduced to the electrostatic potential which results in numerical instabilities.

A different perspective on the local embedding potentials was given by Wesolowski and Warshel[44] in 1993, who formulated the foundation of the exact theory of local embedding potentials (frozen-density embedding theory, FDET).[44−46] In FDET, the local potential is not an approximated quantity, but it is the exact potential associated with constrained optimization of the electron density of the total system, whereas the embedded wavefunction is rather an auxiliary quantity used to optimize the density of the embedded subsystem. This represents the shift of the target, from the embedded orbitals in the pseudopotential theory to embedded density in FDET as well as the change of the fundamental descriptor of the environment, from frozen orbitals to frozen density. As a result, the exact pseudo wave-function and the exact embedded wavefunction in FDET might differ as demonstrated in the analytically solvable case studied in refs 47 and 48. The FDET embedding potential was given the form of a universal functional of charge densities. The FDET embedding potential is expressed using density functionals for the exchange-correlation and noninteracting kinetic energies ($E_{xc}[\rho]$ and $T_s[\rho]$, respectively) known in the Kohn−Sham formulation[49,50] of density functional theory (DFT).[51] Casting the local embedding potential into the form of a functional, which depends on charge densities, made it possible to develop such computational methods in which only charge-densities are used as descriptors of the environment. Such formulation of the embedding problem makes it possible to combine the quantum-mechanical level of description for embedded system with any model based on physical laws which yields the electron density. Note that electron density is a well-defined quantity at any scale (even macroscopic), and it can be measured experimentally.

DOI: 10.1021/cr500502v
Chem. Rev. 2015, 115, 5891−5928

FDET is related to subsystem DFT[52] and partition DFT,[53,54] which are alternative formulations of DFT, i.e., they yield the exact energy and electron density of a given quantum system. The local embedding potential determined by electron densities of individual subsystem is used in all of them. Seen as alternative formulations of density functional theory, these formalisms form a hierarchy. Partition DFT is the most general one. Besides the capacity of reaching the exact electron density and energy of the total system, it provides a meaningful partitioning of the total density. Subsystem DFT is also designed to reach the exact density and energy but lacks the capacity of partitioning the density into meaningful components. Unique partitioning obtained in practical simulations is the result of using approximations used for the nonadditive kinetic energy functional (defined in eq 12). Partition DFT and subsystem DFT formalisms take as an input the external potential and the total number of electrons and yield (a) exact ground-state energy, (b) exact ground-state electron density, and (c) auxiliary quantities such as orbitals for subsystems and their occupancies (integer in case of subsystem DFT and fractional in case of partition DFT). FDET on the other hand, concerns other situations. The input quantities are the external potential, the number of electrons in the selected subsystem (denoted as N_A in the present review), but also a non-negative function denoted with $\rho_B(\vec{r})$ in the present review. The output quantities, the optimal density of the total system, the corresponding minimal energy, and auxiliary quantity (embedded wavefunction), satisfy an additional constraint $(\forall \vec{r}\ \rho(\vec{r})) \geq \rho_B(\vec{r}))$. In this review, we refer to the quantities obtained with these conditions as exact. FDET equations (eqs 3-8 in the present work) hold for any arbitrarily chosen $\rho_B(\vec{r})$, but the FDET energy can lie above the ground-state energy of the whole system. The quality of the obtained results depend on the chosen $\rho_B(\vec{r})$. One of possible choices is to use optimized $\rho_B(\vec{r})$. If the embedded subsystem is described by means of the reference system of noninteracting electrons in FDET and optimized $\rho_B(\vec{r})$ is used, FDET and subsystem DFT yield the same total energy and electron density. Such minimization is usually performed by means of the freeze-and-thaw procedure.[55] It is worthwhile to point out that FDET is formulated not only for the Kohn−Sham type of description of the embedded subsystem[44] but also for the explicitly interacting Hamiltonians.[45]

As far as setting up a FDET based multiscale numerical simulation is concerned, the situation is similar as in any method of the QM/MM type. In both cases, choices must be made concerning (a) the selection of the subsystem to be described by means of the embedded wavefunction and (b) descriptors for the environment. In QM/MM, descriptors such as electric multipole moments, polarizabilities, pair potentials of atoms/molecules in the environment, etc. are used, whereas it is $\rho_B(\vec{r})$ in FDET. Any observable quantity derived from the embedded wavefunction obtained in FDET is a functional of the electron density associated with the environment. In particular, the FDET energy is an upper bound of the total energy. The quality and usefulness of observable quantities derived from the embedded wavefunction depend on the user-decided choice made for $\rho_B(\vec{r})$. This dependence allows the user to verify the quality of the obtained results through the analysis of their sensitivity to variations of $\rho_B(\vec{r})$.

The formal frameworks of subsystem DFT and partition DFT can also be used as a basis for multilevel simulations if different approximations of fundamental nature (density functionals) or technical character (localization and quality of the basis sets) are used for different subsystems. Such calculations involve nevertheles the wavefunction-level of description for each subsystem including the environment. FDET concerns more general situations in which wavefunction level of description for the environment is not available at all. Besides models in which $\rho_B(\vec{r})$ is obtained from some lower level quantum mechanical methods as it is made in subsystem DFT or partition DFT, it makes it possible to combine any model based on laws of physics, which yields electron density, with a quantum-mechanical level of description for the embedded species. In summary, subsystem DFT or partition DFT are alternative formulations of quantum many body problem within the Born−Oppenheimer approximation, whereas FDET provides a universal formal framework besides any empirical QM/MM type of method using local embedding potential.

Another strategy to obtain a local, density-dependent embedding potential follows the common scheme to compensate errors in energy of approximate methods in quantum chemistry, such as the *ONIOM* strategy known under the name introduced by Morokuma and collaborators.[56] Carter and collaborators[57,58] used the ONIOM strategy which resulted in an ad hoc combination of the local embedding potential introduced by Wesolowski and Warshel for multilevel simulations with conventional methods of quantum chemistry (see ref 59 for the most recent overview). Such combination uses also local, charge-density dependent embedding potential. It corresponds, however, to the change of independent variables for the whole system. In FDET it is the embedded wavefuncion and $\rho_B(\vec{r})$, whereas it is the embedded wavefunction and the approximated wavefunction of the whole system in ONIOM. The change of the independent variables puts such methods beyond the scope of FDET because other descriptors for the environment than just its density are used. The success of this combination resulted in great interest in density based embedding methods. Significant further developments by many researchers followed. They concerned understanding the underlying theory, the applicability of the approximations for the density functionals in FDET, applications of FDET for evaluation of properties, and efficient numerical implementations. Extensions going beyond FDET were proposed.

The aim of the present review is to overview these developments. We use FDET as a common formal framework for: (a) development of approximated methods, (b) interpretation of approximations made in practice, (c) interpretation of the results obtained using approximated methods, and last but not least, (d) beyond-FDET formalisms or related approaches using also the embedding potential of the FDET form but requiring other descriptors for the environment besides $\rho_B(\vec{r})$.

In section 2, the formal framework of FDET approach to the embedding problem is provided. The key quantities are defined and discussed. Interpretation of some quantities closely related to similar ones known in multilevel simulation methods is provided. Section 3 concerns beyond-FDET formalisms which, share with FDET the use of the FDET form of the embedding potential. Approximations used in practical calculations are overviewed in Section 4. Application of methods based on FDET and/or its extensions for modeling spectroscopic properties of embedded species (UV/vis, CD, ESR, NMR, etc.) as well as properties of the potential energy surfaces (interaction energies, geometries, transition states, and vibrational frequencies). Such applications of FDET are overviewed in section 5. Although the present review concerns principally the multilevel simulations using the formal framework of FDET, i.e., methods in which the

DOI: 10.1021/cr500502v
Chem. Rev. 2015, 115, 5891−5928

environment is described by means of some arbitrarily chosen density $\rho_B(\vec{r})$ and the embedded wavefunction is obtained from the Euler−Lagrange equations featuring a charge-density depended universal density functional, applications of other subsystem based methods sharing with FDET the form of local embedding potential are also included. The present review complements the one made by one of us published in 2006[60] or by others such as that by Neugebauer,[61] Gomes and Jacob,[62] Jacob and Neugebauer,[63] and Bendavid and Carter.[64] The reviews authored by Neugebauer and Jacob, especially the recent one,[63] cover large class of methods sharing with FDET the use of local embedding potentials approximated as density functionals. The acronyms and abbreviations used for formalisms, approximations, and numerical algorithms discussed in the present review are collected in the Appendix.

Throughout the present review, we try to make a clear distinction between the discussed formalisms (Kohn−Sham DFT, subsystem DFT, partition DFT, and FDET) and approximated methods based on these formalisms which are used in computational practice. In the exact formulation, these formalisms represent different strategies to obtain the ground-state electron density and energy of the whole system (case of Kohn−Sham DFT, subsystem DFT, and partition DFT) or the optimal density and energy in the presence of a given constraint imposed on the electron density (case of FDET). The quantities used to optimize the total energies such as embedded wavefunctions and the corresponding eigenvalues have different interpretations in each of them. In numerical practice, on the other hand, applying particular set of additional approximations may lead to similar working equations. We hope that this perspective will allow both the readers interested in foundations and interpretation of quantities obtained in practical simulations and the ones interested in applications and numerical implementations to be able to find easily the sections covering issues of their interest. In view of large amount of methods developed in the recent years, which share with FDET the use of a charge-density dependent universal embedding potential, giving a full account on all possible approximations used in such simulations seems impossible. For this reasons, the description of the numerical implementation issues of the discussed equations is also limited to the minimum.

Finally, we would like to specify what the reader cannot find in the present review. All considerations (exact theory, approximations, and applications) concern cases where the Born−Oppenheimer approximation is applicable, the temperature of electrons is 0 K, and approximations concern the Hamiltonian or density functionals and do not involve modification of the external potential. Such subsystem based approaches, which do not use local charge-density dependent local potential to couple subsystems but more complicated operators (see refs 65−68 for instance), are not covered in the present review. The present review focuses on methods in which the embedding operator is a local potential and in which this potential is approximated by some density functionals, i.e., methods which retain the basic mathematical structure of FDET. For multilevel simulation methods going beyond the scope of FDET, the reader may wish to consult some of the recent reviews on fragmentation methods such as the ones collected in a special issue of *Accounts of Chemical Research* published in 2014 (vol. 47 issue 9), the comprehensive review by Gordon et al.,[69] or other articles in the present issue of *Chemical Reviews*.

2. FROZEN-DENSITY EMBEDDING THEORY

2.1. Statement of the Problem: Basic Equations

Frozen-density embedding theory[44,45,60] concerns the treatment of a many-electron systems described within the Born−Oppenheimer in the presence of a given in advance constraint imposed on the total electron density ($\forall \vec{r}\ \rho(\vec{r}) \geq \rho_B(\vec{r})$). It is rooted in Hohenberg−Kohn−Sham−Levy density functional theory, from which it borrows the following elements: (a) the two Hohenberg−Kohn theorems,[51] (b) the constrained search definition of density functionals for components of the total energy,[50] (c) the reference system of noninteracting electrons,[49] and (d) effective potentials which are functionals of the electron density.[49] In density functional theory, the exact ground state energy (E_o) for a quantum system comprising N_{AB} electrons in an external potential $v_{AB}(\vec{r})$ is obtained from the Hohenberg−Kohn variational principle for the density functional of the ground-state energy ($E^{HK}_{v_{AB}}[\rho]$):

$$E_o = \min_{\int \rho(\vec{r})\mathrm{d}\vec{r} = N_{AB}} E^{HK}_{v_{AB}}[\rho] = E^{HK}_{v_{AB}}[\rho^{AB}_o] \tag{1}$$

where $\rho^{AB}_o(\vec{r})$ is the exact ground-state density.

In FDET, the optimization of the density is subject to an additional constraint: $\rho(\vec{r}) \geq \rho_B(\vec{r})$, where $\rho_B(\vec{r})$ is an arbitrarily chosen non-negative function integrating to less that N_{AB}.

$$E^{FDET}[\rho_B] = \min_{\substack{\forall \vec{r}\rho(\vec{r}) \geq \rho_B(\vec{r}) \\ \int \rho(\vec{r})\mathrm{d}\vec{r} = N_{AB}}} E^{HK}_{v_{AB}}[\rho] = E^{HK}_{v_{AB}}[\rho^{FDET}_{AB}] \tag{2}$$

Equations 1 and 2 show clearly that E_o and $E^{FDET}[\rho_B]$ can be the same only for particular choices for $\rho_B(\vec{r})$. On the virtue of the second Hohenberg−Kohn theorem, the two energies can be the same only if $\rho_B(\vec{r})$ is never larger than the exact ground-state electron density of the total system ($\rho^{AB}_o(\vec{r})$). For formulations related to FDET, which target the exact ground-state energy of the total system, see section 3.1. The condition $\forall \vec{r}\ \rho(\vec{r}) \geq \rho_B(\vec{r})$ can not be assured in practice, i.e., without knowing the exact ground-state density of the whole system ($\rho^{AB}_o(\vec{r})$). As a result, $\rho^{FDET}_{AB}(\vec{r})$ might differ from $\rho^{AB}_o(\vec{r})$ and E^{FDET} lies above E_o. FDET is an approximate formulation of quantum many-body problem conceived from the start to be used in combination with system-dependent approximations as is any other embedding method for multiscale simulations. Practical applicability of this formulation hinges on the nature of the problem under investigation restricting its use to such cases where some information about electron density of the total system is known in advance.

For the sake of further considerations, eq 2 can be equivalently written as

$$E^{FDET}[\rho_B] = \min_{\substack{\forall \vec{r}\rho_A(\vec{r}) \geq 0 \\ \int \rho_A(\vec{r})\mathrm{d}\vec{r} = N_A}} E^{HK}_{v_{AB}}[\rho_A + \rho_B] = E^{HK}_{v_{AB}}[\rho^{opt}_A + \rho_B] \tag{3}$$

where $N_A = N_{AB} - \int \rho_B(\vec{r})\ \mathrm{d}\vec{r}$.

In principle, various methods can be envisaged to perform the search for the optimal density ($\rho^{opt}_A(\vec{r})$). The straightforward approach to optimize $\rho_A(\vec{r})$ would follow the Thomas and Fermi ideas,[70,71] which lie at the origin of modern orbital-free DFT methods (see the review by Wang and Carter[72] and the recent book edited by Wesolowski and Wang[73]). In view of limited applicability of current orbital-free DFT methods, such an approach to eq 2 will not be considered here. In FDET, following

DOI: 10.1021/cr500502v
Chem. Rev. 2015, 115, 5891−5928

the spirit of density functional theory, an auxiliary quantity, the embedded wavefunction (Ψ_A^{emb}), is used to perform the search for $\rho_A^{opt}(\vec{r})$. The search is performed not directly, i.e., among densities, but among embedded wavefunctions, opening thus the possibilities to use methods of modern quantum chemistry in order to optimize Ψ_A^{emb}. For any trial embedded wavefunction, the corresponding embedded density can be trivially obtained as the expectation value of the density operator $\hat{\rho}(\vec{r})$

$$\rho_A(\vec{r}) = \langle \Psi_A^{emb} | \hat{\rho} | \Psi_A^{emb} \rangle \tag{4}$$

In FDET, the optimal embedded wavefunction is obtained by means of solving the Euler−Lagrange equation:

$$\frac{\delta E_{AB}^{EWF}[\Psi_A^{emb}, \rho_B]}{\delta \Psi_A^{emb}} - \lambda \Psi_A^{emb} = 0 \tag{5}$$

where $E_{AB}^{EWF}[\Psi_A^{emb},\rho_B]$is the total energy expressed as a functional depending on Ψ_A^{emb} and $\rho_B(\vec{r})$, where λ is the Lagrange multiplier associated with the normalization of the embedded wavefunction.

Below, the energy functional $E_{AB}^{EWF}[\Psi_A^{emb},\rho_B]$ is given in the form adopted for multilevel simulations. To this end, the total external potential is partitioned into two components $v_{AB}(\vec{r}) = v_A(\vec{r}) + v_B(\vec{r})$ corresponding to the embedded subsystem (A) and the environment (B). Such partitioning defines a quantum system of N_A electrons in the external potential $v_A(\vec{r})$ with the corresponding Hamiltonian ($\hat{H}_A$). FDET admits various treatments of electron−electron interactions in $\hat{H}_A$: (a) interacting, where the electron−electron repulsion is taken into account explicitly as in conventional wavefunction based methods of quantum chemistry, (b) noninteracting as in Kohn−Sham based methods, or (c) partially interacting as in the "beyond-Kohn−Sham" formulations of DFT such as the ones based on adiabatic connection[74−76] or DFT formulation using multideterminantal auxiliary wavefunctions.[77] Using the density functionals borrowed from the Kohn−Sham formulation of DFT: exchange-correlation energy ($E_{xc}[\rho]$) or kinetic energy in a reference system of noninteracting electrons ($T_s[\rho]$) defined in the Levy constrained search,[50] the FDET functional for the total energy reads:

$$\begin{aligned} E_{AB}^{EWF}[\Psi^A, \rho_B] &= \langle \Psi^A | \hat{H}_A | \Psi^A \rangle + \Delta F^{SC}[\rho_A] \\ &+ \int \rho_A(\vec{r}) v_B(\vec{r}) d\vec{r} + \int\int \frac{\rho_A(\vec{r})\rho_B(\vec{r}')}{|\vec{r} - \vec{r}'|} d\vec{r}' d\vec{r} \\ &+ T_s^{nad}[\rho_A, \rho_B] + E_{xc}^{nad}[\rho_A, \rho_B] \\ &+ E_{v_B}^{HK}[\rho_B] + \int \rho_B(\vec{r}) v_A(\vec{r}) d\vec{r} \end{aligned} \tag{6}$$

where (a) $E_{xc}^{nad}[\rho_A,\rho_B] = E_{xc}[\rho_A + \rho_B] - E_{xc}[\rho_A] - E_{xc}[\rho_B]$, (b) $T_s^{nad}[\rho_A,\rho_B] = T_s[\rho_A + \rho_B] - T_s[\rho_A] - T_s[\rho_B]$, and (c) $\Delta F^{SC}[\rho_A]$ denotes a contribution to the total energy which depends on the form of the embedded wavefunction and the Hamiltonian $\hat{H}_A$ (see below).

Note that, despite the fact that $\hat{H}_A$ might denote either the interacting or noninteracting Hamiltonians, the functionals defined for the noninteracting system (Kohn−Sham system) are used in the above expression. Owing to this "step back" in FDET, the embedding operator can be represented as a multiplicative operator (embedding potential).

The necessary condition for Ψ_A^{emb} to satisfy eq 5 is

$$(\hat{H}_A + \hat{v}_{emb})\Psi_A^{emb} = \epsilon \Psi_A^{emb} \tag{7}$$

where $\hat{v}_{emb}$ is an "embedding operator".

Subject to the condition of v-representability of the optimal density $\rho_A^{opt}(\vec{r})$ (see section 2.2.5), FDET provides a system-independent expression for the embedding operator as a potential. The FDET embedding potential is a functional of two electron densities ($\rho_A(\vec{r})$, $\rho_B(\vec{r})$) and the electron density independent potential generated by the environment $v_B(\vec{r})$:[45]

$$\begin{aligned} &v_{emb}[\rho_A, \rho_B, v_B](\vec{r}) \\ &= v_B(\vec{r}) + \int \frac{\rho_B(\vec{r}')}{|\vec{r}' - \vec{r}|} d\vec{r}' + \frac{\delta T_s^{nad}[\rho_A, \rho_B]}{\delta \rho_A(\vec{r})} \\ &+ \frac{\delta E_{xc}^{nad}[\rho_A, \rho_B]}{\delta \rho_A(\vec{r})} + \frac{\delta \Delta F^{SC}[\rho_A]}{\delta \rho_A(\vec{r})} \end{aligned} \tag{8}$$

It is worthwhile to notice the applied notation for the embedding potential v_{emb}. An equivalent notations for this functional could read either $v_{emb}[\rho_A,\rho_B,\rho_B^{pos}](\vec{r})$, which reflects the fact that the external potential is generated usually by positive charges of the nuclei or just $v_{emb}[\rho_A,\rho_B;\vec{r}](\vec{r})$ indicating its explicit position dependence due to $v_B(\vec{r})$. For the sake of generality, we do not use the shorthand notation $v_{emb}[\rho_A,\rho_B](\vec{r})$ which is used frequently in the literature (including our own works). The shorthand notation carries a silent assumption that all considerations concern fixed partitioning of the total external potential into its components $v_A(\vec{r})$ and $v_B(\vec{r})$. With the notation used in the present review, eq 8 becomes an equation for functionals and not for particular functions.

Throughout this work, we will refer to the formal framework defined by eqs 3−8 as frozen-density embedding theory. The formulas given so far are general. They hold for any variational principle based method used to solve eq 7 including either the Kohn−Sham framework, in which the Hamiltonian does not comprise the explicit electron−electron interaction, or any wavefunction-based method treating electron−electron interaction explicitly (Hartree−Fock, complete active space self-consistent field[78,79] (CASSCF), truncated or full configuration interaction (CI) type of methods of quantum chemistry,[3,4] for instance). In fact, the extension for FDET was formulated also for the case of using embedded spin-less reduced one-particle density matrix.[46] In view of lack of practical applications of this extension, it will not be discussed further here.

Turning back to the $\Delta F^{SC}[\rho_A]$ functional, it is defined differently depending on the treatment of electron−electron correlation in $\hat{H}_A$. In the case of the embedded Kohn−Sham system,[49] i.e., implicit treatment of electron−electron correlation by means of an effective potential, $v_{eff}^{KS}[\rho_A](\vec{r})$, it is defined as

$$\begin{aligned} \Delta F^{SC(KS)}[\rho_A] &= \frac{1}{2}\int\int \frac{\rho(\vec{r})\rho(\vec{r}')}{|\vec{r} - \vec{r}'|} d\vec{r}' d\vec{r} + E_{xc}[\rho_A] \\ &- \int \rho_A(\vec{r})(v_{eff}^{KS}[\rho_A](\vec{r}) - v_A(\vec{r})) d\vec{r} \end{aligned} \tag{9}$$

The functional derivative ($\delta \Delta F^{SC(KS)}[\rho_A]/\delta\rho_A(\vec{r})$) disappears by construction but the term $\Delta F^{SC(KS)}[\rho_A]$ provides a nonzero contribution to the total energy functional given in eq 6. As a result, the expectation value of the noninteracting Hamiltonian (Kohn−Sham) ($\langle \Psi^A | \hat{H}^{KS}{}_A | \Psi^A \rangle$) is not equal to the energy $E_{v_A}{}^{HK}[\rho_A]$. We introduced a descriptive term, Kohn−Sham equations with constrained electron density (KSCED),[55] for the FDET equations in the case of embedding a noninteracting system in a frozen density (eqs 20−21 in ref 44 or eqs 43−45 in the present work). This acronym is also used in the literature (see

DOI: 10.1021/cr500502v
Chem. Rev. 2015, 115, 5891−5928

refs 80−83). The approximate version of eq 43, in which the exact functionals $T_s^{nad}[\rho_A,\rho_B]$ and $E_{xc}[\rho]$ are replaced by their approximated counterparts, for the use in simulations, is the same as the ones in the method by Senatore and Subbaswamy.[84] In the approximated case, the obtained energy may obviously lie below the exact ground-state energy. Moreover, the localization of the embedded orbitals is not only the result of constrained optimization of the total energy but reflects also errors in the used approximation to $T_s^{nad}[\rho_A,\rho_B]$ (see section 4.1). Note also a possible confusion with the term constrained DFT coined by an Voorhis et al.[85,86] It also concerns constraints imposed on Kohn−Sham density (enforcing a particular charge occupancy on selected parts through a strong constraint $C[\rho] = 0$) with the constraint in FDET which is soft $(\forall \vec{r}\ \rho(\vec{r})) \geq \rho_B(\vec{r}))$.

In the case of explicit treatment of the electron−electron correlation in $\hat{H}_A$ as in traditional variational methods of wavefunction based quantum chemistry methods (*WFT*), the role of the $\Delta F^{SC}[\rho_A]$term is different.

The $\Delta F^{SC(WFT)}[\rho_A]$ term is defined by means of the constrained search:

$$\Delta F^{SC(WFT)}[\rho_A] = \min_{\Psi_A\to\rho_A} \langle \Psi_A|\hat{T}_{2N_A} + \hat{V}^{ee}_{2N_A}|\Psi_A\rangle - \min_{\Psi_A^{WF}\to\rho_A} \langle \Psi_A^{WF}|\hat{T}_{2N_A} + \hat{V}^{ee}_{2N_A}|\Psi_A^{WF}\rangle \quad (10)$$

where Ψ_A^{WF} indicates a trial function used in the search procedure of the form admissible in the used wavefunction based method, whereas Ψ_A is a trial wavefunction from the wider class of functions comprising all v-representable densities.[50,87] Ψ_A^{WF} can take any form used in variational-principle conventional wavefunction methods of quantum chemistry (see the textbooks by Szabo and Ostlund,[3,4] and by Helgaker, Olsen, and Jorgensen,[4] for instance) starting from as simple as a single determinant (Ψ_A^{SD}) in the Hartree−Fock method, through the forms in CASSCF or truncated CI methods, until the one in full (CI) calculations.

$\Delta F^{SC(WFT)}[\rho_A]$ is nonpositive, and it is bound from below by

$$\Delta F^{SC(SD)}[\rho_A] = \min_{\Psi_A\to\rho_A} \langle \Psi_A|\hat{T}_{2N_A} + \hat{V}^{ee}_{2N_A}|\Psi_A\rangle - \min_{\Psi_A^{SD}\to\rho_A} \langle \Psi_A^{SD}|\hat{T}_{2N_A} + \hat{V}^{ee}_{2N_A}|\Psi_A^{SD}\rangle \quad (11)$$

$\Delta F^{SC(SD)}[\rho_A]$ is just the correlation functional as introduced by Baroni and Tuncel[88] for treatment of correlation in generalized Kohn−Sham framework using exchange energy evaluated using 100% of exact exchange (the idea mentioned already in the original Kohn−Sham publication[49]). The zero value is reached only in the limit of the embedded wavefunction of the full CI form. For truncated CI forms of the embedded wavefunction, the numerical values of this functional lie between the two limits.

Since the $\Delta F^{SC(WFT)}[\rho_A]$ functional depends on $\rho_A(\vec{r})$ only (no contribution from either $\rho_B(\vec{r})$ or $v_B(\vec{r})$), it is a matter of convention to consider it as an error in correlation energy for truncated CI type of methods or to relate it to embedding (see the relevant discussion in ref 62). Numerical tests show that this term can be most likely neglected in practice because of the use of other approximations leading to larger errors.[89] It is worthwhile to mention here the DFT formulation by Savin[77] (for further recent formal developments see ref 90), where the electron−electron interactions are represented in $\hat{H}_A$ in a hybrid way (explicitly or implicitly depending on the range). Accurate numerical data indicate that limiting the orbital space can be efficiently compensated by a density functional.[91] The interpretation of the $\Delta F^{SC}[\rho]$ functional lies between that in two extreme model situations: that of Kohn−Sham formulation where the search in orbital space is limited to single-determinants and $\Delta F^{SC}[\rho]$ is needed to obtain exact energy expression and that in a full CI) where such term is not needed at all.

Finally, we note that it is not the total energy, which is the target of FDET based simulations, but the difference between the total energy and the energy of the subsystem B. Once the external potential is partitioned into its v_A and v_B components, the latter is given as $H^{HK}_{v_A}[\rho_B]$ which is constant if $\rho_B(\vec{r})$ is frozen. If the investigated process involves changes in the charge densities in the environment, the corresponding changes in energy are not derived from FDET but from the method chosen to describe the environment: using atomic potentials in QM/MM methods, energy obtained from lower quality quantum mechanical method, using optimized orbitals obtained in subsystem DFT calculations, for instance.

2.2. More on Key Features of FDET

In this section, the key quantities of FDET are discussed in more detail. We focus on their interpretation and relations with notions known in methods for multilevel simulations.

2.2.1. Nonadditivity of the Density Functional for the Kinetic Energy. The bifunctional $T_s^{nad}[\rho_A,\rho_B]$is defined using the constrained search procedure:

$$\begin{aligned} T_s^{nad}[\rho_A, \rho_B] &= \min_{\Psi_s\to\rho_A+\rho_B} \langle \Psi_s|\hat{T}|\Psi_s\rangle \\ &- \min_{\Psi_s\to\rho_A} \langle \Psi_s|\hat{T}|\Psi_s\rangle - \min_{\Psi_s\to\rho_B} \langle \Psi_s|\hat{T}|\Psi_s\rangle \\ &= \langle \Psi_s^{AB(opt)}[\rho_A + \rho_B]|\hat{T}|\Psi_s^{AB(opt)}[\rho_A + \rho_B]\rangle \\ &- \langle \Psi_s^{A(opt)}[\rho_A]|\hat{T}|\Psi_s^{A(opt)}[\rho_A]\rangle \\ &- \langle \Psi_s^{B(opt)}[\rho_B]|\hat{T}|\Psi_s^{B(opt)}[\rho_B]\rangle \end{aligned} \quad (12)$$

where Ψ_s denotes an N-electron single-determinant trial wavefunction.

The constrained search definition of $T_s^{nad}[\rho_A,\rho_B]$ shows clearly why this bifunctional can be nonzero despite the fact that, for determinants constructed using a common set of orthogonal orbitals, the kinetic energy is strictly additive. The three constrained searches for the optimal wavefunctions used in the definition of $T_s^{nad}[\rho_A,\rho_B]$ are independent and lead to three sets of orthogonal orbitals. The orbitals from different sets might, however, be nonorthogonal.

For the pair $\rho_A(\vec{r})$ and $\rho_B(\vec{r})$, which are constants (uniform electron gas), the density of the nonadditive kinetic energy $T_s^{nad}[\rho_A,\rho_B](\vec{r})$ can be evaluated analytically. It is non-negative and reads

$$\begin{aligned} &T_s^{nad(TF)}[\rho_A, \rho_B](\vec{r}) \\ &= C_{TF}((\rho_A(\vec{r}) + \rho_B(\vec{r}))^{5/3} - \rho_A^{5/3}(\vec{r}) - \rho_B^{5/3}(\vec{r})) \end{aligned} \quad (13)$$

with $C_{TF} = 2.871$ in atomic units.

The corresponding functional for $T_s^{nad}[\rho_A,\rho_B]$ is obtained by integration of $T_s^{nad}[\rho_A,\rho_B](\vec{r})$

$$T_s^{nad(TF)}[\rho_A, \rho_B] = C_{TF}\int ((\rho_A + \rho_B)^{5/3} - \rho_A^{5/3} - \rho_B^{5/3})\, d\vec{r} \geq 0 \quad (14)$$

DOI: 10.1021/cr500502v
Chem. Rev. 2015, 115, 5891−5928

It diverges for uniform densities but it is one of the simplest approximations for the molecular densities.

It has been shown that $T_s^{nad}[\rho_A,\rho_B]$ is non-negative also for a particular class of pairs of densities discussed in ref 92. The non-negativity of $T_s^{nad}[\rho_A,\rho_B]$ in these two examples is not an exact property. Analytical examples where it can be negative can be easily constructed by dividing a smooth four-electron density into two rapidly varying two-electron components (see ref 48).

Finally, it is worthwhile to underline that the kinetic energy in the noninteracting reference system (T_s) represented as a functional of other quantities than the electron density ($T_s[\gamma]$ for one-particle spin-less density matrix γ or $T_s[\{\phi_i\}]$ for the orbitals $\{\phi_i\}$, for instance) might be an additive quantity. The particular role of the nonadditive kinetic energy in FDET is due to the fact that it is represented as a functional of a pair of electron densities and such functional is not additive (see section 2.2.6).

2.2.2. Relation between the FDET Embedding Potential and Projectors in the Pseudopotential Theory. Equation 7 resembles the equation for pseudo wave-function in approaches founded on the pseudopotential theory formulated by Phillips and Kleinman.[14] Pseudopotential theory is the formal basis for commonly used methods to eliminate the most-tightly bound electrons (core electrons) from explicit considerations (see the overview by Heine[93] or ref 94 for a recent review). Nonlocal embedding operators for practical applications are either transferable pseudpotentials (conventional strategy) or system specific projectors obtained from localized frozen orbitals (such methods trace their origin to the work of Husinaga and Cantu[30]). Methods and formalisms using such nonlocal embedding operators have been developed in several groups. A nonrepresentative (but most likely not all-inclusive) list of methods and formalisms using nonlocal embedding potential developed in several groups comprises: ab initio model potential by Barandiaran and Seijo,[15] effective group potentials by Katsuki,[16] effective fragment potential by Morokuma and collaborators,[17,56] effective group potentials developed in the Toulouse group,[18] atomic and molecular pseudopotentials by Simons and Mazziotti,[19] and effective potentials developed by von Arnim and Peyerimhoff,[20] Colle and Salvetti,[21] Whitten,[22] Assfeld and Rivail,[23] Duarte and Salahub,[24] Beran and Hirata,[25] Moriarty and Phillips,[26] Stoll and collaborators,[27] Mata et al.,[28] and embedding theory by Henderson,[29] Rajchel et al.[31,95] For most recent developments, see refs 32, 68, 96, and 97.

Concerning the relation between FDET and the pseudpotential theory, they target different quantities. The pseudopotential theory aims at wavefunctions (orbitals) whereas FDET at densities. In FDET, the embedding operator is just a potential., i.e., a multiplicative operator, whereas the exact Phillips-Kleinman pseudopotential involves projectors which are intrinsically nonlocal operators. If the exact Phillips-Kleinman pseudopotential is approximated by means of some local potential (see the overviews given in refs 93 and 94 or examples in refs 39, 43, and 98), it is an approximation in the pseudopotential theory. The exact FDET embedding potential, on the other hand, is local. In practical calculations, it is tempting to correct the deficiencies of the used approximations for $T_s^{nad}[\rho_A,\rho_B]$ by addition to a nonlocal pseudopotential to given approximation for $\delta T_s^{nad}[\rho_A,\rho_B]/\delta\rho_A(\vec{r})$. Stefanovich and Truong[99] used such combination to correct the qualitatively wrong results at short separations using an approximated FDET embedding potential (collapse of the embedded density on the cationic center in the environment). On the formal level, with such combination the nonadditive contribution to $T_s^{nad}[\rho_A,\rho_B]$ is counted twice (see the constrained search definition of $T_s^{nad}[\rho_A,\rho_B]$ given in eq 12). Moreover, the subsequent studies of the same system by Dulak and Wesolowski[100] showed that even conventional approximations for the functional $\delta T_s^{nad}[\rho_A,\rho_B]/\delta\rho_A(\vec{r})$ provide a sufficiently repulsive embedding potential to stop the artificial collapse provided the corresponding matrix elements are evaluated using an adequate integration technique.

The originally considered case by Phillips and Kleinman, separation of core and valence electrons, provides a good example illustrating the difference between the pseudopotental and the FDET embedding potential. In the pseudopotential theory, the most tightly bound orbital is frozen, which corresponds to freezing the corresponding orbital density and using it as $\rho_B(\vec{r})$ in FDET. For a model system consisting of four noninteracting electrons in the $-1/r$ potential,[47,48] the exact FDET solutions can be obtained analytically. They reveal the key features, in which FDET and the pseudopotential theory differ. The optimal FDET wavefunction obtained as the lowest energy solution of eq 7 with the FDET embedding operator given in eq 8 is not the same as the exact pseudo wave-function even they both yield the same electron density $\rho_A(\vec{r})$. The difference is not due to just a possible unitary transformation. Since the FDET embedding operator is a potential, the lowest energy orbital obtained as the solution of eq 7 with FDET embedding operator given in eq 8 is nodeless whereas the exact Philips-Kleinman pseudoorbital obtained using a nonlocal operator is not. It is the hydrogenic 2s function which must be orthogonal to the 1s orbital which is frozen. If the two strategies lead to the same total density $\rho_A^{opt}(\vec{r})$ defined in eq 3, the node-containing Phillips-Kleinman pseudoorbital Ψ_A^{pseudo} must yield the same density as Ψ_A^{emb}. This implies that $\Psi_A^{emb} = |\Psi_A^{pseudo}|$. The embedding potential, for which Ψ_A^{pseudo} could be obtained from eqs 7 and 8 of FDET, does not exist. FDET on the other hand admits the function $\Psi_A^{emb} = |\Psi_A^{pseudo}|$ to be lowest-energy orbitals as solutions of eq 7 with the embedding potential given in eq 8. Analytical examples provided in refs 47 and 48 show that the corresponding FDET embedding potential exists but it is not smooth (it comprises Dirac's δ-type of singularities). The target density $\rho_A^{opt}(\vec{r})$ and the corresponding embedded wavefunction $\Psi_A^{emb} = |\Psi_A^{pseudo}|$ can be, nevertheless, approached infinitely closely with a series of smooth embedding potentials.

Another qualitative difference of the pseudopotential theory and FDET is that the FDET embedding potential depends on $\rho_A(\vec{r})$. The exact FDET embedding potential cannot be, therefore, transferable. It depends not only on the environment but also on the state of the embedded species. Approximate pseudopotentials, which are usually nonlocal, are constructed on the other hand, to ensure their transferability. Transferability, is the key feature of approximated pseudopotentials, whereas ρ_A-dependence is the key feature of both exact and approximated FDET embedding potential. The ρ_A-dependence of the FDET embedding potential might be removed by further simplifications such as its linearization (see section 4.1.3) in order to avoid this undesired feature of FDET. The strategy introduced by Carter and collaborators[101] to construct ab initio local pseudopotentials can be seen as a simplified (linearized) version of the FDET embedding potential (see also section 4.1.4).

2.2.3. Polarization of the Environment by the Embedded Species. All quantities obtained in FDET are functionals of $\rho_B(\vec{r})$ (see section 2.1). Choosing $\rho_B(\vec{r})$ is, therefore, an empirical element in any FDET based multilevel simulations. The issue of dependence of the FDET results on

DOI: 10.1021/cr500502v
Chem. Rev. 2015, 115, 5891−5928

$\rho_B(\vec{r})$ is closely related to the strategies used in QM/MM methods to account for the electronic polarization of the environment by the embedded species. In QM/MM methods, where usually the embedding potential includes only the electrostatic component of the whole FDET potential, any change in the charge distribution in the environment is expected to affect the properties of the embedded species in a linear way. This is due to the fact that the electrostatic potential, which is a linear functional of $\rho_B(\vec{r})$, provides the first-order contribution to the intermolecular interaction energy.[102] The higher order terms are associated with such effects as electronic polarization of the environment. In fact, the intermolecular interaction theory is frequently used as a basis to construct embedding potential in QM/MM methods (see refs 103−105 for example).

The situation is not the same in FDET. First of all, different choices for $\rho_B(\vec{r})$ are possible which yield the same total density in eq 2. This leads to ambiguity in the definition of electric polarization of each separated subsystem. Second, FDET energy is obtained from variational calculations where, in contrast to the first-order term in perturbation theory, the dependence of energy on $\rho_B(\vec{r})$ is not linear. Below, we look at this issue in more detail. To this end, we introduce a well-defined quantity, $\rho_B^{(0)}(\vec{r})$, the ground-state electron density of the isolated environment. For any $\rho_B(\vec{r})$ used as an input for FDET, the quantity $\Delta\vec{\mu}_B$

$$\Delta\vec{\mu}_B = \int \vec{r}(\rho_B(\vec{r}) - \rho_B^{(0)}(\vec{r}))\, d\vec{r} \tag{15}$$

might be interpreted as the dipole moment induced in the environment by the embedded species. Such interpretation might be misleading. Whereas $\rho_B^{(0)}(\vec{r})$ is a well-defined quantity, different choices for $\rho_B(\vec{r})$ in eq 3 may lead to the same energy and electron density of the whole system (see discussions of this issue in refs 60, 106, and 107). For instance, two such choices for $\rho_B(\vec{r})$, $\rho_B^{(1)}(\vec{r})$ and $\rho_B^{(2)}(\vec{r})$, can be made that

$$\rho_B^{(1)}(\vec{r}) \le \rho_o^{AB}(\vec{r}) \tag{16}$$

and

$$\rho_B^{(2)}(\vec{r}) \le \rho_o^{AB}(\vec{r}) \tag{17}$$

For the chosen two different frozen densities

$$E_{emb}[\rho_B^{(1)}] = \min_{\substack{\rho_A(\vec{r})\ge 0 \\ \int\rho_A(\mathbf{r})\, d\vec{r}=N_A}} E_v^{HK}[\rho_A + \rho_B^{(1)}] = E_v^{HK}[\rho_A^{opt(1)} + \rho_B^{(1)}] = E_v^{HK}[\rho_o] = E_o \tag{18}$$

$$E_{emb}[\rho_B^{(2)}] = \min_{\substack{\rho_A(\vec{r})\ge 0 \\ \int\rho_A(\vec{r})\, d\vec{r}=N_A}} E_v^{HK}[\rho_A + \rho_B^{(2)}] = E_v^{HK}[\rho_A^{opt(2)} + \rho_B^{(2)}] = E_v^{HK}[\rho_o] = E_o \tag{19}$$

where $\rho_A^{opt(1)}(\vec{r})$ and $\rho_A^{opt(2)}(\vec{r})$ are the optimized densities of subsystem A obtained for these two choices for $\rho_B(\vec{r})$.

The quantities

$$\Delta\vec{\mu}_B^{(1)} = \int \vec{r}(\rho_B^{(1)}(\vec{r}) - \rho_B^{(0)}(\vec{r}))\, d\vec{r} \tag{20}$$

and

$$\Delta\vec{\mu}_B^{(2)} = \int \vec{r}(\rho_B^{(2)}(\vec{r}) - \rho_B^{(0)}(\vec{r}))\, d\vec{r} \tag{21}$$

might be, however, different. The fact that $\Delta\vec{\mu}_B^{(1)}$ and $\Delta\vec{\mu}_B^{(2)}$ are not the same shows that FDET alone cannot deliver a unique partitioning of the total density. Only the total dipole moment is uniquely defined. The notion of the polarization of individual subsystems is, therefore, not well-defined in FDET. The situation is, however, different if approximations are used for the functionals $T_s^{nad}[\rho_A,\rho_B]$ and $E_{xc}^{nad}[\rho_A,\rho_B]$ (see eq 38 in section 4.1). Due to partitioning-dependent errors in the approximated functionals the unique pair is the result of the optimization of the densities of subsystems.

The numerical analyses show that the properties of the embedded subsystem depend weakly on the choice made for $\rho_B(\vec{r})$ in the case of local excitations for electrically neutral but polar chromophore embedded in a hydrogen bonded environment.[107] The weak dependence is a manifestation of the variational basis of FDET. We note that eq 3 admits the possibility of several choices for $\rho_B(\vec{r})$ leading to the same total density. Moreover, the whole FDET embedding potential depends on $\rho_A(\vec{r})$ whereas its dependence on $\rho_B(\vec{r})$ is not linear. In this respect, FDET embedding potential differs from the case where the environment is represented only by the electrostatic potential. This electrostatic component of the FDET alone can be expected to result in linear dependency of the environment induced shifts on $\rho_B(\vec{r})$.

It is important to underline that the above formal observations provide only the justification for the weak dependence of the FDET-derived properties of embedded species on the charge distribution in the environment but not for the lack of such dependence. The results obtained in practice, i.e., when approximate density functionals are used to evaluate FDET embedding potential, depend on $\rho_B(\vec{r})$ for two reasons: (i) lack of possibility to verify a priori whether the condition $\forall\vec{r}\ \rho(\vec{r})) \ge \rho_B(\vec{r})$ is satisfied for a given $\rho_B(\vec{r})$ and (ii) the effect of errors in the used approximation for the nonadditive density functionals (see the discussion in section 3.1). The numerical effect on the FDET results of these two factors cannot be separated in practice. Moreover, none of them relates directly to the electronic polarization of the environment be the embedded species.

2.2.4. Charge-Transfer between Subsystems. The interpretation of the FDET results in terms of charge transfer is not straightforward for the same reasons as interpretation of polarization discussed in the previous section. There are multiple pairs $\rho_A(\vec{r})$ and $\rho_B(\vec{r})$ adding to the same total density and, on the virtue of the Hohenberg−Kohn theorem, to the same total energy in FDET. In approximated methods, this degeneracy of partitioning is lifted as the results of the use of approximated functionals (see eq 38 in section 4.1). In practice, especially, in multilevel simulations the densities $\rho_A(\vec{r})$ and $\rho_B(\vec{r})$ are subject to some localization due to the use of limited number of centers for atomic basis sets. For instance, the centers for the basis sets for $\rho_A(\vec{r})$ might coincide with the atoms defining $v_A(\vec{r})$ and the centers for the basis sets for $\rho_B(\vec{r})$ might coincide with the atoms defining $v_B(\vec{r})$. We refer to such calculations as monomer expansion for embedded orbitals.[108] In ref 108, the numerical significance of this approximation was analyzed in detail in the case of hydrogen-bondend subsystems. Discussion of the numerical effects of such localization of embedded orbitals on calculated properties can be found in several publications.[37,89,108−126] Most of the large-scale simulations using FDET embedding potentials use the monomer expansion as an a priori assumption. Dulak and Wesolowski introduced also an automatic adaptive procedure to construct grid of the reduced

DOI: 10.1021/cr500502v
Chem. Rev. 2015, 115, 5891−5928

size.[127] In such a case, no charge-transfer between the embedded species and the environment is possible even with the exact density functionals in eqs 3−8 and optimization of $\rho_B(\vec{r})$. Taking into account the charge transfer and using monomer expansion requires going beyond FDET or subsystem DFT and use such methods as partition DFT[53,54] (see section 3). If, however, the number of centers used in the basis sets is not limited and includes all centers (supermolecular expansion for embedded orbitals), the redistribution of charges between subsystem can take place in also within the framework of subsystem DFT, i.e., keeping the integer occupancies of subsystems. Subsystem DFT, will not be able to provided the answer concerning the amount of the charge transferred between subsystems. Dealing with charge-transfer within FDET, it does not seem to be practical. One would need to provide such $\rho_B(\vec{r})$ which is either partially localized on the embedded species (in the case of charge-transfer from the environment) or leaves a "hole" for the density of the embedded species localized in the environment (in the case of charge-transfer from the embedded species to the environment). The supermolecular expansion for embedded orbitals is, however, indispensable for studies of the accuracy of the approximations for the nonadditive kinetic energy functionals,[48,108,110,111,126,128−133] using the (freeze-and-thaw procedure to optimize $\rho_A(\vec{r})$ and $\rho_B(\vec{r})$[55] (see section 4.1.1). It is also very useful in assessment of the completeness of smaller basis sets.[134]

2.2.5. *v*-Representability of the Optimal Embedded Density $\rho_A^{opt}(\vec{r})$. Although the total optimal densities obtained from either eq 2 or 3 are *v*-representable (only for such densities the Hohenberg−Kohn density functional for energy exists), $\rho_A^{opt}(\vec{r})$ defined in eq 3 may belong to a wide class of functions called *N*-representable. Conditions of *N*-representability were given by Gilbert[135] and can be easily implemented in the search procedure (eq 3). Performing the search for $\rho_A^{opt}(\vec{r})$ by means of the Euler−Lagrange equation (eq 5) restricts, however, the class of the obtained functions to the *v*-representable ones, i.e., densities which are ground-state densities for some external potential *v*. For a given descriptor used for $\rho_A(\vec{r})$, the corresponding FDET embedding potential given in eq 8 exists only if $\rho_A^{opt}(\vec{r})$ is *v*-representable.[50,87] Equation 5 is, therefore, less general than eq 3.

Concerning *v*-representability, we should distinguish among descriptors. In the case of noninteracting embedded wavefunction, the Euler−Lagrange equation may lead only to pure-state noninteracting *v*-representable[136] densities as in any Kohn−Sham DFT based computational method. If $\rho_A^{opt}(\vec{r})$ defined in eq 3 does not belong to this class, it cannot be obtained using such simple descriptor. The illustration of the practical importance of the *v*-representability condition condition for $\rho_A(\vec{r})$ is given in refs 47 and 48 dealing with an analytically solvable system. It is shown that a density $\rho_A^{opt}(\vec{r})$, which is evidently not pure-state noninteracting *v*-representable (the density of valence electrons in a noninteracting four-electron system in a spherical potential), can be approached infinitely closely using FDET. The corresponding series of smooth FDET embedding potentials for such densities approaching $\rho_A^{opt}(\vec{r})$ was constructed. The issue of *v*-representability of $\rho_A^{opt}(\vec{r})$ defined in eq 3 is crucial for methods using numerical inversion techniques to approximate the FDET embedding potential (see section 4.1.4).

In the case of interacting Hamiltonians used for $\hat{H}_A$, a wider class of densities can be obtained from the Euler−Lagrange equation. They do not have to be pure-state noninteracting *v*-representable. In practice, it means that they can have a multideterminant form. Similarly as in the case of noninteracting $\hat{H}_A$, the conditions of *v*-representability cannot, unfortunately, be verified in advance. In summary, the situation of FDET is similar as any density-functional-theory based computational method as far as *v*-representability of the target density is concerned. As shown in ref 137, even if the density is obtained in Kohn−Sham calculations using a finite basis sets, there is no guarantee that it is pure-state noninteracting *v*-representable.

It is worthwhile noting that the quantity $\rho_{A(target)}(\vec{r}) = \rho_o^{AB}(\vec{r}) - \rho_B(\vec{r})$, where $\rho_o^{AB}(\vec{r})$ is the exact ground-state density of the total system, may not be obtainable even from eq 3, because it might be negative for some choices for $\rho_B(\vec{r})$. If $\rho_o^{AB}(\vec{r}) - \rho_B(\vec{r})$ is negative, it is neither *v*-representable nor even *N*-representable (see also the discussion in ref 106).

2.2.6. Exact Properties of the Nonadditive Density Functionals.

- Uniform electron gas limit for $T_s^{nad}[\rho_A, \rho_B]$

The analytical form of the functional $T_s^{nad}[\rho_A,\rho_B]$ is known in the particular case where $\rho_A(\vec{r})$ = const and $\rho_B(\vec{r})$ = const. It is given in eq 14. A similar expression is available for the exchange component of $E_{xc}^{nad}[\rho_A,\rho_B]$ which is trivially obtainable from the Dirac expression for the exchange-energy of the uniform electron gas.[138]

- Sufficient conditions for $T_s^{nad}[\rho_A,\rho_B] = 0$

$$T_s^{nad}[\rho_A, \rho_B] = 0 \quad \text{for non overlapping } \rho_A \text{ and } \rho_B \tag{22}$$

For demonstration, we consider three sets of orbitals: $\{\phi_i^A\}$, $\{\phi_i^B\}$, and $\{\phi_i^{AB}\}$, used to construct the determinants $\Psi_s^{A(opt)}$, $\Psi_s^{B(opt)}$, and $\Psi_s^{AB(opt)}$ defined in eq 12. Within each set, the orbitals are orthogonal. The orbitals from different sets, $\{\phi_i^A\}$ and $\{\phi_i^B\}$, are also orthogonal due to the zero overlap between $\rho_A(\vec{r})$ and with $\rho_B(\vec{r})$. An auxiliary determinant ($\Psi_s^{AB(antis)}$) constructed using all orbitals from the two sets $\{\phi_i^A\}$ and $\{\phi_i^B\}$, yields the density $\rho_A(\vec{r}) + \rho_B(\vec{r})$. It belongs, therefore, to the set of trial densities in the constrained search definition of $T_s[\rho_A + \rho_B]$. Using $\Psi_s^{AB(antis)}$ as a trial function in the constrained search yields

$$\langle \Psi_s^{AB(antis)} | \hat{T} | \Psi_s^{AB(antis)} \rangle \geq \langle \Psi_s^{AB(opt)} | \hat{T} | \Psi_s^{AB(opt)} \rangle = T_s[\rho_A + \rho_B] \tag{23}$$

On the other hand, the expectation value of the kinetic energy operator evaluated at $\Psi_s^{AB(antis)}$ is known. It is the sum of orbital kinetic energies for the orbitals of the two sets $\{\phi_i^A\}$ and $\{\phi_i^B\}$, i.e., $\langle \Psi_s^{AB(antis)} | \hat{T} | \Psi_s^{AB(antis)} \rangle = T_s[\rho_A] + T_s[\rho_B]$. This relation inserted to eq 23, results in the inequality

$$T_s[\rho_A] + T_s[\rho_B] \geq T_s[\rho_A + \rho_B] \tag{24}$$

Now we continue with showing that the opposite inequality holds as well. To this end, we consider two other auxiliary sets of orbitals: $\{\phi_i^{A(proj)}\}$ and $\{\phi_i^{B(proj)}\}$. Each of them is obtained by means of projecting the orbitals $\{\phi_i^{AB}\}$ onto the one of the localized basis sets $\{\phi_i^A\}$ or $\{\phi_i^B\}$. The projected basis sets are, therefore, also orthogonal. The determinants generated from $\{\phi_i^{A(proj)}\}$ and $\{\phi_i^{B(proj)}\}$ yield $\rho_A(\vec{r})$ and $\rho_B(\vec{r})$, respectively. Each of them belongs, therefore, to the set of trial densities in the constrained search. As for any other trial function

$$\langle \Psi_s^{A(proj)} | \hat{T} | \Psi_s^{A(proj)} \rangle \geq T_s[\rho_A] \tag{25}$$

and

DOI: 10.1021/cr500502v
Chem. Rev. 2015, 115, 5891−5928

$$\langle \Psi_s^{B(proj)} | \hat{T} | \Psi_s^{B(proj)} \rangle \geq T_s[\rho_B] \tag{26}$$

leads to the inequality

$$T_s[\rho_A + \rho_B] \geq T_s[\rho_A] + T_s[\rho_B] \tag{27}$$

The two inequalities hold only if $T_s[\rho_A] + T_s[\rho_B] = T_s[\rho_A + \rho_B]$, i.e., if $T_s^{nad}[\rho_A,\rho_B] = 0$. A similar relation for nonoverlapping densities does not hold for $E_{xc}^{nad}[\rho_A,\rho_B]$. It is worthwhile to mention in this context that the exact Kohn−Sham formulation of DFT is capable to describe long-range dispersion interactions as illustrated by the success of the strategy developed by Langreth, Lundqvist, and collaborators to dispersion in which the exchange-correlation potential (a multiplicative operator in the Kohn−Sham theory) is a nonlocal density functional.[139−141] A less trivial example of pairs, for which $T_s^{nad}[\rho_A,\rho_B] = 0$, was given in ref 142. $T_s^{nad}[\rho_A,\rho_B] = 0$ if ρ_A and ρ_B are orbital densities in any spin-compensated noninteracting four-electron system. Using eq 14 to approximate $T_s^{nad}[\rho_A,\rho_B]$ violates the above condition.

•Sufficient conditions for $T_s^{nad}[\rho_A,\rho_B] \geq 0$.

$T_s^{nad}[\rho_A,\rho_B]$ is non-negative for particular pairs of densities $\rho_A(\vec{r})$ and $\rho_B(\vec{r})$ (called v_{AB}-representable pairs) which are analyzed in ref 92. They are defined as pairs densities, which are obtained form partitioning of any pure-state noninteracting v-representable[136] density, i.e., density obtained as a solution of Kohn−Sham equations, into two components constructed from a subset of orbital densities. An example of such a pair is the density of the core and valence electrons. Another example of pairs of electron densities, for which $T_s^{nad}[\rho_A,\rho_B]$ is non-negative, is given in ref 142. They are constructed using orbital densities $\rho_1(\vec{r})$ and $\rho_2(\vec{r})$ in a spin-compensated noninteracting four-electron system. For any pair $\rho_A(\vec{r}) = \alpha\rho_1(\vec{r}) + (1-\alpha)\rho_2(\vec{r})$ and $\rho_B(\vec{r}) = (1-\alpha)\rho_1(\vec{r}) + \alpha\rho_2(\vec{r})$ with $0 < \alpha < 1$, $T_s^{nad}[\rho_A,\rho_B]$ is positive (it is zero if $\alpha = 1$ or $\alpha = 0$ as discussed above).

•Symmetry of $T_s^{nad}[\rho_A,\rho_B]$.

$T_s^{nad}[\rho_A,\rho_B] = T_s^{nad}[\rho_B,\rho_A]$ by construction (see eq 12). It is worthwhile noting that the corresponding potentials cannot be assumed to be symmetric.

$$\left.\frac{\delta T_s^{nad}[\rho,\rho_B]}{\delta\rho(\vec{r})}\right|_{\rho=\rho_A(\vec{r})} \neq \left.\frac{\delta T_s^{nad}[\rho_A,\rho]}{\delta\rho(\vec{r})}\right|_{\rho=\rho_B(\vec{r})} \tag{28}$$

•Asymptotic condition for the functional $\delta T_s^{nad}[\rho,\rho_B]/\delta\rho(\vec{r})$ at low overlaps.

The condition

$$\left.\frac{\delta T_s^{nad}[\rho,\rho_B]}{\delta\rho(\vec{r})}\right|_{\rho=\rho_A\to 0,\int\rho_B d\vec{r}=2} = \frac{1}{8}\frac{|\nabla\rho_B|^2}{\rho_B^2} - \frac{1}{4}\frac{\nabla^2\rho_B}{\rho_B} \tag{29}$$

was discussed in detail in ref 131. Using eq 14 to approximate $T_s^{nad}[\rho_A,\rho_B]$ (see section 4.1) leads to a gross violation of this condition and to the emergence of a singular well near the distant nuclei in the environment. Gradient expansion based approximations to $T_s^{nad}[\rho_A,\rho_B]$ (see section 4.1) helps only partially by filling only 1/9 of this well. The same concerns generalized gradient expansion type of approximations to $T_s^{nad}[\rho_A,\rho_B]$. The approximation for the functional $\delta T_s^{nad}[\rho,\rho_B]/\delta\rho(\vec{r}$ introduced in ref 131 enforces this condition.

•Asymptotics of the embedding potential at large separation.

Jacob et al.[80] considered the asymptotic behavior of the FDET embedding potential at large separations between the subsystems A and B for $\rho_B(\vec{r})$ approaching locally the exact ground-state density of the total system. In such a case, the FDET embedding potential is constant. A pragmatic approach to reach this constant value was proposed by forcing the embedding potential to disappear at large separations. The exact behavior of the embedding potential was assured, therefore, without constructing an approximation for either the functional $T_s^{nad}[\rho_A,\rho_B]$ or the functional $\delta T_s^{nad}[\rho,\rho_B]/\delta\rho(\vec{r})$.

•Homogeneity of $T_s^{nad}[\rho_A,\rho_B]$ (lack of it).

The functional $T_s[\rho]$ is not order-one ($\lambda = 1$) homogeneous:[136]

$$T_s[\rho] \neq \lambda \int \rho(\vec{r}) \frac{\delta T_s[\rho]}{\delta\rho(\vec{r})}\, d\vec{r} \tag{30}$$

For recent numerical illustrations of the inhomogeneity see the recent work by Borgoo and Tozer.[143] Inhomogeneity of $T_s[\rho]$ results in the fact that the nonadditive kinetic potential $\delta T_s^{nad}[\rho_A,\rho_B]/\delta\rho_A(\vec{r})$ depends on $\rho_A(\vec{r})$. Furthermore, $T_s^{nad}[\rho_A,\rho_B]$ is not order-one homogeneous in either $\rho_A(\vec{r})$ or $\rho_B(\vec{r})$, which leads to the following inequalities:

$$T_s^{nad}[\rho_A,\rho_B] \neq \int \rho_A(\vec{r}) \frac{\delta T_s^{nad}[\rho_A,\rho_B]}{\delta\rho_A(\vec{r})}\, d\vec{r}$$

$$T_s^{nad}[\rho_A,\rho_B] \neq \int \rho_B(\vec{r}) \frac{\delta T_s^{nad}[\rho_A,\rho_B]}{\delta\rho_B(\vec{r})}\, d\vec{r}$$

$$T_s^{nad}[\rho_A,\rho_B] \neq \int \rho_A(\vec{r}) \frac{\delta T_s^{nad}[\rho_A,\rho_B]}{\delta\rho_A(\vec{r})}\, d\vec{r} + \int \rho_B(\vec{r}) \frac{\delta T_s^{nad}[\rho_A,\rho_B]}{\delta\rho_B(\vec{r})}\, d\vec{r} \tag{31}$$

The inhomogeneity of the exchange-correlation energy density functional $E_{xc}[\rho]$[144] results from the similar inequalities for the nonadditive exchange-correlation energy $E_{xc}^{nad}[\rho_A,\rho_B]$. As a result of the above inequalities, neither $T_s^{nad}[\rho_A,\rho_B]$ nor $E_{xc}^{nad}[\rho_A,\rho_B]$ can be obtained as the expectation value of the corresponding terms in the FDET embedding potential (see section 4.1.3).

3. EXTENSIONS AND FORMALISMS RELATED TO FDET

3.1. Formalisms to Reach the Exact Ground-State Energy E_o

FDET leads to the exact results only if $\rho_B(\vec{r})$ is chosen in such a way that the difference $\rho_o^{AB}(\vec{r}) - \rho_B(\vec{r})$ is v-representable. Since this condition cannot be verified in advance, FDET cannot, therefore, be seen as an alternative formulation of DFT. It is rather a formal framework for multilevel simulations which can yield only approximate solutions (upper bound of the total energy and the corresponding electron density) even if the exact FDET embedding potential would be available. The target of such simulations is the embedded species and the effect of the environment on its properties assuming that an adequate density $\rho_B(\vec{r})$ can be constructed so that the variations $\delta\rho_B(\vec{r})$ around $\rho_B(\vec{r})$ affect the investigated property not significantly. An estimation of the sensitivity of the results on the choice for $\rho_B(\vec{r})$ is thus an indispensable preliminary stage of any large-scale multilevel simulation.

Besides the Kohn−Sham formalism, alternative formulations of DFT using subsystems, which are capable to yield exact total density and energy were developed. They share with FDET common elements (nonadditive kinetic energy and the local embedding potential which is a functional of charge densities). In exchange for introducing other-than-charge-density descriptors

DOI: 10.1021/cr500502v
Chem. Rev. 2015, 115, 5891−5928

for the environment, they have the capacity of reaching the exact ground-state energy with the exact functionals and not to an upper limit as does FDET.

Cortona introduced an alternative formulation of DFT using the noninteracting reference wavefunctions for each subsystem into which the whole system was partitioned.[52] We will refer to this formalism as subsystem DFT. The model introduced in refs 145 and 146 and applied for solids[147] is formally the same as the Cortona formulation. This formalism is an alternative to the Kohn−Sham formulation of DFT, but it is not an approximation to it. It builds upon the ideas tracing their origin to various approximate methods developed as ad hoc system specific numerical procedures such as nonvariational Gordon−Kim model for interacting molecules,[148] the Senatore and Subbaswamy model for rare gas crystals,[84] and Ivanov and Maksimov generalization of the Gordon−Kim model for phonons,[149] for instance.

The model and method introduced by Senatore and Subbaswamy,[84] actually predates the publication by Cortona. Moreover, once the approximations are used, the working equations are essentially the same as the ones of subsystem DFT. The publication by Cortona provided interpretation of quantities obtained in the such approximate calculations. The first application of subsystem DFT based calculations reported in the original publication[52] concerned ionic solids. The subsystems corresponded to ions. For molecular systems, subsystem DFT was applied originally by Weber and Wesolowski[55] for the purpose of testing approximations for the nonadditive kinetic energy functional needed to solve both FDET and subsystem DFT equations in practice. The freeze-and-thaw iterative procedure was applied to optimize both $\rho_A(\vec{r})$ and $\rho_B(\vec{r})$[55] as a solution of the coupled Euler−Lagrange equations for different subsystems (eq 43). Interestingly, the interaction energies obtained using such fully variational calculations are frequently better than the results of the Kohn−Sham based calculations using corresponding approximations for the density functional for the exchange-correlation and kinetic energy.[150] Although approximate methods based on this formulation proved very successful especially in the evaluation of interaction energies and geometries of hydrogen- and dipole bonded intermolecular complexes (see refs 112 and 151), this formulation seems to suffer from intrinsic incompleteness: if approximations are used for nonadditive kinetic potential, the partitioning is the result of the error in the used approximation (see eq 38 in section 4.1).

Subsystem DFT admits infinite number of pairs of densities $\rho_A(\vec{r})$ and $\rho_B(\vec{r})$ adding up to the same total density.[60] The unique partitioning obtained in practice is the result of the fact that the difference between the exact and approximated bifunctional for the nonadditive kinetic energy depends on the partitioning, whereas the exact kinetic energy of the total system does not (see the disscusion in ref 107 or sections 2.2.3) and 4.1 in the present work). Despite this formal weakness, subsystem DFT is also used as the basis for various formal extensions concerning: LR-TDDFT treatment for excited states,[152−154] frequency dependent responses of the subsystems,[113] electron transfer processes,[155−157] generation of diabatic states in the empirical valence bond (EVB)[158,159] and Hamiltonian[160,161] or London-dispersion interactions,[162] for instance.

The issue of lack of uniqueness of partitioning cannot be solved without additional conditions/constraints. The partition DFT introduced by Elliott et al.[53,54] offers a way to achieve such uniqueness by imposing that the embedding potential remains the same upon exchanging the roles of subsystems A and B in eq 8. Such unique potential is called partition potential in partition DFT. Compared to subsystem DFT, partition DFT admits an additional degree of freedom: the number of electrons in each subsystem is subject to optimization and the optimal values can be fractional. For a recent overview of the state of methods based on partition DFT see ref 163. Recently, Carter and collaborators showed that the embedding potential, if it exists, is unique even if the subsystems are occupied by integer number of electrons.[164,165] Della Sala and collaborators addressed formally the issue of the uniqueness of partitioning in partition DFT in the context of methods using approximate density functionals.[166] To this end, the functionals of FDET were generalized in order to admit ensemble densities. As a result the optimization of the subsystem densities might lead to fractional occupancies of subsystems. Lifting the constraints of integer occupancies led to noticeable improvement of the optimized densities even if approximate density functionals were used.

Gritsenko and Visscher[167] proposed a formal framework to go over the intrinsic constraint of FDET, which is targeting an upper bound to the total energy instead of the exact ground-state energy and density. The introduced formalisms (density-orbital embedding theory) admits the situation where the difference between the exact density and the chosen $\rho_B(\vec{r})$ is not v-representable[50,87] by means of using another descriptor for the embedded subsystem density orbital. So far, no practical implementation of this formalism was made.

3.2. Extension of Ground-State FDET to Excited States

Section 2.1 provides a complete formal framework to obtain an upper bound of the ground-state energy and the corresponding electron density of the total system. Additionally, an auxiliary quantity, the embedded wavefunction corresponding the lowest-energy solution of eq 7, can be used to evaluate other properties than density and energy at the ground-state. Other than the lowest-energy solutions of eqs 7 and 8 are usually also available and can be used to evaluate properties of the same system at the excited state. Three approaches that extend this framework for excited states are outlined below.

3.2.1. High Symmetry Case. In the case of different symmetries of the ground and excited states, FDET (eqs 3−8) can be used to get information about the lowest-energy state of a given symmetry. Restricting the search for the lowest energy to densities of a given symmetry leads to an upper bound of the lowest energy for the specific symmetry. The situation is similar to that in density functional theory.[75,168−170] In the FDET context, it was used to study excited states of embedded rare-earth elements.[171,172] As in the ground-state case, the obtained energies are upper bounds for the energy in each considered state.

3.2.2. Other than the Lowest-Energy Solutions of the Euler−Lagrange Equations. According to the Perdew−Levy theorem,[173] stationary states of a ground-state density functional correspond to excited states. Although this theorem is known for almost 30 years, it has not been exploited numerically in the DFT context. Khait and Hoffmann[174] proposed to use other-than-ground-state solution of the FDET equations derived in ref 45 as quantities corresponding to the excited state. Additionally, the authors analyzed the effect of optimization of $\rho_B(\vec{r})$ on the obtained states. Daday et al.[175] were the first to pick up on this issue and investigated the effects of dependencies of the FDET embedding potential on $\rho_A(\vec{r})$ and $\rho_B(\vec{r})$ in practice. The numerical data on several embedded chromophores investigated there show that changes of $\rho_B(\vec{r})$ due to its optimization for a

DOI: 10.1021/cr500502v
Chem. Rev. 2015, 115, 5891−5928

given electronic state of the embedded chromophore affects the excitation energies significantly more than the direct effect associated with changing only $\rho_A(\vec{r})$ upon changing the electronic state. Similar conclusions were drawn from the subsequent studies of this issue.[176]

Concerning the practical use of the Perdew–Levy theorem in the FDET based calculations,[177] the $\rho_A(\vec{r})$ dependency of the embedding potential results inevitably in nonorthogonality of embedded wavefunctions corresponding to different electronic states even if $\rho_B(\vec{r})$ is constant.[177] Moreover, such use of the FDET embedding potential merits separate discussion of the cease of interacting and noninteracting Hamiltonians ($\hat{H}_A$ in eq 6). In the noninteracting case, the situation is similar as in the DFT context. All difficulties in constructing sufficiently accurate density functionals to describe adequately both the energy of the ground and excited state are carried on to embedding methods based on FDET. The prospects for its use as a basis for generally applicable methods are rather bleak because of the special conditions required for the excited states (see the discussion in ref 178). Not all excited states are extrema of the ground-state density functional. Moreover, it yields the exact excited-state density only if it is *v*-representable.

If, on the other hand, an interacting Hamiltonian is used for $\hat{H}_A$ in FDET, the perspectives for the practical usefulness of the Perdew–Levy theorem seem promising. The ad hoc combinations of the FDET embedding potential, which is usually subject to further approximations such as its linearization (see section 4.1.3), with interacting Hamiltonians, were pioneered by Carter and collaborators.[57,58]

Approaches combining various wavefunction theory based methods from the quantum chemistry toolbox with the FDET embedding potential have been developed including: Hartree–Fock,[58]

Møller–Plesset perturbation theory (MPn),[58] CASSCF,[179] configuration interaction (CI),[179] coupled cluster methods,[180] etc. In addition to explicit construction of the embedded wavefunction for the excited state, the burden of constructing an approximation for the exchange-correlation density functional describing the ground and excited states with comparable accuracy is removed owing to explicit treatment of electronic correlation for $\rho_A(\vec{r})$ in such methods.

3.2.3. Time-Dependent Linear-Response Theory for Noninteracting System Embedded in Frozen Density. In the case of a noninteracting system embedded in the frozen density,[44,60] excitation energies and oscillator strengths for each transition can be obtained following the linear-response time-dependent DFT strategy (LR-TDDFT).[181] Within the neglect of dynamic response of the environment (NDRE) approximation, i.e., neglecting the frequency dependent response of $\rho_B(\vec{r})$ to a time-dependent perturbation ($\delta\rho_B(\vec{r},\omega)=0$), the extension of the LR-TDDFT framework to embedded system is straightforward.[182] In the absence of the environment, the excitation energies (ω_A) are obtained from the basic equation of LR-TDDFT (Casida equation):[181]

$$\hat{\Omega}_A - {\omega_A}^2 \hat{\mathbf{I}}_A = 0 \tag{32}$$

where the matrix representation of $\hat{\Omega}_A$ reads

$$\Omega^A_{ij\sigma,kl\tau} = \delta_{\sigma,\tau}\delta_{i,k}\delta_{j,l}(\epsilon^A_{l\tau} - \epsilon^A_{k\tau})^2 + 2\sqrt{(f^A_{i\sigma} - f^A_{j\sigma})(\epsilon^A_{j\sigma} - \epsilon^A_{i\sigma})}\, K^A_{ij\sigma,kl\tau} \sqrt{(f^A_{k\tau} - f^A_{l\tau})(\epsilon^A_{l\tau} - \epsilon^A_{k\tau})} \tag{33}$$

where the matrix $K^A_{ij\sigma,kl\tau}$ is defined as

$$K^A_{ij\sigma,kl\tau} = \iint \phi^{A^*}_{i\sigma}(\vec{r})\phi^A_{j\sigma}(\vec{r})\frac{1}{|\vec{r} - \vec{r}'|}\phi^A_{k\tau}(\vec{r}')\phi^{A^*}_{l\tau}(\vec{r}')\, d\vec{r}'\, d\vec{r} + \iint \phi^{A^*}_{i\sigma}(\vec{r})\phi^A_{j\sigma}(\vec{r}) f^A(\vec{r},\vec{r}')\phi^A_{k\tau}(\vec{r}')\phi^{A^*}_{l\tau}(\vec{r}')\, d\vec{r}'\, d\vec{r} \tag{34}$$

with

$$f^A[\rho_A](\vec{r},\vec{r}') = \frac{\delta^2 E_{xc}[\rho_A]}{\delta\rho_A(\vec{r})\delta\rho_A(\vec{r}')} \tag{35}$$

In the above equations, the Roman and Greek indices denote space and spin respectively, and the ordering of indices is such that $f_{i\sigma} > f_{j\sigma}$ and $f_{k\tau} > f_{l\tau}$.

Within the NDRE approximation in the embedding case introduced in ref 182, the Casida equation retains the form given in eqs 32 and 33. The matrix $\hat{\Omega}_A$ is defined using the eigenvalues (ϵ) and occupation numbers (f) obtained not from the Kohn–Sham equations for the isolated system but from the corresponding FDET equations, Kohn–Sham equations with constrained electron density (eqs 20 and 21 in ref 44 or eqs 43–45 in the present work), for the embedded system. Compared to environment-free case, however, the matrix $K^A_{ij\sigma,kl\tau}$ not evaluated using the kernel defined in eq 35 but the kernel which is the functional derivative of the whole FDET effective potential given in eq 45. This kernel can be conveniently represented as

$$f^{A(emb)}[\rho_A,\rho_B](\vec{r},\vec{r}') = f^A[\rho_A](\vec{r},\vec{r}') + f^{emb}[\rho_A,\rho_B](\vec{r},\vec{r}') \tag{36}$$

where the contribution to the kernel due to the embedding potential reads:[182]

$$f^{emb}[\rho_A,\rho_B](\vec{r},\vec{r}') = \frac{\delta^2 T_s^{nad}[\rho_A,\rho_B]}{\delta\rho_A(\vec{r})\delta\rho_A(\vec{r}')} - \frac{\delta^2 E_{xc}^{nad}[\rho_A,\rho_B]}{\delta\rho_A(\vec{r})\delta\rho_A(\vec{r}')} \tag{37}$$

Note that the electrostatic components of the FDET embedding potential do not contribute to $f^{emb}[\rho_A,\rho_B](\vec{r},\vec{r}')$ because they do not depend on $\rho_A(\vec{r})$.

The above extension of FDET is referred to in the present work as FDET/LR-TDDFT. For an extension of FDET going beyond NDRE see section 3.3.

3.3. Beyond Density Embedding for Coupled Chromophores

The subsystem formulation of DFT by Cortona[52] was generalized for LR-TDDFT treatment of excited states by Casida and Wesolowski.[152] Such extension goes beyond FDET for two reasons. Similarly to subsystem DFT, other descriptors than density are used for the environment. The environment and the embedded species are treated on on equal footing. Beyond-density descriptors (embedded orbitals and the corresponding eigenvalues) are used for the environment. NDRE approximation can be expected to be adequate for modeling the environment induced shifts in the excitation energies if they are the result of electrostatic interactions and/or confinement. Going beyond NDRE approximation is indispensable if the environment and the embedded species absorb at the same (dimers) or similar wavelengths. For dimers absorbing in the same spectral range, a straightforward demonstration of the failure of the NDRE approximation was provided in refs 123 and 153. Besides such easy-to-detect cases, NDRE can be also expected to fail if a large number of weakly polarizable molecules

DOI: 10.1021/cr500502v
Chem. Rev. 2015, 115, 5891–5928

couple weakly their electronic state with that of the embedded species (the case of metal cluster in noble gases,[183] for instance). Numerical results reported in ref 123 for beta-cyclodextrin indicate that NDRE lies at the origin of the discrepancies between excitation energies obtained in embedding and supermolecular calculations. In such a case, the use of explicit polarizability of the molecules/atoms is probably the best strategy.

Similarly as for the ground-state, the subsystem formulation of LR-TDDFT suffers from the ambiguity the lack of uniqueness in partitioning of the total density (see section 2.2.3), which becomes unique due to approximations used for the nonadditive functionals (see eq 38).

In the original work introducing this straightforward generalization of subsystem DFT for excited states,[152] no numerical implementations of this formalism was reported. A closer analysis of this formulation and results obtained using approximate functionals revealed that this formalism suffers from numerical instabilities in case of the embedded system comprising identical chromophores (benzaldehyde dimer).[153] Neugebauer made a connection between the coupling term in the phenomenological Hamiltonian used in the Förster,[184] Dexter,[185] or Marcus[186] models and the Casida−Wesolowski generalization of subsystem DFT. As a result, a general subsystem-based formal framework for treating coupled chromophores was developed.[153] Following Neugebauer, we will refer to this formalism as FDEc. Subsequently, this framework was applied to obtain other response properties besides the LR-TDDFT derived excitation energies. Reference 113 provides the outline of the formalism and numerical illustrations.

Recently, Pavanello presented a new derivation of the subsystem DFT for excited states linking them with Dyson equation.[154]

4. APPROXIMATIONS IN FDET FOR MULTILEVEL SIMULATIONS

FDET cannot be applied in practice without further approximations. Exact solutions of eqs 3−8 available in only a few cases, which are discussed in section 2. They are useful for construction of approximations for the relevant density functionals and for interpretations. In this section, the approximations made in practice are discussed. They concern either the approximations for universal density functionals (section 4.1) or the generation of $\rho_B(\vec{r})$ (section 4.2) which are system-dependent. In section 4.3, the group of approximate methods using also the approximated FDET embedding potential, which are introduced usually as variants of the ONIOM strategy,[56] are overviewed.

4.1. Approximations for Density Functionals

The straightforward implementation of FDET for practical simulation uses some approximate expressions ($\tilde{T}_s^{nad}[\rho_A,\rho_B]$ and $\tilde{E}_{xc}^{nad}[\rho_A,\rho_B]$) for the bifunctionals $T_s^{nad}[\rho_A,\rho_B]$ and $E_{xc}^{nad}[\rho_A,\rho_B]$ and using them in eqs 3−8 instead of their exact counterparts. Equations 3−8 remain unaffected by this substitution and the variational principle basis, which lies at the origin of numerical stability of the FDET results even in the approximate case,[36,37] still applies. The variational principle does not apply to $E^{FDET}[\rho_B]$ but to its approximated counterpart:

$$\tilde{E}^{FDET}[\rho_B] = E^{FDET}[\rho_B] + \Delta\tilde{T}_s^{nad}[\rho_A^{opt}, \rho_B] + \Delta\tilde{E}_{xc}^{nad}[\rho_A^{opt}, \rho_B] \quad (38)$$

where $\Delta\tilde{T}_s^{nad}[\rho_A^{opt},\rho_B]$ and $\Delta\tilde{E}_{xc}^{nad}[\rho_A^{opt},\rho_B]$ denote the difference between the exact and the approximate functional (its error). The above equations show clearly that, although the exact FDET equations (eqs 3−8) lead to a upper bound of the exact energy, the use of approximations for the nonadditive density functionals might lead to the energies which are below the exact $E^{FDET}[\rho_B]$.

Another qualitative difference between the exact and approximate FDET is the removal of degeneracy of partitioning the total density (see section 2.2.3). In the exact theory, there are multiple pairs of densities $\rho_A(\vec{r})$ and $\rho_B(\vec{r})$ which add up to the optimal total density[60] (see refs 47 and 48 for analytical examples). In the approximated case, the optimization of $\rho_A(\vec{r})$ is affected by the partition-dependent terms $\tilde{T}_s^{nad}[\rho_A,\rho_B]$ and $\tilde{E}_{xc}^{nad}[\rho_A,\rho_B]$. As a result, optimization of both $\rho_A(\vec{r})$ and $\rho_B(\vec{r})$ through the minimization of the total energy given in eq 38 leads to a unique pair.

Equation 38 relates also to the issue of the state-specificity of the FDET embedding potential in calculations targeting excited states. State-specificity has a clear interpretation in FDET as its ρ_A-dependence[177] for a given $\rho_B(\vec{r})$. In the literature, the term state-specificity is used as the dependence of the embedding potential on $\rho_B(\vec{r})$ obtained in freeze-and-thaw optimization made for different electronic states of the embedded species.[175,176]

The effect of optimization of $\rho_B(\vec{r})$ on the obtained properties of the embedded species in different electronic states cannot, however, be attributed to the differential electronic polarization of the environment. The differences in the optimized $\rho_B(\vec{r})$ for different electronic states are also affected by the errors in the used approximation for the nonadditive functionals which might be also state-dependent.

4.1.1. Explicit Approximations for $T_s^{nad}[\rho_A,\rho_B]$ and $E_{xc}^{nad}[\rho_A,\rho_B]$.

For approximating $T_s^{nad}[\rho_A,\rho_B]$, the most common strategy (decomposable approximations) is to apply one of existing approximations for the functional $T_s[\rho]$ (for a comprehensive list of semilocal approximations to $T_s[\rho]$ see ref 187) in the definition of $T_s^{nad}[\rho_A,\rho_B]$

$$T_s^{nad}[\rho_A, \rho_B] \approx \tilde{T}_s[\rho_A + \rho_B] - \tilde{T}_s[\rho_A] - \tilde{T}_s[\rho_B] = \tilde{T}_s^{nad}[\rho_A, \rho_B] \quad (39)$$

In the case of gradient-dependent approximations for $T_s[\rho]$, which is the most commonly used in practice, the corresponding expression reads

$$\tilde{T}_s^{nad(GGA)}[\rho_A, \rho_B] = C_{TF} \int (\rho_A + \rho_B)^{5/3} F_T\left(\frac{|\nabla(\rho_A + \rho_B)|}{(\rho_A + \rho_B)^{4/3}}\right) d\vec{r} - C_{TF}\int \rho_A^{5/3} F_T\left(\frac{|\nabla\rho_A|}{\rho_A^{4/3}}\right) d\vec{r} - C_{TF}\int \rho_A^{5/3} F_T\left(\frac{|\nabla\rho_B|}{\rho_B^{4/3}}\right) d\vec{r} \quad (40)$$

where the function $F_T(x)$ with $x = |\nabla\rho|/\rho^{4/3}$ (enhancement factor) is specific for each gradient-dependent approximation. $F_T(x) = 1 + (x^2/72C_{TF})$ for the second order gradient expansion approximation to $T_s[\rho]$, for instance. The contribution to the FDET embedding potential due to $\tilde{T}_s^{nad(GGA)}[\rho_A,\rho_B]$ can also be obtained analytically as a functional derivative of the first two terms in eq 40 using the following expression for each of them

DOI: 10.1021/cr500502v
Chem. Rev. 2015, 115, 5891−5928

$$\frac{\delta \tilde{T}_s^{GGA}[\rho]}{\delta\rho(\vec{r})} = \frac{5}{3}C_{TF}\rho^{2/3}\left(F_T(x) - xF_T'(x) + \frac{4}{5}x^2F_T''(x)\right) + C_{TF}D\frac{\rho^{1/3}}{|\nabla\rho|^3}(F_T'(x) - xF_T''(x)) - C_{TF}\frac{F_T'(x)}{x}\frac{\nabla^2\rho}{\rho} \quad (41)$$

where $D = \sum_{i=1}^{3}\sum_{j=1}^{3}\partial_i\rho\partial_i\partial_j\rho\partial_j\rho$.

For the enhancement factors used in the GGA approximations for $T_s[\rho]$, Lee, Lee, and Parr formulated a never-proven conjointness conjecture[188] concerning the relation between explicit approximations for the exchange energy ($E_x[\rho]$) and $T_s[\rho]$. The conjecture builds on previous observations made by March and Santamaria concerning the exchange- and kinetic energies in Hartree−Fock case,[189] which is directly related to the DFT functionals $E_x[\rho]$ and $T_s[\rho]$ defined in Levy constrained search.[50] Following this conjecture, for a given GGA approximations for $E_x[\rho]$ an approximation for $T_s[\rho]$ can be constructed. The conjoint approximations for $E_x[\rho]$ and $T_s[\rho]$ shares the same analytical form of the enhancement factor which represents the same physical approximation for the one-particle reduced density matrix. As a result, the conjoint approximations for $E_x[\rho]$ and $T_s[\rho]$ are expected to have the same quality. Moreover, fine-tuning of the parameters in the enhancement factor keeping its analytical form lies also within the assumptions of the conjecture. Lee, Lee, and Parr used the enhancement factor of the Becke's (B88)[190] to illustrate the usefulness of this approach to construct approximations for $T_s[\rho]$. Investigations by several authors provided further numerical confirmations of the conjointness conjecture for several the enhancement factors of the common GGA exchange functionals: Fuentealba and Reyes[191] for that of the Perdew−Wang (PW86),[192] Lembarki and Chermette[193] for that of the Perdew−Wang (PW91),[194] Tran and Wesolowski[195] for that of Perdew−Burke−Ernzerhoff (PBE),[196] and Karasiev, Trickey, and Harris[197] for that of the modified PBE[198] functional, for instance. The conjointness conjecture strategy was recently applied by Constantin et al.[199,200] to construct two approximations for $T_s[\rho]$ (APBEK and revAPBEK) conjoint to the approximations to $E_x[\rho]$ obtained from semiclassical atom theory.

The decomposable strategy hinges on the assumption that the errors in $\tilde{T}_s[\rho]$ do compensate for the three densities $\rho_A(\vec{r}) + \rho_B(\vec{r})$, $\rho_A(\vec{r})$, and $\rho_B(\vec{r})$ in eq 39. In fact it is not the case for the functionals originating in the regular gradient expansion for the kinetic energy[201] such as the Thomas−Fermi functional, second-order gradient expansion, and the functionals of the GGA form. Numerical results show that there is no correlation in errors in decomposable approximations for $\tilde{T}_s^{nad}[\rho_A,\rho_B]$ with the errors in the corresponding parent approximation for $\tilde{T}_s[\rho]$.[48,130] The same concerns errors in $\delta\tilde{T}_s^{nad}[\rho_A^{opt},\rho_B]/\delta\rho_A(\vec{r})$.[48,129,130,160] A closer look at the decomposable strategy shows that imbalance of errors in the density of the kinetic energy $\tilde{t}_s[\rho](\vec{r})$ evaluated for the three densities $\rho_A(\vec{r}) + \rho_B(\vec{r})$, $\rho_A(\vec{r})$, and $\rho_B(\vec{r})$. The imbalance of errors has its origin in a different role, which the von Weizsäcker functional[202] plays near and far from the embedded subsystem. This functional is the exact functional for one electron and spin-compensated two-electron systems, but if divided by 9 it is the second-order term in the gradient expansion. We illustrate the imbalance of such approximations in the case of two molecules (say molecule A and molecule B) and attribute the role of the environment in FDET to the molecule B. Within B, the gradient expansion can be expected to provide much better approximation for $t_s[\rho_A + \rho_B](\vec{r})$ than for $t_s[\rho_A](\vec{r})$. In the second-order gradient expansion, the Thomas−Fermi functional enters entirely and the von Weizsäcker functional is divided by 9 in second-order gradient expression. Far from the molecule A, the von Weizsäcker the density $\rho_A(\vec{r})$ decays exponentially and is dominated by one orbital. The exact functional for $t_s[\rho_A](\vec{r})$ is given by the entire von Weizsäcker functional (not divided by 9) without any contribution from the Thomas−Fermi functional.

These considerations explain the disappointing results obtained using the second-order gradient expansion approximation.[44,129] The convergence problems reported in ref 110 originate probably from this flaw of the second-order gradient expansion. Within the decomposable strategy, a pragmatic solution was made to minimize the errors due to the above imbalance of errors. Instead of using the second-order gradient-expansion approximation, a specially chosen GGA functional is used in which the second-order contribution to $t_s[\rho](\vec{r})$ is smoothly damped by an appropriately chosen enhancement factor ($F_T(x)$) in eq 40.[108,160] The desired enhancement factor has the same analytical form as the one in the GGA functional for the exchange energy introduced by Perdew and Wang[194] and parametrized for the kinetic energy[193] by Lembarki and Chermette. The origin of this approximation is reflected by a nonhomogeneous nomenclature in the literature; it is called differently by different authors depending on which quantity is referred to the GGA97 label is used to specify approximation for $T_s^{nad}[\rho_A,\rho_B]$ (see refs 100 and 203−206), PW91K (in refs 80, 114, and 207−211 for instance) or LC94 (see refs 200 and 212 for instance) for $T_s[\rho]$, or just PW91 for the enhancement factor $F(x)$.[108,115,180,213]

Damping the second order contribution at low densities cures also another problem of the second-order gradient expansion. In contrast to the zeroth-order term in $T_s^{nad}[\rho_A,\rho_B]$, which is non-negative (see eq 14), the second-order term in $T_s^{nad}[\rho_A,\rho_B]$ is nonpositive (see eq 27 in ref 44). $T_s^{nad}[\rho_A,\rho_B]$ is non-negative for a large class of electron densities (see section 3.1), but the second-order gradient expansion provides always nonpositive contribution to $T_s^{nad}[\rho_A,\rho_B]$. Damping this term reduces the negative error in the total energy occurring when the second-order gradient expansion is used to approximate $T_s^{nad}[\rho_A,\rho_B]$.[44,110]

The desired features of the Perdew−Wang enhancement factor are (a) $F_T(x = 0) = 1$, which assures the correct homogeneous electron gas limit, (b) its quadratic growth at low values of $|\nabla\rho|/\rho^{4/3}$, and (c) the monotonic decrease to zero at large values of $|\nabla\rho|/\rho^{4/3}$ providing the desired damping factor if one of the densities is small.

This deficiency of the decomposable strategy to approximate $T_s^{nad}[\rho_A,\rho_B]$ stems from the so-called λ vs γ controversy[214] concerning the choice for the dominant contribution to the good approximation for $T_s[\rho]$, either the exact uniform electron gas expression, which is exact for the uniform electron gas, or the von Weizsäcker functional, which is exact expression for spin-compensated two-electron systems. The two functionals have completely different analytical forms. It is rather unlikely that the corresponding potentials obtained from them as functional derivatives have a similar error if evaluated at $\rho_A(\vec{r}) + \rho_B(\vec{r})$, $\rho_A(\vec{r})$, and $\rho_B(\vec{r})$ at a given point in space. An alternative strategy was proposed in ref 131 in which approximation for $T_s^{nad}[\rho_A,\rho_B]$ is constructed directly without approximating $T_s[\rho]$, i.e., without the intermediate step in eq 39. Targeting $T_s^{nad}[\rho_A,\rho_B]$ directly and not through approximations to of $T_s[\rho]$ makes it possible to build in the exact properties of this bifunctional in a straightforward way. For instance, the non-decomposable approximation using

DOI: 10.1021/cr500502v
Chem. Rev. 2015, 115, 5891−5928

second derivatives (NDSD) to $T_s^{nad}[\rho_A,\rho_B]$ introduced in ref 131 assures satisfying the exact condition for the nonadditive kinetic potential given in eq 29. The functional $\tilde{T}_s[\rho]$ corresponding to NDSD as in eq 39 does not exist.

$$T_s^{nad}[\rho_A, \rho_B] \approx \tilde{T}_s^{nad}[\rho_A, \rho_B] \tag{42}$$

Dedicated studies of approximations for the nonadditive kinetic energy functional[108,128,129,215] indicate that the simple GGA type of approximations are only applicably if the densities $\rho_A(\vec{r})$ and $\rho_B(\vec{r})$ are weakly overlapping. Trying to apply them in the case of covalent bonds using for any reasonably chosen $\rho_B(\vec{r})$ (or $\rho_B(\vec{r})$ optimized by means of the freeze-and-thaw procedure) lead usually to failure.[110,116,216] With increasing overlap between $\rho_A(\vec{r})$ and $\rho_B(\vec{r})$, the exact and approximated nonadditive kinetic potentials became qualitatively different if simple gradient-dependent functionals are used for $\tilde{T}_s^{nad}[\rho_A,\rho_B]$ as shown in model analytically solvable systems[48] and partitioned molecular densities.[215]

Compared to $T_s^{nad}[\rho_A,\rho_B]$, much less work has been devoted to approximations to the $E_{xc}^{nad}[\rho_A,\rho_B]$ functional. In the case of embedded noninteracting reference system[44] and semilocal approximations for the exchange-correlation functional, a separate approximation for $E_{xc}^{nad}[\rho_A,\rho_B]$ is, in principle, not needed. The Euler−Lagrange equation for the embedded wavefunction take the form of the Kohn−Sham equations for constrained electron density (eqs 20 and 21 in the original work of Wesolowski and Warshel[44]), which using the notation of the present work read

$$\left(-\frac{1}{2}\nabla^2 + v_A(\vec{r}) + \int \frac{\rho_A(\vec{r}')}{|\vec{r}' - \vec{r}|}\,d\vec{r}' + v_{xc}[\rho_A](\vec{r}) + v_{emb}[\rho_A, \rho_B, v_B](\vec{r})\right)\phi_i = \epsilon_i\phi_i \quad \text{for} \quad i = 1,\ N_A \tag{43}$$

The effective potential in eq 43

$$v_{eff}(\vec{r}) = v_A(\vec{r}) + \int \frac{\rho_A(\vec{r}')}{|\vec{r}' - \vec{r}|}\,d\vec{r}' + v_{xc}[\rho_A](\vec{r}) + v_{emb}[\rho_A, \rho_B, v_B](\vec{r}) \tag{44}$$

can be written equivalently as

$$v_{eff}(\vec{r}) = v_{AB}(\vec{r}) + \int \frac{\rho_A(\vec{r}') + \rho_B(\vec{r}')}{|\vec{r}' - \vec{r}|}\,d\vec{r}' + v_{xc}[\rho_A + \rho_B](\vec{r}) + \frac{\delta T_s^{nad}[\rho_A, \rho_B]}{\delta\rho_A(\vec{r})} \tag{45}$$

The functional for the exchange-correlation component of the effective potential in eq 45 ($v_{xc}[\rho_A + \rho_B](\vec{r})$) is the same for any pair of densities adding up to the same sum: $\rho_A(\vec{r}) + \rho_B(\vec{r})$. Also the corresponding expression for the total exchange-correlation energy depends on the total density $\rho_A(\vec{r}) + \rho_B(\vec{r})$ ($E_{xc}[\rho_A + \rho_B]$). Partitioning the total exchange-correlation energy in the exact version of the FDET equations (eqs 3−8) as well in the case of semilocal approximations for the exchange-correlation energy as in

$$E_{xc}[\rho_A + \rho_B] = E_{xc}[\rho_A] + E_{xc}[\rho_B] + E_{xc}^{nad}[\rho_A, \rho_B] \tag{46}$$

represents thus just rewriting them.

Different approximations for $E_{xc}[\rho_A]$ and $E_{xc}^{nad}[\rho_A,\rho_B]$ are needed if the functional for the exchange-correlation energy is not approximated by an explicit density functional but by an orbital-dependent expression, the case of generalized Kohn−Sham methods using orbital-dependent approximations.[217] In such a case the corresponding approximation for the total exchange-correlation energy is not available. As a consequence, different approximations for $E_{xc}[\rho_A]$ and $E_{xc}^{nad}[\rho_A,\rho_B]$ must be used

$$E_{xc}[\rho_A + \rho_B] \approx \tilde{E}_{xc}^{(a)}[\{\phi_i[\rho_A]\}] + \tilde{E}_{xc}^{(b)}[\rho_B] + \tilde{E}_{xc}^{nad(c)}[\rho_A, \rho_B] \tag{47}$$

The different approximations are indicated with (a), (b), and (c) in the above formula. The superscript a denotes any approximation for the exchange-correlation energy (including the orbital-dependent expressions), whereas c is used for an explicit expression for the nonadditive exchange-correlation energy. The approximation used for $\tilde{E}_{xc}^{(b)}[\rho_B]$ is not relevant for the present considerations because this term is constant in FDET.

The generalized version of eqs 43−45 for orbital-dependent approximations for the exchange-correlation energy was developed by Della Sala and collaborators.[82,132,218] The differential treatment of approximations for $E_{xc}[\rho_A]$and $E_{xc}^{nad}[\rho_A,\rho_B]$ can be also a pragmatic necessity even in the case of using only semilocal exchange-correlation functionals. For example, if the $E_{xc}[\rho_A]$ functional conjoint to the one used for $T_s^{nad}[\rho_A,\rho_B]$ (and/or the corresponding potentials) is not adequate to describe the properties of the isolated subsystem A or if the energy functional for the used potential does not exist as it is the case of the SAOP potential[219,220] (see ref 111).

The numerical evidence concerning environments of such embedded systems, which are not linked to the environment by covalent bonds but by weaker interactions, indicates that the results of FDET calculations depend significantly less on the choice made for the approximation to $E_{xc}^{nad}[\rho_A,\rho_B]$ than that for $T_s^{nad}[\rho_A,\rho_B]$.[175] It is worthwhile to underline that the proper asymptotic behavior of the dispersion interactions can be assured only by $E_{xc}^{nad}[\rho_A,\rho_B]$. Even exact $T_s^{nad}[\rho_A,\rho_B]$, not to mention the semilocal approximations, does not contribute to the energy if the overlap between $\rho_A(\vec{r})$ and $\rho_B(\vec{r})$ disappears (see section 2.2.6). In beyond-FDET embedding methods based on projectors, approximation for $T_s^{nad}[\rho_A,\rho_B]$ are not needed at all, but $E_{xc}^{nad}[\rho_A,\rho_B]$ must still be approximated (see the formula for the energy in section 2 of ref 96).

The quality of an approximation for $\tilde{T}_s^{nad}[\rho_A,\rho_B]$ can be easily tested in practice using any implementation of eqs 43−45. The procedure proposed by Wesolowski and Weber for this purpose[55] consists of the following elements: (a) the total electron density $\tilde{\rho}_{AB}$ and energy $\tilde{E}_o^{KS}$ obtained from reference Kohn−Sham calculations with some approximation for the exchange-correlation energy ($\tilde{E}_{xc}[\rho]$) and for a given basis set; (b) a pair of optimized densities for the two subsystems $\tilde{\rho}_A^{opt}(\vec{r})$ and $\tilde{\rho}_B^{opt}(\vec{r})$ optimized by means of the freeze-and-thaw optimization of electron densities of subsystems; (c) analysis of the differences between quantities obtained from reference Kohn−Sham- and subsystem DFT calculations. If technical parameters (grids, basis sets, and common exchange-correlation approximation) are the same in all calculations, any deviations from the reference results can be attributed only to the approximation used for the nonadditive kinetic energy.

DOI: 10.1021/cr500502v
Chem. Rev. 2015, 115, 5891−5928

As far as stage (c) is concerned, various analyses are possible for different purposes. The visual inspection of differences between reference Kohn−Sham and subsystem DFT densities ($\Delta\rho_{AB}(\vec{r}) = \tilde{\rho}_A^{opt}(\vec{r}) + \tilde{\rho}_B^{opt}(\vec{r}) - \tilde{\rho}_{AB}(\vec{r})$) in 3D reveals region in space where the tested approximation for the nonadditive kinetic potential is most deficient.[129] Differences of the dipole moments associated with $\tilde{\rho}_A^{opt}(\vec{r}) + \tilde{\rho}_B^{opt}(\vec{r})$ and $\tilde{\rho}_{AB}(\vec{r})$ reveal artificial charge flow between subsystems resulting from the errors in the nonadditive kinetic potential.[100] Differences between reference the Kohn−Sham and subsystem DFT energies are of the greatest practical interest and reflect both the errors in the used approximation for the nonadditive kinetic functional directly as well as the errors in the corresponding potential (its functional derivative). Finally, using Euclidean metrics for $\Delta\rho_{AB}(\vec{r})$ makes it possible to order the quality of approximations for the nonadditive kinetic potentials.[130] Other than Euclidean matrices can be used as a measure for $\Delta\rho_{AB}(\vec{r})$.[218,221]

The freeze-and-thaw calculations converge quickly if $\rho_A(\vec{r})$ and $\rho_B(\vec{r})$ exchange their roles in eq 43. They represent practical realization of subsystem DFT.[52] In contrast to the exact subsystem DFT formulation, in which such a pair is not unique (see the discussion in ref 60 or examples provided in refs 47 and 48), the use of approximations leads to an unique pair (see eq 38). If the same basis set (the same atomic basis functions and the same number of atomic centers in all calculations) is used in the reference Kohn−Sham calculations and in the freeze-and-thaw optimization of subsystem densities, the difference between $\tilde{\rho}_{AB}(\vec{r})$ and the sum $\tilde{\rho}_A^{opt}(\vec{r}) + \tilde{\rho}_B^{opt}(\vec{r})$ can be attributed to the accuracy of the used $((\delta\tilde{T}_s^{nad}[\rho_A,\rho_B])/(\delta\rho_A(\vec{r})))$. Due to the fact that the potential $((\delta\tilde{T}_s^{nad}[\rho_A,\rho_B])/(\delta\rho_A(\vec{r})))$ (and its error) is a local property the errors in the potential are not related to global properties such as energy, dipole moment, energy contributions, or the norm $|\tilde{\rho}_{AB}(\vec{r}) - \tilde{\rho}_A^{opt}(\vec{r}) - \tilde{\rho}_B^{opt}(\vec{r})|$, for instance. The dipole moments, the norm, or any total energy component besides the kinetic energy are especially useful because the difference between their deviations from the reference Kohn−Sham values are due to the errors in $((\delta\tilde{T}_s^{nad}[\rho_A,\rho_B])/(\delta\rho_A(\vec{r})))$. The difference between the total FDET energy evaluated at $\tilde{\rho}_A^{opt}(\vec{r})$ and $\tilde{\rho}_B^{opt}(\vec{r})$ and $\tilde{E}_0^{KS}$ can be attributed to two sources of error: that of $((\delta\tilde{T}_s^{nad}[\rho_A,\rho_B])/(\delta\rho_A(\vec{r})))$ which determines the quality of the electron density and that of $\tilde{T}_s^{nad}[\rho_A,\rho_B]$ which determines the errors in the energy.

The freeze-and-thaw optimization was subsequently used by us in studies of the accuracy of various decomposable approximations for $\tilde{T}_s^{nad}[\rho_A,\rho_B]$ of the GGA form[48,108,128−130] and the nondecomposable approximation[131] based on the asymptotic condition given on eq 29. The freeze-and-thaw optimization was performed to test approximations developed by Della Sala and collaborators[126,132,133] for $T_s[\rho]$. Jacob and Visscher used it in the benchmarking studies of approximations to $T_s^{nad}[\rho_A,\rho_B]$.[110,111]

4.1.2. Spin-Density Generalization of $T_s^{nad}[\rho_A,\rho_B]$. For any considered kinetic-energy functional defined for spin-compensated systems, the Oliver−Perdew spin-density generalization can be applied:[222]

$$T_s[\rho^{\uparrow}, \rho^{\downarrow}] = \frac{1}{2}(T_s[2\rho^{\uparrow}] + T_s[2\rho^{\downarrow}]) \tag{48}$$

The spin-density generalization of approximate functionals for the nonadditive kinetic energy is, therefore, straightforward[207] for any nondecomposable approximation for $T_s^{nad}[\rho_A,\rho_B]$ in order to obtain an approximate expression for $T_s^{nad}[\rho_A^{\uparrow},\rho_A^{\downarrow},\rho_B]$. In principle, the same can be made for $\rho_B(\vec{r})$. In practice, however, the choices for subsystems A and B are made usually in such a way that the environment is not spin-polarized.[37,117,207,223] Reference 224 provides an example of simulations in which this constraint on $\rho_B(\vec{r})$ was removed leading to mutual spin-polarization of subsystems.

4.1.3. Linearization of the Functionals $T_s^{nad}[\rho_A,\rho_B]$ and $E_{xc}^{nad}[\rho_A,\rho_B]$. The dependence of the FDET embedding potential (see eq 8) on $\rho_A(\vec{r})$ is an essential feature of FDET. Despite the simplicity of the embedding operator of the form of the FDET embedding potential, the nonlinear dependence of energy on $\rho_A(\vec{r})$ may result in strong modification of the algorithms used to solve eq 7, which were developed for methods where the external potential is density-independent. This inconvenient feature can be treated through expanding the functionals $T_s^{nad}[\rho_A,\rho_B]$ and $E_{xc}^{nad}[\rho_A,\rho_B]$ in $\Delta\rho_A(\vec{r}) = \rho_A(\vec{r}) - \rho_A^{ref}(\vec{r})$ and retaining only the linear term (linearization). Dulak and Wesolowski investigated numerically the adequacy of such an approximation for $\tilde{T}_s^{nad}[\rho_A,\rho_B]$[225] and for $\tilde{T}_s^{nad}[\rho_A,\rho_B]$ and $\tilde{E}_{xc}^{nad}[\rho_A,\rho_B]$ together[226] in the case of semilocal functionals. With linearized expression for the energy components, the FDET embedding potential is $\rho_A(\vec{r})$-independent and reads

$$\begin{aligned} v_{emb}[\rho_A, \rho_B, v_B](\vec{r}) &\approx \tilde{v}_{emb}[\rho_A^{lin}, \rho_B, v_B](\vec{r}) \\ &= v_B(\vec{r}) + \int \frac{\rho_B(\vec{r}')}{|\vec{r}' - \vec{r}|}\, d\vec{r}' + \left.\frac{\delta T_s^{nad}[\rho_A, \rho_B]}{\delta\rho_A(\vec{r})}\right|_{\rho_A(\vec{r})=\rho_A^{ref}(\vec{r})} \\ &\quad + \left.\frac{\delta E_{xc}^{nad}[\rho_A, \rho_B]}{\delta\rho_A(\vec{r})}\right|_{\rho_A(\vec{r})=\rho_A^{ref}(\vec{r})} \end{aligned} \tag{49}$$

where the functional $v_{emb}[\rho_A,\rho_B,v_B(\vec{r})]$ is evaluated at $\rho_A^{ref}(\vec{r})$ and not at the actual one $\rho_A(\vec{r})$.

Linearization of $T_s^{nad}[\rho_A,\rho_B]$ and $E_{xc}^{nad}[\rho_A,\rho_B]$[177] involves modification of the FDET expression for the total energy, into which $\rho_A^{ref}(\vec{r})$ enters in the way assuring self-consistency of the embedding potential, energy, and the embedded wavefunction

$$\begin{aligned} T_s^{nad}[\rho_A, \rho_B] &\approx T_s^{nad}[\rho_A^{ref}, \rho_B] \\ &\quad + \int (\rho_A - \rho_A^{ref}) \left.\frac{\delta T_s^{nad}[\rho_A, \rho_B]}{\delta\rho_A(\vec{r})}\right|_{\rho_A(\vec{r})=\rho_A^{ref}(\vec{r})} d\vec{r} \end{aligned} \tag{50}$$

$$\begin{aligned} E_{xc}^{nad}[\rho_A, \rho_B] &\approx E_{xc}^{nad}[\rho_A^{ref}, \rho_B] \\ &\quad + \int (\rho_A - \rho_A^{ref}) \left.\frac{\delta E_{xc}^{nad}[\rho_A, \rho_B]}{\delta\rho_A(\vec{r})}\right|_{\rho_A(\vec{r})=\rho_A^{ref}(\vec{r})} d\vec{r} \end{aligned} \tag{51}$$

We underline that, in most of the applications of FDET based methods, the environment interacts weakly with the embedded species. In such a case, the electrostatic terms, for which the corresponding density functionals are known exactly, are already linear in $\rho_A(\vec{r})$. The nonelectrostatic terms are usually approximated by means of semilocal approximations. The approximated nonadditive kinetic term in the potential is usually short-ranged and strongly repulsive if approximated using gradient-expansion type of functionals (see section 4.1.1) due to the overlap-dependent and strongly repulsive zeroth-order term (eq 14). In such situations, linearization can be expected to be a good practical solution.

In case of weakly bound intermolecular complexes, linearization of semilocal approximations for the functionals $T_s^{nad}[\rho_A,\rho_B]$

DOI: 10.1021/cr500502v
Chem. Rev. 2015, 115, 5891−5928

and $E_{xc}^{nad}[\rho_A,\rho_B]$ was shown to be a very efficient way of treating ρ_A-dependence of the embedding potential.[226] Fully self-consistent solutions of the approximate (semilocal functionals were used) version of eqs 3−8, were obtained using a quickly converging double-SCF procedure based on linearization.

Approximation given in eq 49 is frequently used as an a priori approximation in methods combining the FDET embedding potential with interacting Hamiltonians $\hat{H}_A$ used in eq 7.[57,58,118,157,175,180,209−211,213] Making the embedding potential ρ_A-independent simplifies greatly the numerical implementation. For ground-state calculations, it is a fully controllable approximation. The FDET embedding potential and the embedded wavefunction corresponding to the optimized $\rho_A(\vec{r})$ can be easily constructed by means of an iterative process,[57] which was shown to converge quickly in the case of weak interactions between the embedded species and the environment.[226] For excited-state calculations, however, linearization remains an approximation unless different $\rho_A^{ref}(\vec{r})$ are used for different electronic states (see section 3.2.2).

Finally, it is worthwhile to underline that in the case of linearization of the approximated functionals used for $T_s^{nad}[\rho_A,\rho_B]$ and $E_{xc}^{nad}[\rho_A,\rho_B]$, the corresponding energy components in eq 6 are given by neither

$$T_s^{nad}[\rho_A, \rho_B] \approx \tilde{T}_s^{nad}[\rho_A, \rho_B] \tag{52}$$

$$E_{xc}^{nad}[\rho_A, \rho_B] \approx \tilde{E}_{xc}^{nad}[\rho_A, \rho_B] \tag{53}$$

nor

$$T_s^{nad}[\rho_A, \rho_B] \approx \tilde{T}_s^{nad}[\rho_A^{ref}, \rho_B] \tag{54}$$

$$E_{xc}^{nad}[\rho_A, \rho_B] \approx \tilde{E}_{xc}^{nad}[\rho_A^{ref}, \rho_B] \tag{55}$$

because they are not consistent with the potential. The self-consistent expressions for the energy are obtained using the linearized approximations for the nonadditive functionals (eqs 50 and 51) in evaluation of the total energy (eq 6).

4.1.4. Embedding Potentials from Numerical Inversion Procedures. If the Kohn−Sham calculations for the total system using some approximate exchange-correlation functional are doable, the approximated nonadditive kinetic potential or even the whole FDET embedding potential can be obtained following the inversion strategy. The strategy relies on the unique correspondence between the Kohn−Sham potential ($v_s[\rho](\vec{r})$) and the ground-state density:[50]

$$\left(-\frac{1}{2}\nabla^2 + v_s[\rho](\vec{r})\right)\phi_i = \epsilon_i\phi_i \quad \text{with } \rho = \sum_{i=1}^{N} 2|\phi_i|^2 \tag{56}$$

where $2N$ is the number of electrons (the spin-compensated version of Kohn−Sham equations is given here for the sake of simplicity).

Note that $v_s[\rho](\vec{r})$ denotes the density functional (unique correspondence) and not the explicit expression for the Kohn−Sham effective potential. This correspondence can be applied for $\rho_A^{opt}(\vec{r})$, and for $\rho_A^{opt}(\vec{r}) + \rho_B(\vec{r})$ defined in eq 3, to obtain two potentials $v_s[\rho_A^{opt}](\vec{r})$ and $v_s[\rho_A^{opt} + \rho_B](\vec{r})$. On the other hand, Kohn−Sham formalism and FDET provide expressions for these potentials for a given external potential. The potential corresponding to $\rho_A^{opt}(\vec{r}) + \rho_B(\vec{r})$ is given in the Kohn−Sham theory and reads

$$v_s(\vec{r}) = v_{AB}(\vec{r}) + \int \frac{\rho_A^{opt}(\vec{r}) + \rho_B(\vec{r}')}{|\vec{r}' - \vec{r}|}\, d\vec{r}' + v_{xc}[\rho_A^{opt} + \rho_B](\vec{r}) \tag{57}$$

The functinal for the potential corresponding to $\rho_A^{opt}(\vec{r})$ is given in FDET and reads

$$v_s[\rho_A^{opt}](\vec{r}) = v_s[\rho_A^{opt} + \rho_B](\vec{r}) + \frac{\delta T_s^{nad}[\rho_A, \rho_B]}{\delta\rho_A(\vec{r})} \tag{58}$$

Note that eq 57 is an equation for functions and eq 58 is an equation for functionals. Once the potentials given in eqs 57 and 58 are available numerically, it is possible to evaluate $\delta T_s^{nad}[\rho_A,\rho_B]/\delta\rho_A(\vec{r})$ numerically as a difference without constructing approximations for the density functional $T_s^{nad}[\rho_A,\rho_B]$. Such construction is analytically possible only for some model systems.[47,48] Exact potentials are also available analytically for particularly partitioned (such that $\rho_A(\vec{r})$ integrates to 2) molecular densities obtained form Kohn−Sham calculations[215] using approximated exchange-correlation potential. Such constructions are useful for development of approximations and interpretations. For a more general case, the numerical inversion must be used in order to obtain at least one of the potentials given in eqs 57 and 58 numerically.

Unfortunately, procedures for the numerical inversion are not robust and do not lead to unique potentials if the finite basis sets are used.[227] Moreover, using a finite basis sets to obtain $\rho_A^{opt}(\vec{r}) + \rho_B(\vec{r})$ does not guarantee that the obtained density is pure-state noninteracting v-representable, i.e., whether the potential $v_s[\rho_A^{opt} + \rho_B](\vec{r})$ exists for this density.[137] The first generation of numerical inversion procedures such as the ones proposed by Zhao, Morrisson, and Parr[144] or by Gritsenko, van Leeuwen, and Baerends[228] were improved (see the methods by Wu and Yang[229] and by Jacob[230]).

With additional approximations (such as linearization, which makes the embedding potentials ρ_A-independent), the numerical inverted potentials can be used also for evaluation of the whole FDET embedding potential. Carter and collaborators introduced this strategy to develop local pseudopotentials for solids.[101] The numerical inversion methods for the FDET embedding potentials were further refined and applied by others.[81,116,231,232] The work of Fux et al.,[116] for instance, demonstrated that the numerical inversion strategy is much more efficient than using simple approximations for $\delta T_s^{nad}[\rho_A,\rho_B]/\delta\rho_A(\vec{r})$ for covalently bound environments.

4.2. Generation of $\rho_B(\vec{r})$

Most of the applications of FDET based simulation concern embedded species which are not linked with the environment by covalent bonds (molecules physisorbed at surfaces, molecules in clusters, guest molecules in guest−host complexes, etc.). In such cases, N_A and $v_A(\vec{r})$ are determined in a straightforward manner. As a consequence, N_B and $v_B(\vec{r})$ cannot be chosen freely because of the conditions $N_{AB} = N_A + N_B$ and $v_{AB}(\vec{r}) = v_A(\vec{r}) + v_B(\vec{r})$. The case when choosing N_A is ambiguous (if the charge-transfer between subsystem is possible, for instance), lies rather outside of the scope of FDET based methods, and will not be considered here. Methods such as those based on partition DFT (see section 3.1) should be considered instead. In practical FDET based calculations, even if N_B is fixed, $\rho_B(\vec{r})$ still must be generated. Freezing $\rho_B(\vec{r})$, which lies at the origin of the fact that FDET cannot yield the ground-state energy but its upper bound, is an additional approximation on top of the ones made in practice

DOI: 10.1021/cr500502v
Chem. Rev. 2015, 115, 5891−5928

concerning $T_s[\rho_A,\rho_B]$ and $E_{xc}[\rho_A,\rho_B]$, i.e., the universal approximations discussed in the previous section, and the treatment of correlation in $\hat{H}_A$. The strategy to generate $\rho_B(\vec{r})$ can be expected to be strongly system specific. As a consequence, many system-specific strategies to generate the frozen density are in use. Below we outline the major ones.

4.2.1. $\rho_B(\vec{r})$ As a Ground-State Density from the Quantum-Mechanical Calculations for the Whole Environment. The most straightforward strategy to generate $\rho_B(\vec{r})$ is to use some inexpensive quantum mechanical method to generate the ground-state density of the isolated subsystem B. Such strategy is especially suitable if the environment is not significantly polarizable such as in the case of embedding a species in a noble gas matrix.[207] This strategy is also applicable for polarizable environments due to the weak dependence of the FDET derived properties of the embedded species on variations of $\rho_B(\vec{r})$ as discussed in section 2.2.3 (see the examples for local excitations provided in ref 107). But generation of $\rho_B(\vec{r})$ by means of the quantum-mechanical calculations for the whole environment has some drawbacks. In the case of large environments, the computational effort to generate such $\rho_B(\vec{r})$ might be prohibitive. Moreover, obtaining self-consistent solutions using some inexpensive Kohn−Sham based calculation might be difficult.[233,234]

4.2.2. Superposition of Densities of Fragments. This method to generate $\rho_B(\vec{r})$ seems a natural choice for cases where conventional QM/MM type of calculations are applicable. Instead of additive pair potentials in QM/MM, superpositions of densities of fragments are used to generate $\rho_B(\vec{r})$ for FDET calculations. Such additive $\rho_B(\vec{r})$ is obtained as

$$\rho_B(\vec{r}) = \sum_{i=1}^{\mathrm{NfragB}} \rho_B^i(\vec{r}) \tag{59}$$

where NfragB is the number of fragments in the environment, $\rho_B^i(\vec{r})$ denotes the electron density of the isolated ith fragment. The superposition strategy was used in our original applications of FDET where the fragments were water molecules in the case of solvatation[160,235] or fragments of proteins.[236] The fragments in the above expression can be just atoms or ions (see refs 210 and 233, for instance), the whole molecules (see refs 114, 120, 180, 208, 209, 223, and 237 for instance), or parts of larger molecules (see refs 119 and 234 for instance). Equation 59 leads to linear scaling of the computational effort needed to generate $\rho_B(\vec{r})$ and can be expected to be a good approximation if the environment comprises weakly interacting species. In the case of chains formed by hydrogen-bonded molecules in the environment of the organic chromophore (7-hydroxyquinoline), neglecting the mutual polarization of the molecules in the chain (eq 59) affects the environment induced shifts in the excitation energies by up to 20%.[107,238] We notice that the density of each fragment used in the superposition might correspond not to the isolated fragment but to the fragment in a condensed phase. For instance, the magnitude of the dipole moment for the water molecule equals 1.85 D, whereas its liquid phase counterpart is about 40% larger.[239] Such effective densities of fragments were considered the FDET studies of solvatochromism,[240] in simulating dipole moment fluctuations in liquid water,[241] solvent effect on NMR shieldings,[119] for instance.

4.2.3. Optimized $\rho_B(\vec{r})$ from Subsystem DFT Calculations. Simultaneous optimization of $\rho_A(\vec{r})$ and $\rho_B(\vec{r})$ using the freeze-and-thaw procedure[55] leads to a unique optimized pair of densities if approximations are used for the nonadditive density functionals (see eq 38 in section 4.1). The uniqueness is the artifact due to the use of approximations for the nonadditive functionals in subsystem DFT.[52] Optimization of $\rho_B(\vec{r})$ in procedures such as freeze-and-thaw affects the FDET results through two indistinguishable factors: the physical effect of electronic polarization of the environment by the embedded species and maximization of the absolute error in the used approximation for the nonadditive kinetic energy (see the relevant discussion in section 4.1). Only in the extreme case of a charged/polar embedded species and highly polarizable environment, the former effect clearly dominates.[37,171] Optimization of $\rho_B(\vec{r})$ was shown to qualitatively improve results (bring them closer to experimental ones) in such cases as a charged (+3e) the embedded species (Ln^{3+}) in anionic environment (six Cl^- anions). The polarization of $\rho_B(\vec{r})$ by $\rho_A(\vec{r})$ leads to the increase of the environment induced property (the ligand-field splittings of f-levels) by about factor two.[171] In the case of biliverdin in anionic enzymatic pocket,[37] the use of not optimized $\rho_B(\vec{r})$ (taken from Kohn−Sham calculations for isolated environment) leads to qualitative wrong results. The effect of the environment on g-tensor is properly described with freeze-and-thaw optimized $\rho_B(\vec{r})$.

Optimization of $\rho_B(\vec{r})$ jeopardizes, however, the principal advantage of the embedding strategy, reduction of the quantum mechanical description level to only a small fragment of a larger system. Nevertheless, the freeze-and-thaw algorithm although introduced for the purpose of testing approximations to $T_s^{nad}[\rho_A,\rho_B]$ (see section 4.1) also can be useful in practical simulations (see section 5.6). For instance, in a preliminary stage of any large-scale simulation it can be applied to small model system to test the procedure to generate $\rho_B(\vec{r})$ or if optimization of $\rho_B(\vec{r})$ is doable.

4.2.4. Polarized $\rho_B(\vec{r})$. In cases where the electron density is expected to be strongly affected by the embedded species, taking into account the electronic polarization of the environment by the embedded species must be unavoidable despite the weak dependence of the FDET results on variations in $\rho_B(\vec{r})$.[107] Since optimization of both $\rho_A(\vec{r})$ and $\rho_B(\vec{r})$ in subsystem DFT, which can be achieved through the freeze-and-thaw iterations,[55] lacks clear physical interpretation (see section 2.2.3), it is rather more appropriate to use simplified techniques to take into effect the polarization of the environment by the embedded species. For instance, by adding the dominant component of the external electric field generated by the embedded species in the generation of $\rho_B(\vec{r})$.[171,172]

4.2.5. Average $\langle\rho_B\rangle(\vec{r})$ from Statistical Ensembles for Structurally Flexible Environments. In the approximate schemes based on FDET discussed so far, $\rho_B(\vec{r})$ has a quantum-mechanical origin. It was associated with some molecular system at a given geometry. Equations 3−8 admit wider choices for $\rho_B(\vec{r})$. FDET might be used as a basis for a truly multilevel strategy to evaluate the averaged effect of the solvent on molecular properties in which $\rho_B(\vec{r})$ is a statistically averaged electron density (denoted here with $\langle\rho_B\rangle(\vec{r})$). Equations 3−8 remain the same with $\rho_B(\vec{r})$ being replaced by the statistical ensemble averaged electron density, which is denoted with $\langle\rho_B\rangle(\vec{r})$ throughout this work and with $\langle v_B\rangle(\vec{r})$ being the ensemble averaged potential generated by the nuclei in the environment. Such use of FDET was introduced by Kaminski et al.[240] for studies of solvatchromism. Similarly to commonly used polarizable dielectric continuum models such as PCM[12] or COSMO,[13] $\langle\rho_B\rangle(\vec{r})$, it provides a continuum representation of

DOI: 10.1021/cr500502v
Chem. Rev. 2015, 115, 5891−5928

the solvent. In contrast to dielectric models, it takes into account the specific solvent−solute interactions in a statistical manner.

In principle, any method can be used to generate the average quantities $\langle\rho_B\rangle(\vec{r})$ and $\langle v_B\rangle(\vec{r})$. The most straightforward way is to use explicit atomic level simulation of the solvated system and average the needed quantities. Such an approach has been applied to average the electrostatic potential generated by the solvent[242,243] which can be seen as an approximate FDET method in which the last two terms of the FDET embedding potential (eq 8) are completely neglected. Yet another procedure to obtain these average quantities was applied in refs 240 and 244. The procedure is based on classical statistical mechanics theory of liquids. In the first step, the 3D-RISM equations[245] with Hirata-Kovalenko closure[246] are used to obtain the site probabilities, i.e., the probability of finding a particular atom in a given volume element which is a function in R^3. In the next step, $\langle\rho_B\rangle(\vec{r})$ is obtained as a sum of contributions due to each type of atom in the system. $\langle\rho_B\rangle(\vec{r})$ and eqs 3−8 are coupled in a self-consistent manner. The 3D-RISM site probabilities depend on the net charges on atoms of the embedded species, i.e., on $\rho_A(\vec{r})$, whereas the embedded density depends on $\langle\rho_B\rangle(\vec{r})$ through the ρ_B dependency of the embedding potential. In practical calculations, assuring the self-consistency between these quantities might be numerically unstable[240] due to lack of uniqueness in casting electron density of the solvated chromophore in the form of atomic point charges. The problem can be expected to aggravate in the case of emission due to large charge delocalization of the electron density and possible large solvent effect on the geometry of the chromophore in excited state. Recently, we proposed a simplified treatment of self-consistency of charge distribution.[247]

4.2.6. 3-FDE Scheme. Jacob and Visscher[221] proposed a pragmatic approach to handle the systems where the embedded species is linked with the environment with covalent bonds. To avoid using approximations for the nonadditive kinetic energy functional at strongly overlapping pairs densities, a buffer zone comprising capping atoms with the corresponding third component of the total density was introduced. In the 3-FDE calculations, the two weakly overlapping subsystem densities are optimized by means of the conventional freeze-and-thaw procedure while keeping the capping density fixed. The advantages of such treatment of a covalently bonded environment were demonstrated in the case of proteins with sulfide bonds and charged side chains.[221,248]

4.3. FDET-Like Approximate Methods Based on the ONIOM Strategy

The ONIOM strategy introduced by Morokuma and collaborators[56] relies on the following Ansatz for the total energy of the whole system using two different approximate methods

$$E_{AB} \approx E_{AB}^{ONIOM} = E_{AB}^{method_I} + E_{A}^{method_{II}} - E_{A}^{method_I} \tag{60}$$

where the method of the lower quality ($method_I$) can be applied to the whole system and that of the higher quality ($method_{II}$) only to the embedded part.

Upon introducing the quantity $E_{AB}^{int} = E_{AB}^{method_I} - E_{A}^{method_I} - E_{B}^{method_I}$, eq 60 takes an alternative form

$$E_{AB}^{ONIOM} = E_{A}^{method_{II}} + E_{AB}^{int} + E_{B}^{method_I} \tag{61}$$

which shows that ideal systems for the ONIOM Ansatz are such where the lower quality method provides adequate interaction energies.

FDET embedding potential is sometimes introduced in the literature as the functional derivative of the E_{AB}^{int} in the ONIOM expression for the total energy (see the recent review by Severo Pereira Gomes and Jacob,[62] for instance). In the original work by Carter and collaborators,[57] the ONIOM Ansatz was used to introduce the first combination of the approximated FDET embedding potential with interacting Hamiltonian for $\hat{H}_A$. Since both FDET and ONIOM approaches to multilevel simulations hinge on approximations, the differences between them might appear to be of technical nature. In fact, the differences between the ONIOM strategy and the methods based on FDET concern the underlying principles and interpretation of the obtained quantities.

4.3.1. Independent variables. The pair of densities $\rho_A(\vec{r})$ and $\rho_B(\vec{r})$ is needed to evaluate the FDET embedding potential (eq 8). Equation 61 implies that only the density $\rho_A(\vec{r})$ and the total density $\rho_{AB}(\vec{r})$ are available in ONIOM. This pair of densities is considered as independent variables[57,58] and not $\rho_A(\vec{r})$ and $\rho_B(\vec{r})$ as in the FDET case. $\rho_B(\vec{r})$ is not directly available in ONIOM type of calculations. The quantities

$$\tilde{\rho}_B(\vec{r}) = \rho_{AB}^{method_I}(\vec{r}) - \rho_{A}^{method_I}(\vec{r}) \tag{62}$$

and

$$\tilde{\rho}_B(\vec{r}) = \rho_{AB}^{method_I}(\vec{r}) - \rho_{A}^{method_{II}}(\vec{r}) \tag{63}$$

might not be even N-representable. No constraint assures that these functions are non-negative. So they cannot be used in eq 8 without additional approximations concerning either $\rho_A(\vec{r})$ or $\rho_B(\vec{r})$. For instance, in the methods proposed in ref 57, the embedding potential was calculated at a fixed total density (obtained from Kohn−Sham calculations for the total system) whereas $\rho_A(\vec{r})$ varied during the optimization. The corresponding $\rho_B(\vec{r})$ was not available. Due to the fact that the three quantities $\rho_A(\vec{r})$, $\rho_B(\vec{r})$, and $\rho_{AB}(\vec{r})$ such that $\rho_{AB}(\vec{r}) = \rho_A(\vec{r}) + \rho_B(\vec{r})$ are not available in ONIOM calculations, further approximations must be made concerning the densities used in the evaluation of the embedding potential.

4.3.2. The total ONIOM electron density. Despite the availability of the electron density $\rho_A(\vec{r})$ obtained from the higher-level calculations, the total density of the whole system has the quality determined by of the low-level method $\rho_{AB}^{method_I}(\vec{r})$. The *ONIOM* Ansatz made for the total energy (eq 60) cannot be applied for the total density. The quantity

$$\tilde{\rho}_{AB}(\vec{r}) = \rho_{AB}^{method_I}(\vec{r}) + \rho_{A}^{method_{II}}(\vec{r}) - \rho_{A}^{method_I}(\vec{r}) \tag{64}$$

cannot be interpreted as the electron density of the total system because it might not be N-representable.

4.3.3. The embedded wavefunction in FDET vs the ONIOM wavefunction. In ONIOM calculations, the embedding potential is usually made ρ_A-independent in the procedure to obtain the embedded wavefunction (see point (a)). It is evaluated at some fixed density $\rho_A^{ref}(\vec{r})$ instead of using the actual density $\rho_A(\vec{r})$ corresponding to the embedded wavefunction[57,180] (see section 4.1.3). Such ρ_A-independent embedding potential is just an addition to usual external potential for isolated subsystem A. For each electronic state, the ONIOM wavefunction is, therefore, a legitimate one for evaluation the expectation value of any quantum operator. The use of the embedded FDET wavefunction lacks such justification except for one-particle operators. From the start, it is just an auxiliary object used to optimize the embedded density.

DOI: 10.1021/cr500502v
Chem. Rev. 2015, 115, 5891−5928

4.3.4. The total energy of the whole system in exact case. In contrast to the issues discussed above, the exact FDET (exact density functionals) and exact ONIOM (exact method$_{II}$) are not available in practice. For the purpose of improving the existing approximate methods, it is worthwhile to consider how the two strategies behave at the exact limits. With the exact functionals, FDET energy never falls below the exact total energy regardless the choice of $\rho_B(\vec{r})$. In the case of ONIOM, even if the full CI calculations were used as method$_{II}$, the total energy given in eq 60 might lie above or below the exact one depending on the choice made for method$_I$. If the environment disappears, FDET energy converges toward the exact energy of subsystem A regardless the form of the embedded wavefunction whereas the ONIOM energy reaches the same limit only if full CI is used as method$_{II}$. In the absence of the environment, the FDET energy expression represents just another formulation of DFT which uses limited number of determinants to represent the reference system (one in case of Kohn−Sham formulation of DFT and more than one in formulations of DFT based on artificial reference system constructed with a limited number of determinants[77]). For this reason, the $\Delta F^{SC}[\rho_A]$ term (see eq 10) of the FDET expression for the total energy functional is not considered in ONIOM calculations using correlated methods as method$_{II}$.

4.3.5. Variational principle. ONIOM calculations can combine any pair of approximated methods. FDET, on the other hand, is based on the Euler−Lagrange equations, and it is formulated only for such methods where the embedded wavefunction is obtained from variational calculations.

5. NUMERICAL SIMULATIONS USING APPROXIMATED FDET EMBEDDING POTENTIALS

The present section provides an overview of numerical simulations based on various formal frameworks sharing the use of the local embedding potential of the FDET form (eq 8). Most of the reviewed applications concern the straightforward application of eqs 3−8 in their approximated version. In eqs 5−8, the functionals $T_s^{nad}[\rho_A,\rho_B]$ and $E_{xc}^{nad}[\rho_A,\rho_B]$ are replaced by their approximated counterparts ($\tilde{T}_s^{nad}[\rho_A,\rho_B]$ and $\tilde{E}_{xc}^{nad}[\rho_A,\rho_B]$) and are used for some $\rho_B(\vec{r})$ generated in a procedure chosen by the user. Besides such simulations, we include also applications of several beyond-FDET formalisms sharing with FDET the used of the local embedding potential of the form given in eq 8. They include (a) extensions of FDET to evaluate properties beyond energy and density using quantities obtained from eqs 5−8 (for excitation energies[182] and NMR chemical shifts,[115] for instance); (b) alternative formulations of DFT such as subsystem DFT[52] or partition DFT[53,54]), in which the environment density is also optimized owing to the use of other descriptors than just $\rho_B(\vec{r})$; (c) alternative formulations of LR-TDDFT based on subsystems;[113,152−154] and (d) approximate methods based on the ONIOM Ansatz, in which the basic variables are not $\rho_A(\vec{r})$ and $\rho_B(\vec{r})$ but $\rho_A(\vec{r})$ and the total density.[57,58] The present section is an attempt to summarize the current stage of applications of the approximated FDET embedding potential in numerical simulations. It focuses on properties rather than the used methods and approximations.

5.1. Electronic Excitations

5.1.1. Solvatochromism. The computational advantages of the embedding strategy manifest themselves most evidently in modeling solvatochromism. The structural flexibility of the solvent in a finite temperature results in fluctuations of the instantaneous contribution of the solvent to the excitation energy of the chromophore. Simulating the shape of the absorption or emission bands and even calculation of solvatochromic shifts involves thus repetitive calculations of excitation energies for a statistical ensemble of structures.

Neugebauer et al. pioneered the use of the FDET embedding potential in LR-TDDFT based simulations of solvated chromophores.[208] The solvatochromic shift in the lowest $n \rightarrow \pi^*$ transition in hydrated acetone was investigated. The excitation energies were evaluated for hundreds of instantaneous geometries taken from classical and Car−Parrinello[249] molecular dynamics simulations. Two principal computational advantages of the FDET/LR-TDDFT calculations over the conventional LR-TDDFT treatment of the whole system were demonstrated: (a) a great reduction of the computational effort (the time-consuming LR-TDDFT calculations are only carried in embedded region) and (b) simplicity in the analysis and interpretation of the results (the removal of spurious solvent−solute charge-transfer excitations due the approximations in exchange-correlation potential and the corresponding kernel). The subsequent application of the same FDET/LR-TDDFT method[109] concerned the solvatochromism of aminocoumarin C151 in polar (water) and nonpolar (*n*-hexane) solvents. The shifts of the absorption maximum corresponding to the $\pi \rightarrow \pi^*$ band shapes of UV−vis absorption spectra were evaluated using up to 400 instantaneous geometries for large model of the solvent consisting of up to 300 molecules. The experimental shift between *n*-hexane and water as solvents (−0.22 eV) was qualitatively reproduced (−0.08 eV) even using the simplest approximation for $\rho_B(\vec{r})$ (all solvent molecules were frozen and mutual polarization among them were neglected). Changing the partitioning of the cluster and including the nearest solvent molecules into $\rho_A(\vec{r})$ resulted in the improvement of the calculated shift bringing it to −0.17 eV.

Concerning the comparison of FDET with other embedding methods, Jacob et al.[114] simulated the lowest excitation energy of a water molecule in a cluster (up to 127 water molecules) using both FDET/LR-TDDFT and discrete reaction field (DRF) model.[105,250,251] The results of the two types of embedding calculations were compared with the ones of reference LR-TDDFT calculations for the whole cluster. For water-cluster-induced shift in the lowest excitation energy of the isolated water molecule, the FDET/LR-TDDFT result (0.54 eV) was closer than the DRF result (0.32 eV) to the reference one (0.67 eV).

Kaminski et al.[240] introduced an alternative strategy to simulate the solvatochromic shifts in absorption without modeling explicitly the absorption band shapes. FDET/LR-TDDFT calculations were solved using the ensemble averaged solvent density $\langle\rho_B\rangle(\vec{r})$ derived from classical statistical mechanics based model of the solvent (see section 4.2.5). The obtained numerical results for four chromophores (acetone, aminocoumarin 151, acrolein, or benzophenone) in four solvents (water, methanol, diethyl ether, or *n*-hexane) are very encouraging. Most of the calculated shifts in lowest-lying excitations and their experimental counterpart were in excellent agreement (within 0.03 eV). Using the same methodology, Zhou et al.[244] modeled the shifts in the $\pi \rightarrow \pi^*$ absorption band of coumarin 153 in nine solvents of different polarity. The deviations between the calculated and measured solvatochromic shifts within a narrow range (0.02 eV) demonstrate the strength of the proposed strategy to treat the solvent in FDET/LR-TDDFT. Applications of the same strategy for solvatochromic shifts in emission involves additional practical issue, coupling

DOI: 10.1021/cr500502v
Chem. Rev. 2015, 115, 5891−5928

between the electronic state of the embedded species and the averaged electron density of the environment $\langle\rho_B\rangle(\vec{r})$. Whereas the effect of $\langle\rho_B\rangle(\vec{r})$ on $\rho_A(\vec{r})$ is taken into account in the FDET embedding potential explicitly, modeling the opposite effect involves additional approximations which were analyzed by Shedge and Wesolowski[247] using coumarin 153 in various solvents of different polarity as a test case. The quality of the solvatochromic shifts in emission obtained using the proposed approximations was very good but slightly worse than that found for the solvatochromic shifts in absorption. The deviations of the calculated solvatochromic shifts in emission from experimental values were within 0.05 eV.

The environment induced shifts in excitation energies are often calculated for smaller systems in order to test the approximations and methods for use in full scale simulations. In such cases, the quality of the obtained results is not discussed using experimental data as a reference but the results of other calculations. A number of such studies applying approximated FDET embedding potentials were reported in the literature. Daday et al.[175,176] used several solvated systems (*p*-nitroaniline, acrolein, methylenecyclopropene, or *p*-nitrophenolate in various solvents). The optimization of $\rho_B(\vec{r})$ for different electronic states of the embedded chromophore was discussed in detail and interpreted as "state-specificity". We bring to the readers attention that the state-specificity is an inherent feature of the FDET embedding potential and it is associated with the $\rho_A(\vec{r})$ -dependence (see eq 8). The authors estimated also the effect of changing $\rho_A(\vec{r})$ on the embedding potential and found it negligible as compared with that due to optimization of $\rho_B(\vec{r})$. In view of the fact discussed in sections 2.2.3 and 2.2.4 indicating the unphysical origin of partitioning of the total density obtained in approximate subsystem DFT calculations, the relative importance of the $\rho_A(\vec{r})$ and $\rho_B(\vec{r})$ dependency cannot be interpreted in the straightforward manner. The FDET/LR-TDDFT study by Humbert-Droz et al.[107] revealed a very weak dependence of the excitation energy shifts on $\rho_B(\vec{r})$ for various embedded chromophores: keto-7-hydroxy-4-methylcoumarin in four water molecules, P-nitro aniline solvated by six water molecules, and 4-hydroxybenzylidene-2,3-dimethylimidazolinone anion in 50 water molecules. These studies indicate a need for more dedicated studies on this issue.

Höfener et al.[180,211,252] studied the solvatochromic shift in hydrated uracil for testing the proposed method using coupled cluster calculations combined with linearized FDET embedding potential.

5.1.2. Chromophores in Biological Environments. The simulation of chromophores in biological environments is another area of applicability of multilevel simulations such as the ones based on FDET. Even if the environment is static, i.e., represented by means of a fixed geometry, the huge size of biological macromolecules makes supermolecular strategy impractical. Wesolowski introduced the method for treatment of local electronic excitations embedded in a frozen density combining the FDET and LR-TDDFT framework. The strengths of such combination (FDET/LR-TDDFT)[182] were demonstrated for the low lying local excitations in hydrogen-bonded nucleobases in their classical Watson–Crick geometries. The calculations showed that the complexation induced shifts in the excitation energies is a result of a subtle balance between long-range electrostatic effect and the short-ranged intermolecular Pauli repulsion.

Neugebauer[234] investigated a more complicated biological system, the light-harvesting complex 2 of the purple bacterium *Rhodopseudomonas acidophila*. The shift in site energy (the excitation energies of individual pigments in their binding pocket of a protein-pigment complex) of the chromophore in induced by protein environment were evaluated using the FDET/LR-TDDFT calculations (called "uncoupled FDE" or "FDEu" there). Since the studied system comprises several chromophores, treating each of them as one embedded system FDET/LR-TDDFT is not adequate. The shifts in the absorption bands due to chromophore–chromophore couplings were evaluated by means of the beyond-FDET approach of Neugebauer (coupled FDE or FDEc;[153] see section 3.3).

Neugebauer et al.[118] studied the spectroscopic properties (absorption, circular dichroism, and nuclear magnetic resonance spectra) of another biological system, carotenoid astaxanthin in crustacyanin protein that occur in the shell of the lobster *Hommarus gammarus*, using both FDET/LR-TDDFT calculations and FDEc methods. Several possible mechanisms proposed in the literature for the observed bathochromic shift (more than 0.5 eV) in the absorption spectrum of astaxanthin in crustacyanin were analyzed.

Goez et al.[253] calculated also the excitation energies of Fenna–Matthews–Olson pigment–protein complex for testing the performance of the 3-FDE scheme (see section 4.2.6) to deal with deficiencies of the approximated FDET potentials in the case of covalently bound environments.

Zhou et al.[254] studied the lowest $\pi \rightarrow \pi^*$ excitations of retinal in rhodopsin and three visual cone pigments by means of the FDET/LR-TDDFT calculations. Based on the analysis of the factors determining the spectral shifts, models of mutated rhodopsin with fine-tunned spectral properties were proposed.

5.1.3. Local Excitations in Solid-State Environments. Klüner et al.[179,255] introduced the method combining the approximated FDET embedding potential with interacting Hamiltonians for embedded species and applied it to study excited states of the carbon monoxide molecule adsorbed on a Pd(111) surface. The CO/Pd_n (for $n = 3$ or 6) cluster was treated as embedded system, for which the interacting Hamiltonian was used (either Hartree–Fock, MPn, CASSCF, or CI). A significant effect of the crystal environment (about 5.1 eV) on the vertical excitation energy of the $^1(5\sigma/1\vec{\pi}\ 2\pi^*)$ transition in CO was found.

A single magnetic adatom Co on the Cu(111) surface, which is a strongly correlated system exhibiting the Kondo effect, was studied with similar methods for CO/Pd(111) by Huang et al.[256] Although the main interest of this study was in the Kondo ground state, the low-lying excited states of Co/Cu_n (for $n = 3$ or 7) cluster embedded in periodic crystal environment were also studied using methods combining either CASSCF or multireference singles-and-doubles configuration interaction (MRSDCI) levels of description with an approximated FDET embedding potential. It was found that the embedding potential affects the low-lying excited states of adsorbed Co atom by up to 1.42 eV.

Huang et al.[257] also studied the excited states of this Co/Cu(111) system, but the used methods were slightly different from the ones used in previous studies.[179,255,256] The applied method uses nonlocal embedding operator which puts it beyond the formal framework of FDET.

Kanan et al.[258] investigated the excited states of MgO crystal using cluster models Mg_nO_n ($n = 2$ or 4) embedded in a MgO supercell which generated an approximated FDET embedding potential. For the ground state the cluster was described by means of a CASSCF whereas CASSCF or other correlated

DOI: 10.1021/cr500502v
Chem. Rev. 2015, 115, 5891–5928

methods (CASPT2 or MRSDCI) was used for the excited state. It was found that the quality of the calculated band gap lies between that from standard periodic DFT method and that from more expensive Green's function methods.

Libisch et al.[259,260] studied the hot-electron-induced dissociation of H_2 on gold surface, Au(111), by calculating the ground-state and excitation-energy potential-energy surface using an approximated FDET embedding potential for the H_2/Au_{12} cluster carved from the (111) surface of Au. The embedded cluster was described by means of CASSCF for ground state and CIS for excited state. The dissociation barrier on the excited state potential energy surface was found lower than that for the ground state.

A simplified ligand-filed type of model using the FDET embedding potential was used to calculate the ligand field splitting energies for lanthanides (Ln^{3+}) in octahedral environment by Zbiri et al.[172,261] The calculated splittings agreed very well with experiments: the splitting between the $a_{2u}-t_{2u}$ levels oscillated around experimental values for the whole lanthanide series, whereas the splitting between the $a_{2u}-t_{1u}$ levels were systematically underestimated by about 25%. Moreover, the calculations allowed to determine the role of different factors affecting the splitting parameters such as electronic polarization of the environment by the embedded cation, orbital localization, and Pauli repulsion.

Gomes et al.[209] investigated the f–f spectrum of a NpO_2^{2+} impurity in a $Cs_2UO_2Cl_4$ crystal. The embedded region (NpO_2^{2+} or $NpO_2Cl_4^{2-}$) was described by means of the interacting Hamiltonian of the intermediate Hamiltonian Fock-space coupled-cluster method (IHFSCC).[262−264] The effect of crystal environment on the cluster was decomposed into two parts. A intermediate region (20 $UO_2Cl_4^{2-}$ and 90 Cs^+) surrounding the embedded cluster was described by the approximated FDET embedding potential and the component due to the remaining crystal was represented by means of a Madelung potential. The method introduced in ref 209 was subsequently applied by Tecmer et al.[213] for the f–f transitions in the CUO molecule embedded with noble gas matrices and Gomes et al.[210] to study the f–f transitions in UO_2^{2+} (uranyl cation) in a $Cs_2UO_2Cl_4$ crystal, with embedded region also described by means of the IHFSCC method.

Optical and ESR properties of Mn^{2+} impurity in doped cubic fluoroperovskites AMF_3 (for A = K or Rb and M = Mg, Zn, and Cd) were investigated using the FDET embedding potential by García-Lastra et al.[203] in order to determine the local structure of the environment which is consistent with spectroscopic data.

5.1.4. Induced Circular Dichroism in Guest–Host Complexes. Neugebauer and Baerends[123] applied FDET/LR-TDDFT calculations for simulation of induced circular dichroism (ICD) spectra and optical rotatory strength of a nonchiral molecule forming the complex with a chiral one, benzoic acid-amphetamin complex for instance, ferrocenecarboxylic acid crown ether complexed with L-leucine and phenol in β-cyclodextrin. ICD spectra obtained from FDET resembled closely the reference ones which were obtained by means of conventional Kohn–Sham calculations for the whole system. The calculations showed that the FDET/LR-TDDFT methods represent an efficient tool for modeling of ICD spectra of nonchiral compounds due to their ability to treat large systems. However, the FDET/LR-TDDFT calculations which neglect the dynamic response of the environment (see section 3.2.3) are not applicable if the embedded species and the environment absorb in the same spectral range (coupled excitation; see sections 3.3 and 5.1.5). Such a situation was reported in the case of excitonic coupling in the CD spectra and its intensities for the astraxanthin dimer in β-crustacyanin proteins.[118]

5.1.5. Coupled Chromophores and Charge-Transfer Excitations from Excited-State Subsystem DFT. In the study case of the benzaldehyde dimer,[153] Neugebauer presented a clear case of failure of FDET/LR-TDDFT calculations and proposed a solution through going beyond NDRE. This was achieved by means of other then $\rho_B(\vec{r})$ descriptors for the environment, which was treated and the on the same footing as the embedded species. The dynamic response of the environment is possible and results in couplings between excited states is necessary. Such coupling is indispensable if the environment and the embedded species absorb at similar frequencies. The reported FDEc excitation energies for short distances between the chromophores were qualitative better than the ones derived within NDRE approximation (i.e., FDET/LR-TDDFT or "uncoupled FDE" as they are referred to in the works by Neugebauer). Many successful applications of FDEc followed.

Neugebauer and collaborators investigated excitonic coupling in the CD spectra and its intensities for the astraxanthin dimer in β-crustacyanin proteins.[118] The astraxanthin molecule shows bathochromic shift in absorption spectra on complexation with crustacyanin protein. The prominent effects responsible for the shift are a point of debate. Experimental observations indicate the excitonic coupling, which show couplet like signatures in the CD spectra. Thus, the aim of the study reported in ref 118 was to investigate the role of these effects on observed shift. The strength of the FDEc methods lies in its ability to take into account the coupling effect and, at same time, to treat large systems efficiently. The FDEc simulated CD spectra were consistent with experiment observations.

König et al.[204] calculated the absorption spectra of the Fenna–Matthews–Olson pigment–protein complex, using FDET/LR-TDDFT and FDEc calculations. The study concerned the structural and environmental effects on the site energy, excitonic couplings, and UV–vis absorption spectra. The largest model constructed for the entire protein-pigment network contained more than 7000 atoms. It was found that the site energies were quite sensitive to structural and environmental changes in the model setup, but excitonic couplings were more robust.

Neugebauer and Mennucci reported the first study using the FDEc method to study charge-transfer excitation in a perylene dimer in water.[155] The comparison was made with the results obtained using polarizable QM/MM calculations and demonstrated that the both FDET and empirical QM/MM models describe the long-range screening adequately.

Pavanello et al.[157] used embedded wavefunctions obtained form subsystem DFT calculations to evaluate the coupling terms in empirical Hamiltonian describing charge-transfer states excitation energies isolated molecular clusters (water dimer, ethylene dimer, and π-stacked nucleobases). The obtained excitation energies agreed very well with reference CASPT2 results. The developed methodology (referred to as FDE-ET) was then applied for larger clusters used as the model of the liquid. More recently, the developed methodology for charge-transfer excitations was applied in the following complexes: ethylene dimer, ethylene-tetrafluoroethylene, NH_3-F_2, and X-tertacyanoethylene (for X = benzene, toluene, *o*-oxylene, and naphtalene).[265]

DOI: 10.1021/cr500502v
Chem. Rev. 2015, 115, 5891−5928

5.2. NMR

Jacob and Vischer[115] extended the FDET framework for evaluation of the nonrelativistic NMR shieldings. The use of the FDET for this purpose is not straightforward because the functional for the nonadditive kinetic energy depends not only on the pair of electron densities but on the two components of the total paramagnetic current. In the provided numerical examples, however, this dependence was neglected. The developed method was tested for calculation of the nitrogen shielding of acetonitrile in several solvents: water, chloroform, cyclohexane, and benzene, represented as clusters. The calculated solvent induced shift of the sheldings were in good agreement with the reference results obtained using Kohn–Sham calculations for the whole cluster (the differences between the shieldings obtained in embedding and supermolecular calculations amounted to about 2 ppm). Bulo et al.[120] applied the method introduced by Jacob and Visscher for more realistic models of the solvent (cyclohexane, chloroform, or water). The large set of conformations for the solvated acetonitrile represented by means of a molecular cluster was taken from either classical molecular dynamic and Car–Parrinello molecular dynamic simulations Car–Parrinello.[249] The differential effect of the two solvents (water and cyclohexane) observed experimentally (19.7 ppm) was reasonably well reproduced (20.8 ppm). The differential solvent effect of cyclohexane and chloroform was, however, underestimated in the simulations. In the case of the chloroform, the average solvent effect was shown to depend on the conformations used. Whereas using the instantaneous geometries from classical simulations led to underestimation of the effect of chloroform compared to cyclohexane (3.5 ppm), using the structures from Car–Parrinello trajectories for the averaging improved the result (11.6 ppm) bringing it closer to the experimental value of 8.8 ppm. Implementation of new procedures to generate the density $\rho_B(\vec{r})$ for FDET calculations by Jacob et al.[237] facilitated treatment of large environment efficiently. The NMR shieldings for water in the liquid phase were evaluated to test the new procedures and the implementation.

Recently, the FDET based approach introduced for NMR shieldings was generalized for calculation of nuclear spin–spin coupling constants.[119] In addition to approximations used in the evaluation of NMR shieldings, the contribution of environment to spin magnetization density was also neglected. The method was applied to evaluate the environment induced effect on the NMR coupling constants (ΔJ) in hydrogen bonded dimers, water clusters, and complexes of Hg CH_3X (for X = Cl, I, and Br) with dimethyl sulfoxide. Several ways to obtain the frozen density were considered. $\rho_B(\vec{r})$ was the density of the isolated environment, freeze-and-thaw optimized density of the entire system, or superposition of densities of fragments (either isolated or freeze-and-thaw optimized). FDET simulations reproduced 94% (for NH_3–H_2O) and 78% (for H_2O) of the effect of the environment on the shieldings obtained from reference Kohn–Sham calculations for the whole system. Unlike the case of the water dimer, the FDET calculations underestimated the environment effect on the coupling constants for hydrogen bonded hydrogen fluoride dimer (Δ^1J(F,H) for hydrogen bond donor subsystem, 5.7 Hz vs 17.9 Hz obtained from reference Kohn–Sham calculations for the whole system. In case of strongly interacting complexes of $HgCH_3X$ (for X = Cl, I, and Br) with dimethyl sulfoxide, FDET calculations recovered only from 67% to 79% of the environment effect on the coupling constants. This underestimation was attributed to the inability of the used approximations in FDET to describe solvent-to-metal charge donation. The tested approximations in FDET were applied to evaluate the solvent effect on the coupling constants in larger system consisting of 17 molecules. A good agreement with the environment induced shifts in coupling constants obtained from reference Kohn–Sham calculations for the whole cluster was reported (Δ^1J(O,H) and Δ^1J(O,H′) is 14.4 Hz) even using nonoptimized $\rho_B(\vec{r})$ in FDET: −15.0 Hz and −14.2 Hz for Δ^1J(O,H) and Δ^1J(O,H′), respectively. The freeze-and-thaw optimization of $\rho_B(\vec{r})$ improved the agreement even further.

5.3. ESR

Density functional theory based methods have been successfully applied for deriving the hyperfine structure parameters (g-tensor and isotropic hyperfine coupling constants) and hyperfine structures of radicals (for review, see refs 266–268). Accurate determination of the hyperfine coupling parameters require good description of electronic correlation and sever criteria for the basis set completeness. Compared to conventional post-SCF ab initio methods, the DFT calculations make it possible to include electron correlation effects on spin density at lower computational cost and rapid convergence with basis set. But for large systems, even DFT based calculations for the whole system, which are adequate for evaluation of ESR properties, are practically impossible. In such cases embedding strategy is a good alternative especially if the spin-density is known in advance to be localized in a smaller part of a larger system. FDET based embedding methods are particularly suitable for such applications due to the fact that the FDET embedding potential, which determines the spin density of the embedded species, comprises also the nonelectrostatic components.

The spin-polarized version of FDET was introduced in ref 207 and used to calculate isotropic hyperfine coupling constant (hfcc), A^{iso} of Mg^+ embedded in Ne or Ar matrices. In this system, the electrostatic components of the embedding potential are negligible (environment comprises noble gas atoms) and the difference between Fermi contact terms A^{iso} of the hyperfine tensor for Mg^+ in the two matrices arises due to difference in the Pauli repulsion between the close-shell $\rho_B(\vec{r})$ and the spin density of the Mg^+ cation. A simple model of the matrix consisting only of the nearest noble-gas atoms was used. $A^{iso}([MgNe_8]^+)$ and $A^{iso}([MgAr_8]^+)$ are equal to −80 and −75 MHz, respectively. These values compare very well with the corresponding experimental values (−79 and −76 MHz).

FDET was also applied for calculation of isotropic *g*-tensors for model systems consisting of the biliverdin IXa radical and nearest neighbor amino acids of the protein phycocynobilin to biliverdin in the biliverdin-phycocynobilin complex,[37] i.e., systems where the electrostatic components of the embedding potential can be expected to play a more important role. The study revealed that the nonelectrostatic component of the embedding potential must be included in order to get numerically stable results even in such a case. To this end, the conventional Kohn–Sham calculations were used as a reference. Using approximate functional for nonelectrostatic component of embedding potential could reproduce 50–90% of environment induced shift in *g*-tensor obtained from the reference Kohn–Sham calculations. Moreover, it was found that molecular $\rho_B(\vec{r})$ corresponding to the isolated environment is an adequate choice if it comprises neutral of cationic amino acids. In the presence of negatively charged amino acid in the environment, better agreement with reference results was obtained using optimized

DOI: 10.1021/cr500502v
Chem. Rev. 2015, 115, 5891–5928

$\rho_B(\vec{r})$. Nonoptimized $\rho_B(\vec{r})$ leads even to a wrong direction of the shift.

Besides purely electronic effects, the interactions with the environment may affect the structure of the embedded species. The environment effects on hfcc depend strongly on the structure of the molecule of interest. In modeling solvated radicals, additionally the environment must be treated as a statistical ensemble of several structures. In practice it involves repetitive calculations of hfcc for many geometries of the whole systems. This leaves embedding strategy as the most efficient for modeling. Neugebauer et al.[117] applied FDET based methods to the H_2NO radical in clusters of H_2O comprising two, four, and 75 molecules. This molecule is particularly suitable for such studies because of a strong dependence of the hfcc on the out-of-plan bending angle of the NO group from the H−N−H plane. The values of the constant A^{iso} for hydrogen and nitrogen calculated with the smallest cluster (H_2NO−$4H_2O$) equal to +11.85 and −38.75 MHz, respectively. These numerical values compare well with corresponding reference results from Kohn−Sham calculations for the whole system (+12.78 MHz for N^{14} and −38.75 MHz for H^1). For more realistic modeling of solvent, the Car−Parrinello dynamics was performed to generate an ensemble of structures. The bulk effect of the solvent was obtained by means of averaging the coupling constants derived from FDET calculations for 200 instantaneous geometries. 75 water molecules were used to generate $\rho_B(\vec{r})$ as a sum of densities of molecular densities. The freeze-and-thaw optimization of $\rho_B(\vec{r})$ was estimated to affect the coupling constants by only 0.02 MHz.

More recently, Kevorkyants et al.[223] applied FDET embedding potential for calculation of isotropic hfcc for guanine radical cation in the presence of one water and one chlorine or either of the two molecules. The freeze-and-thaw optimized $\rho_B(\vec{r})$ was used. Larger models of the crystal environment consisting of 7 and 36 guanine molecules was also considered. A obtained with the largest model (36 guanine) equals 15.5 MHz which compares well with the experimental result (16.8 MHz).

5.4. Multipole Moments and Polarizabilities

The dipole moment and polarizabilities are fundamental properties of molecule. These properties are routinely calculated with quantum chemical methods. Wesolowski and Warshel[44] made the first attempt to calculate the dipole moment and its fluctuations for a water molecule in liquid phase using embedding strategy based on FDET. For the nearest solvent molecules, the electron density $\rho_B(\vec{r})$ was generated using superposition of molecular fragments. The electrostatic potential generated by more distant molecules was generated using net atomic charges. Solvent density was kept frozen during the calculation. It was found that the magnitude of the dipole increases by only 0.2 D compared to the gas phase and does not vary noticeably. The magnitude of this increase was underestimated compared to experimental observations (0.6 D). This underestimation was attributed to the small basis set used for calculation. Later, Jacob et al.[114] calculated the dipole moment and quadrupole moment of the solvated water molecule using the triple-ζ quality basis set with diffuse functions. The properties obtained from FDET calculations were compared with the DRF results. The solvent induced increase of the dipole moment derived from FDET calculations with not-optimized $\rho_B(\vec{r})$ was smaller (+0.65 D) than its DRF counterpart (+0.86 D). Optimization of $\rho_B(\vec{r})$ resulted in the further increase of the effect (+0.91 D) in FDET calculations. More recently, Hodak et al.[241] took the dipole moment of the water molecule in the liquid under scrutiny using also the approximated FDET embedding potential to study its fluctuations along the molecular dynamics trajectory. The reported value of the magnitude of the dipole moment equals 2.85 D using the sum of fragments strategy for generation of $\rho_B(\vec{r})$ with fragments being the individual water molecules of the dipole moment set to be equal to 3 D.

Both the total dipole moment or complexation induced dipole moment are useful quantities to analyze the accuracy of the densities obtained from subsystem DFT calculations. The induced dipole moment related directly to the quality of the approximations for the FDET embedding potential (see refs 44, 108, 111, 114, 131, and 216 for instance). With sufficiently large basis set (supermolecular expansion, see section 2.2.4), the induced dipole moment are very sensitive to the variations in the embedding potential. Such study was reported in ref 225 concerning the linearization approximation (see section 4.1.3) to the nonadditive kinetic energy component of the FDET embedding potential by analyzing results of complexation induced dipole moments for weakly bound intermolecular complexes. The linearization scheme for the nonadditive-kinetic, as well as exchange-correlation, components of the FDET embedding potential was examined for the same set of complexes in ref 226. Beyhan et al.[216] analyzed dipole moments in weak covalently bond complexes, such as NgAuF (for Ng = Ar, Kr, and Xe) in the study of the accuracy of several approximations to the density functional for the nonadditive kinetic energy. FDET results were compared to that of conventional Kohn−Sham calculations to the whole complex. It was found that none of the considered functional could describe adequately a weak covalent bond. Among the considered decomposable approximations for $T_s^{nad}[\rho_A,\rho_B]$, only the one introduced by Karasiev et al. in ref 269 for $T_s[\rho]$(PBE2) could produce the induced dipole moment close to the reference Kohn−Sham results if a nonrelaxed $\rho_B(\vec{r})$ was used in FDET equations. The reported magnitudes of the interaction induced dipole moment for Ar, Kr, and Xe complexes are equal to 1.78, 2.26, and 2.88 D, respectively. The corresponding supermolecular Kohn−Sham reference values are 1.80, 2.15, and 2.67 D. The freeze-and-thaw optimization of $\rho_B(\vec{r})$ led to worse dipole moments. These results confirm the conclusions from earlier studies of approximations for the nonadditive kinetic energy functional[108,128−130] which show that the simple GGA type of approximations for $T_s^{nad}[\rho_A,\rho_B]$ are applicably only if the densities $\rho_A(\vec{r})$ and $\rho_B(\vec{r})$ are weakly overlapping. In covalently bound environments, the ρ_A−ρ_B overlaps for any reasonably chosen $\rho_B(\vec{r})$ are too large and the errors in the approximated functional for the FDET embedding potential are unacceptable.

For the dipole-polarizabilities, the first application of FDET/LR-TDDFT was reported in ref 114 concerning solvated water molecules. FDET/LR-TDDFT polarizabilities were compared with the results of the DRF calculations. It was found that the two considered embedding methods (DFT and FDET based) lead to opposite effects of the environment on the polarizability of the embedded species. The DRF calculations yield increased mean static polarizability due to the solvent from 9.40 a.u. (gas phase) to 9.62 a.u. (solvent). The FDET shows an opposite solvent effect, decrease from 9.40 a.u. (gas phase) to 8.77 a.u. in the solvent. A similar trend was observed for frequency dependent mean polarizability. On the other hand, although DRF can account for the polarization of the solvent by the solute, it does not take into account the Pauli repulsion in the embedding potential as does FDET. To analyze the environment response

DOI: 10.1021/cr500502v
Chem. Rev. 2015, 115, 5891−5928

contribution to static polarizability, the finite field calculations were made in which the environment density was also optimized by means of freeze-and-thaw procedure. The contribution to the static polarizability obtained using the two embedding methods was similar and equal to 0.30 a.u. and 0.40 a.u. for FDET and DRF, respectively. (Note that interpreting the effect of the optimization of $\rho_B(\vec{r})$ as the electronic polarization of the solvent by the solute is not straightforward in FDET; see eq 38 in section 4.1.) However, such analysis can be done only for static polarizabilities. The authors attributed this qualitative difference to the lack of coupling between excitations in the embedded species and the environment which we refer to as the NDRE approximation in the present work.

The qualitative differences between the polarizabilties obtained from FDET and DRF calculations reported in ref 114 were attributed to neglecting of couplings between excited states of the embedded species and the environment (i.e., to the NDRE approximation). Indeed, the FDEc dynamic polarizabilities where consistent with DRF.[113]

5.5. Density Analysis

In previous sections, we discussed assessment of results obtained for molecular properties using density embedding methods along with the performance for chosen approximation and limits of the method. Accuracy of these properties depends upon a more fundamental quantity such as electron density. FDET calculations make it possible to investigate the effect of the environment described by a fixed $\rho_B(\vec{r})$ on the electron density of the embedded species. Subsystem DFT[52] calculations such as the ones using the freeze-and-thaw optimization of both $\rho_A(\vec{r})$ and $\rho_B(\vec{r})$[55] provide a unique pair of optimized densities if the approximated functionals are used for $T_s^{nad}[\rho_A,\rho_B]$ or $E_{xc}^{nad}[\rho_A,\rho_B]$ (see eq 38 in section 4.1). Several studies were reported showing that such a unique pair of densities are nevertheless meaningful.

References 121, 122, and 270, for instance, provide a systematic analysis of electron densities and their topologies obtained from subsystem DFT, and the corresponding Kohn–Sham DFT calculations were reported. Such quantities as (a) difference between the Kohn–Sham density of the whole system and the sum of densities of isolated fragments, (b) the difference between the Kohn–Sham density of the whole system and the sum $\rho_A(\vec{r})$ and $\rho_B(\vec{r})$ obtained through the freeze-and-thaw optimization, and (c) negative Laplacian of the optimized densities in the subsystems were analyzed and discussed. Distinct features of such densities in the bonding region were pointed out. Kiewisch et al.[122] studied systems with hydrogen bonds such as HOH-F^-, a strong hydrogen bond such as FH-F^-, and nucleic acid base pair. With the topology analysis it was reconfirmed that freeze-and-thaw calculations lead to densities reflecting the qualitative features of hydrogen bonds. Fux et al.[121] extended this study to weak dative bonds such as, for instance, $H_3N\cdots BH_3$ and compounds with ionic characters such as $TiCl_4$. The densities obtained in freeze-and-thaw calculations reflect the qualitative features of the bonding these systems. For coordination compounds with strong covalent bonds, however, the freeze-and-thaw densities are less useful even in qualitative analyses.

Recently, Fabiano et al.[166] discussed the results obtained using an approach related to that of partition DFT, in which the subsystem particle number can be noninteger. The effect of allowing a fractional particle number of subsystems on the density was analyzed in a representative set of noncovalent complexes such as Ne–Ne, Ne–Ar, Ar–AuF, H_2S–HCl, HF–NCH, $(NH_3)_2$, NH_3–ClF, and NaCl. The necessity to go beyond the integer particle number was shown for NH_3–ClF and Ar–AuF. For Ar–Ne, H_2S–HCl, and HF–NCH, on the other hand, allowing for the fractional particle number appeared not to be necessary. In the same work, the authors introduced the definition of chemical descriptors such as Fukui functions[271] and global hardness for subsystems.

Solovyeva et al.[224] analyzed the spin-density distributions obtained in freeze-and-thaw calculations in several systems such as the H_2NO radical in a cluster consisting of 20 water molecules, a guanine-thymine DNA base pair dimer radical cation, and a radical cation in protein binding pocket represented either as small cluster including only the nearest nighbors or a bigger cluster comprising 750 atoms in total. It was found that the total spin densities obtained from freeze-and-thaw calculations are more localized than the ones obtained from the Kohn–Sham calculations for the whole system.

The freeze-and-thaw optimized subsystem densities can provide the essential information concerning the used approximation for the functional derivatives of the nonadditive kinetic energy functional (see the relevant part in section 4.1 or ref 55). Such direct analyses of freeze-and-thaw optimized subsystem densities were made subsequently for various systems and approximations for the functional $T_s^{nad}[\rho_A,\rho_B]$.[100,128−130]

Della Sala and co-workers[126,200] used the electron densities to study the accuracy of several semilocal functionals for nonadditive kinetic energy component. The test calculations were performed on 20 molecular systems with weak interactions, dipole–dipole interactions, and hydrogen bonded interactions. All considered approximations lead to almost the same global error in the total density. The mean absolute error in density varied by 5% from functional to functional, indicating that each of them yields the embedding potential of the same quality. Larichia et al.[218] performed a similar study of the approximations for the embedding potential within the framework of generalized Kohn–Sham context, i.e., orbital-dependent approximations for the exchange-correlation energy such as in commonly used hybrid functionals B3LYP, BHLYP, and PBE0.[196,272−276] The test calculations were made for weakly bound systems such as H_2–NCH, HF–NCH, benzene–HCN, thymine with six water molecules, and nucleic acid base pairs guanine–cytosine and adenine–thymine.

Stefanovich and Truong[99] reported the case of qualitative wrong shape of the potential energy curve at short separations between charged and neutral subsystems (F^-–H_2O and Li^+–H_2O). This artificial behavior was attributed to unphysical charge-transfer between subsystems caused by the violation of orthogonality between embedded orbitals in different subsystems. Dulak and Wesolowski[100] showed that the erroneous behavior reported by Stefanovich and Truong for this systems was due to the flaws in numerical implementation for the evaluation of the FDET embedding potential. The density obtained as a sum of freeze-and-thaw optimized subsystems densities and the reference density from Kohn–Sham calculations for the whole complex did not show any artificial charge transfer at short and intermediate separations between charged and neutral subsystems.

Trail and Bird analyzed the conventional Kohn–Sham densities and their FDET counterparts in aluminum.[277] The electron density on the [111] direction for fcc aluminum was examined to test the approximation semilocal and nonlocal approximations nonadditive kinetic energy functional. The reference Kohn–Sham densities were reproduced reasonably well using a nonlocal functional.

DOI: 10.1021/cr500502v
Chem. Rev. 2015, 115, 5891−5928

Genova et al.[212] analyzed recently the subsystem DFT densities for periodic systems and compared them to the ones obtained form conventional Kohn−Sham calculations. The method was applied to model systems such as a water molecule adsorbed on platinum surface and perylene diimide on gold surface. Authors concluded that the method is successful to study weakly interacting molecules adsorbed on a metal surface, and accurate results can be obtained when there is no possible hybridization between orbitals of adsorbed molecule and bands of metal.

5.6. Properties of the Ground-State Potential Energy Surface

In practical calculations, both $T_s^{nad}[\rho_A,\rho_B]$ and $E_{xc}^{nad}[\rho_A,\rho_B]$ as well as the corresponding terms in the embedding potential $\delta T_s^{nad}[\rho_A,\rho_B]/\delta\rho_A(\vec{r})$ and $\delta E_{xc}^{nad}[\rho_A,\rho_B]/\delta\rho_A(\vec{r})$ are replaced by their approximated counterparts. The quality of the energies obtained using approximated functionals is determined by the errors in each of these four quantities. Unfortunately, the errors in the energy components and in the corresponding potentials are not related for simple approximations applicable in practical calculations. This was demonstrated for $T_s^{nad}[\rho_A,\rho_B]$ and $\delta T_s^{nad}[\rho_A,\rho_B]/\delta\rho_A(\vec{r})$[48,130] and originates from the inequality given in eq 31. Moreover, the errors in $T_s^{nad}[\rho_A,\rho_B]$ and $E_{xc}^{nad}[\rho_A,\rho_B]$ are not related and should, therefore, be considered as independent unless the approximated density functionals are obtained from conjoint approximations (see section 4.1.1) for the functionals $T_s[\rho]$ and $E_{xc}[\rho]$. The quality of the properties discussed in the previous sections are determined by the used approximated embedding potential and hence on the errors in the used approximations for $\delta T_s^{nad}[\rho_A,\rho_B]/\delta\rho_A(\vec{r})$ and $\delta E_{xc}^{nad}[\rho_A,\rho_B]/\delta\rho_A(\vec{r})$ only. The quality of the energy is influenced additionally by the errors in the used approximations for $T_s^{nad}[\rho_A,\rho_B]$ and $E_{xc}^{nad}[\rho_A,\rho_B]$. Approximated functionals $\tilde{T}_s^{nad}[\rho_A,\rho_B]$ and $\tilde{E}_{xc}^{nad}[\rho_A,\rho_B]$ are used in the FDET functional for the total energy (eq 6) to evaluate it at the density $\tilde{\rho_A}$ which is not equal to ρ_A^{opt} because of the approximations in the functional for the embedding potential. It is, therefore, very difficult to formulate general recommendations for the functionals to be used for evaluation of the energy. In subsystem DFT calculations, the errors of the energy are determined by the errors in four quantities: $\tilde{T}_s^{nad}[\rho_A,\rho_B]$ and $\tilde{E}_{xc}^{nad}[\rho_A,\rho_B]$ and the corresponding functional derivatives. In FDET calculations, the difference between the obtained energy and the exact one depends additionally on ρ_B (as any other property derived from FDET). These errors are unrelated and the used approximations must be rather chosen on a case-by-case basis. Nevertheless, the use of local density approximation for all approximated quantities ($\tilde{T}_s^{nad}[\rho_A,\rho_B]$ and $\tilde{E}_{xc}^{nad}[\rho_A,\rho_B]$ and the corresponding functional derivatives) together with the freeze-and-thaw optimization of $\rho_B(\vec{r})$ leads to astonishingly good results in many cases and should be considered as the starting point. Without using any empirically adjusted parameters, it leads to excellent interaction energies geometries for hydrogen-bonded and dipole bound intermolecular complexes and even some weak dispersion bound complexes. For hydrogen-bonded or dipole bound intermolecular complexes, the quality of the interaction energies[112,124] and geometries[151] exceeds that of the results of conventional Kohn−Sham calculations. For small dispersion bound complexes, the local density approximation in subsystem DFT calculations results in relative errors in the interacting energy from 5% to 50%.[150] Unfortunately, using even conjoint approximation for $T_s^{nad}[\rho_A,\rho_B]$ and $E_{xc}^{nad}[\rho_A,\rho_B]$ of the GGA type does not lead to a systematic improvement of the interaction energy.[125,150] At another end of stronger interactions, local density approximation as well as simple gradient-dependent approximations to $T_s^{nad}[\rho_A,\rho_B]$ lead to large errors.[110,216] Semilocal approximations for the nonadditive kinetic potential known to good accuracy for model systems[116,215] are rather not to be expected to capture even the qualitative features of the exact embedding potential in such cases.

This section provides the overview of the applications of various computational methods using the embedding potential of the FDET form for evaluation of the energy of the embedded species.

5.6.1. Chemical Reactions in Condensed Phase. Warshel and collaborators studied reaction profiles and activation energies of simple chemical reactions such as proton transfer in model systems such as $(FHF)^-$ anion in liquid water,[160] a water dimer in cluster model $(Im)_3Zn^{2+}$ of carbonic anhydrase enzyme,[236] autodissociation of water using an embedded cluster consisting of 10 water molecules,[161] and realistic model of such large enzymes as DNA polymerase and itriptophosphate isomerase.[278] The approximated FDET embedding potential was used to generate diabatic surfaces and to evaluate off-diagonal elements in EVB Hamiltonian[158,159] calculations for the S_N2 reactions in condensed phase.[279,280] Except for small model systems, for which the tests of procedures to generate $\rho_B(\vec{r})$ were made such as that in ref 236, $\rho_B(\vec{r})$ was not optimized in such procedures and the calculations followed the approximate FDET framework.

Olsson et al.[281] evaluated the redox potentials for the blue copper proteins plastocyanin and rusticyanin. The FDET energies were used in a more general context of the applied model for evaluating the free-energies differences based on linear response approximation.[282]

Leopoldini et al.[283] studied the oxidative half-reaction of oxygen atom transfer from nitrate to Mo^{IV} in *Desulfovibrio desulfuricans* nitrate reductase to compare the reaction barriers on potential energy surfaces corresponding to singlet and triplet configuration of molybdenum complex.

5.6.2. Intermolecular Complexes. Most of the results reported in the literature on intermolecular complexes concerns small systems, for which the reference results obtained from accurate wavefunction based methods or experiments were available. We start with the literature concerning benchmarking and/or testing approximations for $T_s^{nad}[\rho_A,\rho_B]$.

The first application of FDET to evaluate intermolecular interaction energies concerned the H_2O-Li^+ complex.[44] The density of $\rho_B(\vec{r})$ (water molecule) was not optimized and two approximations to $T_s^{nad}[\rho_A,\rho_B]$ (obtained from zeroth- and second-order gradient expansion for $T_s[\rho]$) were tested. It was found that including the second-order gradient expansion term in the decomposable approximation for $T_s^{nad}[\rho_A,\rho_B]$ instead of improving the energies obtained using only the zeroth order term (LDA) worsens the energy (overestimated depth of the minimum on the potential energy surface). This was a puzzling results because the optimization of $\rho_B(\vec{r})$ could only worsen the results further by deepening the minimum. This unexpected behavior is the result of the different role the von Weizsäcker functional plays in the interior and far from molecular centers (see section 4.1.1). Subsequent studies by Wesolowski and collaborators on various intermolecular complexes used freeze-and-thaw optimized $\rho_B(\vec{r})$ and included such systems as charged complex H_2O-Li^+,[131,226] charge-transfer complexes NH_3-ClF,[226] dipole bound complexes (H_2S dimer, HCl dimer,

DOI: 10.1021/cr500502v
Chem. Rev. 2015, 115, 5891−5928

CH_3Cl−HCl, HCN−CH_3SH, and HCl-CH_3SH[151]), hydrogen bonded complexes (water dimer at equilibrium geometry[108,128,226,235] and at other stationary points on the potential energy surface,[124] H_2−NCH,[55] HF-NCH,[108,128] HF dimer,[108] HCl dimer,[108] and NH_3−H_2O),[226] weaker intermolecular complexes (C_6H_6-X (for X = O_2, N_2, and CO),[284] benzene dimer,[285] carbazole-X (for X=Ne, Ar, CH_4, CO, N_2),[125] and other typical dispersion bound complexes such as Ne−Ne, F_2−Ne, N_2−N_2, N_2−Ar, Ar−Ar, F_2−Ar,[150] Ne−Ne, CH_4−CH_4, and C_2H_2−C_2H_2.[226] The potential energy curve for same set of van der Waals complexes were recently reinvestigated using subsystem DFT for three different conjoint approximations LDA/TF, PW91/PW91k, and BP86/LLP91 for exchange and nonadditive kinetic energy.[286] The reported studies concerned also larger sets of reference data including that of ref 287 (S22) and that of ref 288 (S66). The results of comprehensive benchmarking of energies and geometries obtained from subsystem DFT, with freeze-and-thaw optimization of $\rho_A(\vec{r})$ and $\rho_B(\vec{r})$, can be found in refs 112 and 151.

In most cases, using the local density approximation for all approximated density functionals leads to good or very good interactions and energies competing in accuracy with that of conventional MP2 calculations. In the case of π-stacking, the tendency to compensate the errors in the local density approximation functional breaks. Concerning testing the nonadditive kinetic functionals, these studies were complemented by the results reported in ref 110 including also more strongly bound complexes such as the coordination complexes.

Kevorkyants et al.[162] reported a study of the LDA and GGA approximations to $T_s^{nad}[\rho_A,\rho_B]$ as well as their extension of subsystem DFT including London dispersion forces for such hydrogen-bonded and dispersion bonded intermolecular complexes as $(NH_3)_2$, $(H_2O)_2$, $(HCOOH)_2$, $(CH_4)_2$, $(C_2H_4)_2$, benzene dimer, benzene−HCN, benzene−amonia, benzene−methane, and benzene−water.

Manby et al.[96] tested the proposed beyond-FDET embedding method that enforce Pauli exclusion via the projection technique and not through the nonadditive kinetic potential to model complexes including water clusters. In ref 231, the interactions between H_2 and a hydrogen chain were investigated using the method applying inversion technique to generate the embedding potential.

Subsystem DFT based calculations were applied also for larger complexes not for testing purposes but to make actual predictions of properties of the studied complexes. Tran et al. studied dimers formed by nitrogen-containing planar polycyclic aromatic hydrocarbons $(C_{30}H_{15}N)_2$ and $(C_{36}H_{15}N)_2$[289] and for H_2 molecule absorbed on polycyclic hydrocarbons.[290] Either studies concerned conformational preferences of the studied complexes and estimation of barriers for transitions between local minima.

To test the used approximations in FDET calculations for modeling blue copper proteins (plastocyanin and rusticyanin), Olsson et al.[281] investigated potential energy surfaces in small model complexes H_2O−CH_3OH and H_2O−CH_3SH which were shown to compare favorably with the results of conventional Kohn−Sham calculations.

5.6.3. Solids and Interfaces. The use of the approximated FDET embedding potential for studies of molecules absorbed at interfaces was pioneered by Carter and collaborators.[57,58] The applied method followed the ONIOM strategy and used explicitly interacting Hamiltonian of the molecule absorbed at the surface (CO on the Cu(111) surface). The performance of the proposed method was tested on a model system (the complex of Li_2 and Mg_2) for which high-level wavefunction based calculations of the full CI quality could be applied. The proposed model was subsequently applied for absorption of CO adsorbed on the Pd(111) surface using periodic DFT calculations to get the total density and such interacting Hamiltonians for the embedded species as that of CASSCF, CI, and MP4 methods.[179,255] Further studies by Carter and collaborators using improved version of the originally proposed method, which made it possible to treat covalently bound adsorbated, concerned binding energy of Co on Cu(111),[256,257,291] CO on Cu(111),[292] or dissociation of H_2 on gold nano particles.[259,260]

Lahav and Kluner[293] reported the absorption energies for CO adsorbed on the Pd(111) surface calculated using a modified version of the method used in the original publications.[179,255] The modifications concerned approximations for the subsystem densities and the used approximation for the nonadditive kinetic potential functional.

Recently, Pavalone and collaborators[212] reported studies of methane on Pt(100), water on Pt(111), perylene diimide on Au(111) using the implementation of the subsystem DFT calculations for periodic systems.

Only a few studies reported using the FDET calculations to evaluate vibrational properties of embedded species. They include studies of embedded CO on metal oxide surfaces, CO molecule physisorbed on the MgO(100) or ZnO(1010) surfaces,[294,295] or embedded clusters carved out from the ionic solids: CO stretching frequency in the M^+-CO (for M = Li, Na, and K) complex embedded in the framework of the ZSM5 zeolite or vibrational and optical properties of the $(MnF_6)^{-4}$ complexes in cubic fluoroperovskites.[296]

5.6.4. Simulations of Statistical Ensembles for Average Structures and Thermochemistry. In the first FDET based simulation of the free energy differences, the FDET energies obtained at instantaneous geometries from the statistical ensembles were used to determine the difference in the free energy of hydratation for methane[235] using a free-energy perturbation scheme.

Iannuzzi et al.[297] used the subsystem DFT calculations for liquid water in NVT ensemble at 320 K. In contrast to freeze-and-thaw algorithm, in which the subsystem densities obtained from FDET are optimized in iterative process, the densities in all subsystem (individual water molecules) were optimized simultaneously.

Reference 298 reports the molecular dynamics simulation performed for the CdSe using subsystem DFT calculations. The calculations featured enormous size of the whole studied system comprising more than 32 thousands of atoms.

Stefanovich and Truong[99] studied the solid−liquid interfaces. The test calculations are performed to generate potential energy surface for several model systems He, Ar dimers, X−H_2O complexes for X = Li^+, Na^+, K^+, F^-, and Cl^- and water absorbed on the NaCl(001) surface. Both the approximated FDET embedding potential as well as an embedding method using a nonlocal embedding operator were used.

Hodak et al.[241] used FDET embedding potential to represent solvent effect using molecular dynamics simulations to model binding of the copper ion to the prion protein. The embedded system consisted five amino acids of prion protein (72 atoms) and embedding solvent consisted 3101 water molecules.

DOI: 10.1021/cr500502v
Chem. Rev. 2015, 115, 5891−5928

6. CONCLUDING REMARKS

In the present review, we overviewed both the applications of the FDET formalism as an alternative to empirical QM/MM methods for multilevel simulations as well as applications of the approximated FDET embedding potential given in eq 8 in several beyond FDET extensions. The provided examples show that the area of applicability of universal density-dependent local embedding potentials is vast.

Concerning first type of applications, due to limiting the description to the environment by such simple quantity as $\rho_B(\vec{r})$, FDET can target not the total density but an upper bound to it and the corresponding self-consistent embedded wavefunction obtained from the Euler−Lagrange equations. Compared to empirical QM/MM methods the modeler must make a system-dependent decision concerning generation of the frozen density instead of choosing or fitting empirical parameters. An additional advantage of FDET facilitating this task is the sublinear dependence of the environment induced shifts of the properties of the embedded species on $\rho_B(\vec{r})$[107] and the availability of a freeze-and-thaw[55] procedure which can be applied on model systems to obtain optimized $\rho_B(\vec{r})$.

6.1. Universal Applicability of the Density Embedding Methods and Their Limitations

The present review shows that local embedding potentials of the form given in FDET found very wide area of applications as far as systems and properties are concerned. The approximated FDET framework as well as related methods using an approximated FDET embedding potential were applied in multilevel simulations of systems such as molecular clusters, solvated systems, interfaces, biomolecules, and solids. The number of reports of successful simulations of the effect of environment on electric moments, polarizabilities, electronic excitations, and magnetic properties (NMR and EPR) is growing. Accurate results were reported in the literature concerning the ground-state potential energy surface (interaction energies, geometries, barriers, and vibrational spectra). FDET is especially suited for simulating properties rather than just the ground-state potential energy surface. FDET provides a variational principle based self-consistent energy and embedded wavefunction, which can be used to evaluate other observables than just the energy. If the ground-state potential energy is the target of the simulation and not electronic structure related properties, empirical QM/MM types of approaches might be more suitable. Owing to empirical parametrization of the components of the total energy, QM/MM methods yield accurate energies. The lack of self-consistency between energy and the embedded wavefunction is acceptable.

The overviewed applications show clearly that methods applying approximated FDET embedding potential are applicable in many areas even if simple approximations for the universal density functionals are used. The domain of applicability of the current approximations is defined not by systems or properties but rather by the type of interactions between the embedded species and the environment. If the environment generates noticeable electric fields as in the case of hydrogen bonding between the embedded system and the environment or if ions or polar species are present in the environment, simple explicit density functionals for the FDET embedding potential are usually adequate. Approximations for the total kinetic energy functional, which are not accurate enough to be used in orbital-free DFT calculations (see refs 72 and 73), are quite successful if used for approximating the nonadditive kinetic energy and potential in FDET, where they are used to take into account the confinement effects (Pauli repulsion).

In the FDET embedding potential, the electrostatic field is taken into account exactly, whereas the presence of approximate terms representing the nonelectrostatic contributions eliminates the possible artificial effects of overpolarization in most cases.

The applications of the FDET based methods revealed also the limitations of the currently available approximations. In the presence of covalent bonding between the environment and embedded species, the commonly used approximations for the nonadditive density functionals usually fail.[110] The numerical inversion procedure to generate the embedding potential, in which the explicit functionals are not used, provides one of the possible solutions.[116] Similarly, if the attribution of the integral number of electrons to the embedded species is not straightforward, FDET probably should not be used. Approaches based on partition DFT,[53,54] which involves optimization of the occupancy of each subsystem, are probably better suited for such applications. Finally, going beyond FDET by means of the optimization of $\rho_B(\vec{r})$, as it is made in subsystem DFT[52] or in partition DFT,[53,54] might be indispensable. The FDET is only applicable if it is possible to generate such $\rho_B(\vec{r})$ that the variation of $\rho_B(\vec{r})$ results in acceptable variations of the calculated properties. If the dependence is strong, the optimization of both $\rho_A(\vec{r})$ and $\rho_B(\vec{r})$, as it is made in subsystem DFT or partition DFT, is probably a better solution. A closely related alternative to subsystem DFT or partition DFT is to retain from FDET only the form of the embedding potential in order to couple subsystems described by means of traditional quantum chemistry methods (see ref 180 for instance). Treating excited states then by means of LR-TDDFT extension of FDET[182] which neglects the frequency dependent response of the environment, fails if the environment and embedded species absorb in the same range.[153] In such cases, methods based on the generalization of subsystem DFT for excited states[152] such as the ones developed in refs 113, 153, and 154 should rather be applied.

6.2. Beyond the FDET Embedding Potential

The embedding operator in FDET is a local potential and is a universal functional of charge densities. This results in its system-independence which is a desired feature but makes its construction of universally applicable approximation for this potential a difficult task.

Another undesired consequence of the ρ_A-dependence of the FDET embedding potential relates to methods using interacting Hamltonians as $\hat{H}_A$. Being ρ_A-dependent, the FDET embedding potential cannot be combined in a straightforward manner with traditional quantum-chemistry methods developed for linear operators. Linearization of the FDET embedding potential, for instance by means of evaluating it at some fixed $\rho_A^{ref}(\vec{r})$[226] which makes it ρ_A-independent, is a pragmatic approximation. For the ground-state calculations, this approximation is fully controllable and the ρ_A-dependence of the FDET embedding potential can be easily recovered through an iterative process,[57] which was shown to converge quickly to a self-consistent solution in the case of weak interactions between the embedded species and the environment.[226] Such an iterative procedure has been applied recently to obtain self-consistent solutions in the case of embedding a system treated by means of density matrix renormalization group methods (DMRG)[299−302] in a frozen environment.[303] For excited-state calculations, however, linearization remains an approximation unless different $\rho_A^{ref}(\vec{r})$ are used for different electronic states (see discussion in ref 177).

DOI: 10.1021/cr500502v
Chem. Rev. 2015, 115, 5891−5928

Abandoning the central idea of FDET, i.e., locality of the embedding potential, and returning to embedding methods applying the nonlocal potentials, which are linear operators, might be more efficient for some cases. In view of the limits of the currently available density-dependent approximations for the FDET functional for the embedding potential, the use of orbitals for the environment and enforcing the orthogonality between the embedded orbitals and the orbitals of the environment[83,96,257] might be a more efficient alternative especially in the case of strong overlap between $\rho_A(\vec{r})$ and $\rho_B(\vec{r})$. For such cases, the numerical inversion strategy to generate the FDET embedding potential without the use of nonadditive density functionals, which appears to be a promising strategy for dealing with strongly overlapping $\rho_A(\vec{r})$ and $\rho_B(\vec{r})$,[116] also requires constructing orbitals for more than just for the embedded species. Also in the studies of solids, it is rather unlikely that approximate FDET potentials would become competitive with nonlocal pseudopotentials because transferable atomic/ionic pseudopotentials are available.

Construction of a sufficiently accurate approximated FDET embedding potential might be impractical for modeling the long-range correlations effects occurring at dissociation of chemical bonds or in metals, for instance. Neither the nonelectrostatic components of the FDET embedding potential nor by nonlocal molecular pseudopotentials provide a practical solution in such cases. The recent work of Chan and collaborators on embedding systems described by means of embedded density matrices[66,67] within the density DMRG framework or the dynamic mean-field theory by Georges, Kotliar, Krauth, and Rozenberg[304] which uses local Green's functions should rather be used.

6.3. Frozen-Density Embedding Theory vs Frozen-Density Embedding Approximations

The basic equations of FDET (eqs 3−8) are not used in practice in their exact form. Approximations ($\tilde{T}_s^{nad}[\rho_A,\rho_B]$, $\tilde{E}_{xc}^{nad}[\rho_A,\rho_B]$, and $\Delta\tilde{F}^{SC}[\rho_A]$) are used for the exact functionals $T_s^{nad}[\rho_A,\rho_B]$, $E_{xc}^{nad}[\rho_A,\rho_B]$, and $\Delta F^{SC}[\rho_A]$. Following terminology advocated by Levy concerning density functional theory, we use the acronym FDEA (frozen-density embedding approximations) in this section referring to the approximated version of eqs 3−8. The use of approximated density functionals in eqs 3−8 does not only affects the obtained results but also leads to emergence of new qualitative features of the approximated scheme.

(a) Removal of the degeneracy of the partitioning in subsystem DFT due to the used approximations (see eq 38 in section 4.1), which lead to unique partitioning of the optimal total electron density. In FDEA the difference between electron density of the isolated environment and the unique $\rho_{B(opt)}(\vec{r})$ obtained in the freeze-and-thaw optimization cannot be attributed only to the electronic polarization because the uniqueness is the result of maximization of the absolute error in the used approximations for the nonadditive functionals.

(b) The optimal embedded density $\rho_{A(opt)}(\vec{r})$ and energy $E^{FDET}[\rho_B]$ (defined in eq 2) can be obtained from the Euler−Lagrange equations (eq 5) only if it is v-representable, i.e., if there exists a local potential $v(\vec{r})$ for which the ground-state density is $\rho_{A(opt)}(\vec{r})$. If the approximations for density functionals are used, the solutions of the approximated Euler−Lagrange equations are restricted to v-representable solutions by construction. In FDET, the Euler−Lagrange equations associated with eq 2 might not exist for some choices of $\rho_B(\vec{r})$, whereas in FDEA they do.

(c) The FDET embedding potential exists only if both the densities $\rho_{A(opt)}(\vec{r}) + \rho_B(\vec{r})$ and $\rho_{A(opt)}(\vec{r})$ are v-representable. However, the embedding potential in FDEA can be evaluated for any density. The condition that $\rho_{A(opt)}(\vec{r}) + \rho_B(\vec{r})$ is v-representable is not needed in FDEA. The density $\rho_{A(opt)}(\vec{r}) + \rho_B(\vec{r})$ can even integrate to a number which is not an integer. Equations 2 and 3 are thus equivalent in FDET but not in FDEA. Equation 3 is more general than eq 2 in FDEA. Even densities comprising a fractional number of electrons can be used as $\rho_B(\vec{r})$ in the FDEA version of eq 3. As a result, FDEA can be used in multilevel simulations where the considered levels are not limited to quantum chemistry methods. Any other method based on law of physics yielding electron density can be used to generate $\rho_B(\vec{r})$ regardless if $\rho_{A(opt)}(\vec{r}) + \rho_B(\vec{r})$ is v-representable or not. An example of such use of FDEA is the nonuniform continuum model of the solvent.[240]

6.4. Challenges

The present overview shows that the development of multilevel simulation methods based on using the local potential of the FDET form is far from complete. Improvements are desired and expected concerning the following issues.

6.4.1. Approximations for Nonadditive Density Functionals. The difficulty to approximate $T_s^{nad}[\rho_A,\rho_B]$ and the corresponding potential at high overlaps between $\rho_A(\vec{r})$ and $\rho_B(\vec{r})$[48,130,215] reported in dedicated studies on model systems results in failure of semilocal approximations for $T_s^{nad}[\rho_A,\rho_B]$ at short distances between atoms of the embedded species and the environment.[108,128,129,215] More importantly, such applications fail when the embedded species and the environment are linked by covalent bonds.[110,116,215,216] This limits the applicability of such approximations to noncovalently bound environments.

However, even for such applications of approximated FDET embedding potential, the universal criterion, i.e., independent of the system and investigated property, of applicability of a particular approximation would be useful. Concerning $T_s^{nad}[\rho_A,\rho_B]$, we advocate a simple criterion based on the numerical value of $\tilde{T}_s^{nad}[\rho_A,\rho_B]$. If the magnitude of $\tilde{T}_s^{nad}[\rho_A,\rho_B]$ (approximate component of the interaction energy) is comparable or larger than that of the electrostatic component of the interaction energy (exact component of the interaction energy), the FDET results might not be reliable.

At the other extreme of small overlap, the decomposable approximations to $T_s^{nad}[\rho_A,\rho_B]$ obtained from semilocal functionals $\tilde{T}_s[\rho]$ do not ensure a proper behavior of the embedding potential near the nuclei in the environment due to the imbalance of errors in $\delta\tilde{T}_s[\rho_{AB}]/\delta\rho_{AB}(\vec{r})$ and $\delta\tilde{T}_s[\rho_A]/\delta\rho(\vec{r})$. This might result in a wrong redistribution of charges between subsystem (charge leak).[80,100] A decomposable approximation for $T_s^{nad}[\rho_A,\rho_B]$ assuring the correct behavior of $\delta\tilde{T}_s^{nad}[\rho_A,\rho_B]/\delta\rho(\vec{r})$ near the nuclei in the environment such as the one would built into the nondecomposable functional introduced in ref 131 would be very useful and would make the link between FDET and the orbital-free DFT methods.

Concerning approximations to $E_{xc}^{nad}[\rho_A,\rho_B]$ not much work on them has been done so far. In the case of noninteracting $\hat{H}_A$ (eqs 43−45), approximations are needed for the whole exchange-correlation energy $E_{xc}[\rho_A + \rho_B]$. The approximations to the separated $E_{xc}^{nad}[\rho_A,\rho_B]$ component are needed only for interacting $\hat{H}_A$, where usually other approximations affect the quality of the results (linearization of the FDET embedding potential, source of $\rho_B(\vec{r})$, and the treatment of correlation). With the expected progress in approximating $T_s^{nad}[\rho_A,\rho_B]$ and advancements in beyond-FDET embedding methods based on projections.[68,96,97] In such methods there is no need to approximate $T_s^{nad}[\rho_A,\rho_B]$

DOI: 10.1021/cr500502v
Chem. Rev. 2015, 115, 5891−5928

because of the use of nonlocal projector operators. A recent study by Goodpaster et al.[68] indicates that indeed approximating $E_{xc}^{nad}[\rho_A,\rho_B]$ emerges as a new challenge because it determines the overall quality of the results.

6.4.2. Conjointness Conjecture. The good quality of the interaction energies obtained using the Gordon−Kim model for noble gas dimers[148] is a long-standing unresolved issue. Subsystem DFT, which can be seen as a variational extension of this model, leads to astonishingly good interaction energies and geometries in hydrogen or dipole bonded intermolecular complexes, if the nonadditive exchange and kinetic functionals are approximated by conjoint density functionals (even in the case of the simplest conjoint case, local-density approximation[112,124,151]). Apparent compensation of errors in the functionals for energy and potential takes place. However, what is the underlying source of this compensation is currently not well understood.

6.4.3. Partitioning of Densities in Subsystem DFT. The unique partitioning in approximate version of subsystem DFT is the result of the use of approximations for $T_s^{nad}[\rho_A,\rho_B]$, which penalizes the overlap between the densities if it is evaluated using decomposable approximations comprising the repulsive Thomas−Fermi component eq 14. Among the multiple possible solutions of the optimal pair of densities in the exact subsystem DFT, the approximated version of subsystem DFT picks up the one with the smallest overlap. Localized embedded wavefunctions have obvious computational advantages. More importantly, the localized embedded wavefunctions are meaningful.[166] They were shown to be very useful in treatment of coupled excitations,[113,153] obtaining parameters in empirical Hamiltonians.[153,160,161] On the other hand the partition DFT in the exact formulation leads also to unique partitioning although it starts from a completely different assumption, the unique embedding potential for all subsystems. The relation between the two approaches to localization of the density merits further investigation.

AUTHOR INFORMATION

Corresponding Author

*Phone: +41 (0)223796101. Fax: +41 (0)223796518. E-mail: tomasz.wesolowski@unige.ch.

Notes

The authors declare no competing financial interest.

Biographies

Tomasz A. Wesolowski was born in Trzcianka (Poland). He earned his Ph.D. (with Professor David Shugar) in 1991 awarded by the Faculty of Physics at the University of Warsaw for his work on modeling cooperative binding of calcium ions in proteins. In 1991, he joined the group of Professor Arieh Warshel (University of Southern California, Los Angeles) where he started working on multilevel simulation methods and density functionals for coupling the quantum-mechanical descriptors with the environment in particular. In 1994, he moved to the University of Geneva, working initially as a postdoctoral researcher, then Lecturer and Research Group Leader, and since 2012, as associate professor in the Physical Chemistry Department. His research concerns mainly the theory of embedding a quantum system and its applications in multilevel simulations of embedded chemical species. His other research interests include density functional theory formulation of quantum many-electron problem, orbital-feee density functional theory methods, and all sorts of molecular simulations.

Sapana Shedge was born in Pune, India. She completed her Ph.D. in Computational Chemistry from the University of Pune in September 2012. During her Ph.D., she worked on the development of a noniterative method for calculation of electric response properties in deMon2k software; the work was done in Dr. Sourav Pal's lab at the National Chemical Laboratory (CSIR-NCL). Subsequently she moved to the University of Geneva in October 2012 to work as a postdoctoral researcher in Prof. T. A Wesolowski's lab. Since then she is working on simulating UV/vis spectra in liquids and in biological environments.

Xiuwen Zhou was born in Hunan, China. She received her M.Sc. degree in Physics in 2010 from the University of Shanghai for Science and Technology, where she worked in the group of Prof. T. Liu. Later, she received her Ph.D. degree from the University of Geneva in 2014, where she worked in the group of Prof. T. A. Wesolowski, and her research was in the field of multiscale simulations of the UV−vis absorption spectra of organic chromophores in the condensed phase. Then she moved to the University of Queensland in January 2015, where she works with Prof. B. Powell and Prof. P. Burn on the simulations of the phosphorescent complexes in OLEDs.

DOI: 10.1021/cr500502v
Chem. Rev. 2015, 115, 5891−5928

ACKNOWLEDGMENTS

T.W. is grateful to Professor Andreas Savin and Drs. Francesco Aquilante and Piotr De Silva for a critical reading of section 2. This research was supported by grants from Swiss National Science Foundation (200021_152779) and Swiss Federal Office of Science and Education (COST Action CM1002).

APPENDIX ABBREVIATIONS AND ACRONYMS USED FOR FORMALISMS, METHODS, AND ALGORITHMS

CASSCF:[78,79]	Complete Active Space Self-Consistent Field
CASPT2:[305−307]	CASSCF with second-order perturbation theory
CI[3,4]	Configuration interaction
COSMO:[13]	COnductor-like screening Solvent MOdel, continuum dielectric model of the solvent for embedding calculations
DFT:[136]	Density Functional Theory, formulation of quantum many body problem based on Hohenberg−Kohn theorems[51]
DRF:[105,250,251]	Discrete Reaction Field, QM/MM type of embedding method taking into account the electronic polarization of the environment
DMRG:[299−302]	Density Matrix Renormalization Group
EVB:[158,159]	Empirical Valence Bond
FDET:[44−46]	Frozen-Density Embedding Theory, formulation of the embedding problem based on eqs 3−8 in the present work
FDET embedding potential:	The embedding operator in FDET (eq 8 in the present work)
FDEc:[153]	Coupled frozen-density embedding, method based on subsystem DFT for excited states[152]
FDE-ET:[157]	Subsystem DFT based method for charge-transfer states excitations
freeze-and-thaw:[55]	The procedure to optimize the subsystem densities in subsystem DFT using coupled equations of FDET
GGA:[188,308,309]	Generalized Gradient Approximation, semilocal approximations in DFT for exchange-, correlation-, and kinetic-energy functionals, in which the density of the energy is expressed by means of a function depending on electron density and its gradients which differs from that of gradient expansion approximation
IHFSCC:[262−264]	Intermediate Hamiltonian Fock-Space Coupled-Cluster method
KSCED:	Kohn−Sham equations with Constrained Electron Density (eqs 20−21 in ref 44)
LDA:[51]	Local Density Approximation, approximation in DFT for exchange-, correlation-, and kinetic-energy functionals, in which the density of the energy is expressed by means of a function depending only on electron density derived from properties of uniform electron gas
LR-TDDFT:[181]	Linear-Response Time-Dependent DFT, formulation of DFT for excited states
NDRE:[182]	Neglect of the Dynamic Response of the Environment, approximation in subsystem DFT for excited states[152]
MPn:[310]	Møller−Plesset perturbation theory (n denotes the order)
MRSDCI:[311]	Multireference Singles-and-Doubles CI
ONIOM:[56]	Energy error compensation scheme for approximate methods (eq 60 in the present work)
orbital-free DFT:[73]	A class of simulation methods being modern realizations of the Thomas-Fermi model[72]
partition DFT:[53,54]	formulation of DFT
PCM:[12]	Polarizable Continuum Model of the solvent for embedding calculations
subsystem DFT:[52]	Formulation of DFT
QM/MM:	Quantum Mechanical/Molecular Mechanics methods, generic term used in the present work for embedding methods using classical descriptors for the environment
WFT:	WaveFunction Theory, generic term used in the present work for conventional methods of quantum chemistry based on approximations to the wavefunction and not on the Hamiltonian
3D-RISM:[245]	Classical statistical-mechanical model for liquids
3-FDE:[221]	A scheme to compensate the errors in approximations to $T_s^{nad}[\rho_A,\rho_B]$ in subsystem DFT calculations by introducing capping atoms

REFERENCES

(1) Schleyer, P. R., Ed.; *Encyclopedia of Computational Chemistry*; John Wiley & Sons, Ltd.: New York, 1998.
(2) Cramer, C. J. *Essentials of Computational Chemistry: Theories and Models*; Wiley: New York, 2005.
(3) Szabo, A., Ostlund, N. S. *Modern Quantum Chemistry. Introduction to Advanced Electronic Structure Theory*; McGraw-Hill: New York, 1982.
(4) Helgaker, T., Olsen, J., Jorgensen, P. *Molecular Electronic-Structure Theory*; Wiley: New York, 2013.
(5) Åquist, J.; Warshel, A. Simulation of Enzyme-Reactions Using Valence-Bond Force-Fields and Other Hybrid Quantum-Classical Approaches. *Chem. Rev.* **1993**, *93*, 2523−2544.

DOI: 10.1021/cr500502v
Chem. Rev. 2015, 115, 5891−5928

(6) Bakowies, D.; Thiel, W. Hybrid Models for Combined Quantum Mechanical and Molecular Mechanical Approaches. *J. Phys. Chem.* **1996**, *100*, 10580−10594.
(7) Cramer, C. J.; Truhlar, D. G. Implicit Solvation Models: Equilibria, Structure, Spectra, and Dynamics. *Chem. Rev.* **1999**, *99*, 2161−2200.
(8) Sauer, J.; Ugliengo, P.; Garrone, E.; Sounders, V. Theoretical Study of van der Waals Complexes at Surface Sites in Comparison with the Experiment. *Chem. Rev.* **1994**, *94*, 2095.
(9) Tomasi, J.; Mennucci, B.; Cammi, R. Quantum Mechanical Continuum Solvation Models. *Chem. Rev.* **2005**, *105*, 2999−3093.
(10) Senn, H. M.; Thiel, W. QM/MM Methods for Biomolecular Systems. *Angew. Chem., Int. Ed.* **2009**, *48*, 1198−1229.
(11) Gao, J. *Reviews in computational chemistry*; VCH Publishers, Inc.: Weinheim, Germany, 1996; Vol. 7, pp 119−186.
(12) Mennucci, B.; Tomasi, J. Continuum Solvation Models: A New Approach to the Problem of Solutes Charge Distribution and Cavity Boundaries. *J. Chem. Phys.* **1997**, *106*, 5151−5158.
(13) Klamt, A.; Schüürmann, G. COSMO: A New Approach to Dielectric Screening in Solvents with Explicit Expressions for the Screening Energy and its Gradient. *J. Chem. Soc., Perkin Trans. 2* **1993**, 799−805.
(14) Phillips, J. C.; Kleinman, L. New Method for Calculating Wave Functions in Crystals and Molecules. *Phys. Rev.* **1959**, *116*, 287−294.
(15) Barandiaran, Z.; Seijo, L. The Ab Initio Model Potential Representation of the Crystalline Environment - Theoretical-Study of the Local Distortion on NaCl-Cu^+. *J. Chem. Phys.* **1988**, *89*, 5739−5746.
(16) Katsuki, S. The Spectral Representation Technique for an Active-Electron-Only Molecular-Orbital Calculation Applied to the Case of Nonspherical Frozen Charge. *J. Chem. Phys.* **1993**, *98*, 496−501.
(17) Ohta, K.; Yoshioka, Y.; Morokuma, K.; Kitaura, K. The Effective Fragment Potential Method - An Approximate Ab initio MO Method for Large Molecules. *Chem. Phys. Lett.* **1983**, *101*, 12−17.
(18) Poteau, R.; Ortega, I.; Alary, F.; Solis, A.; Barthelat, J.; Daudey, J. Effective Group Potentials. 1. Method. *J. Phys. Chem. A* **2001**, *105*, 198−205.
(19) Simons, G.; A, M. Atomic and Molecular Pseudopotential Studies Using Gaussian Orbitals. *J. Chem. Phys.* **1970**, *52*, 2449.
(20) Vonarnim, M.; Peyerimhoff, S. D. Effective Potentials for Spectator Groups in Molecular-Systems - Transition Energies and Transition Moments. *Chem. Phys. Lett.* **1993**, *210*, 488−494.
(21) Colle, R.; Curoni, A.; Salvetti, O. A Nonlocal Representation of the Effective Potential Due to a Molecular Fragment. *Theor. Chim. Acta* **1993**, *86*, 451−465.
(22) Whitten, J. Theoretical-Studies of Surface-Reactions - Embedded-Cluster Theory. *Chem. Phys.* **1993**, *177*, 387−397.
(23) Assfeld, X.; Rivail, J. Quantum Chemical Computations on Parts of Large Molecules: The Ab Initio Local Self Consistent Field Method. *Chem. Phys. Lett.* **1996**, *263*, 100−106.
(24) Duarte, H. A.; Salahub, D. R. Embedded Cluster Model for Chemisorption Using Density Functional Calculations: Oxygen Adsorption on the Al(100) Surface. *J. Chem. Phys.* **1998**, *108*, 743−756.
(25) Beran, G. J. O.; Hirata, S. Fragment and Localized Orbital Methods in Electronic Structure Theory. *Phys. Chem. Chem. Phys.* **2012**, *14*, 7559−7561.
(26) Moriarty, J. A.; Phillips, R. 1^{st}-Principles Interatomic Potentials for Transition-Metal Surfaces. *Phys. Rev. Lett.* **1991**, *66*, 3036−3039.
(27) Stoll, H.; Paulus, B.; Fulde, P. On the Accuracy of Correlation-Energy Expansions in Terms of Local Increments. *J. Chem. Phys.* **2005**, *123*, 144108.
(28) Mata, R. A.; Werner, H.-J.; Schütz, M. Correlation Regions Within a Localized Molecular Orbital Approach. *J. Chem. Phys.* **2008**, *128*, 144106.
(29) Henderson, T. M. Embedding Wave Function Theory in Density Functional Theory. *J. Chem. Phys.* **2006**, *125*, 014105.
(30) Huzinaga, S.; Cantu, A. A. Theory of Separability of Many Electron Systems. *J. Chem. Phys.* **1971**, *55*, 5543−5549.
(31) Rajchel, Ł; Żuchowski, P. S.; Szcześniak, M. M.; Chałasiński, G. Density Functional Theory Approach to Noncovalent Interactions via Monomer Polarization and Pauli Blockade. *Phys. Rev. Lett.* **2010**, *104*, 163001.
(32) Pruitt, S. R.; Addicoat, M. A.; Collins, M. A.; Gordon, M. S. The Fragment Molecular Orbital and Systematic Molecular Fragmentation Methods Applied to Water Clusters. *Phys. Chem. Chem. Phys.* **2012**, *14*, 7752−7764.
(33) Winter, N. W.; Pitzer, R. M.; Temple, D. K. Theoretical-Study of a Cu^+ Ion Impurity in a NaF Host. *J. Chem. Phys.* **1987**, *86*, 3549−3556.
(34) Sugano, S.; Shulman, R. Covalency Effects in $KNiF_3$.III. Theoretical Studies. *Phys. Rev.* **1963**, *130*, 517.
(35) Laio, A.; VandeVondele, J.; Rothlisberger, U. A Hamiltonian Electrostatic Coupling Scheme for Hybrid Car-Parrinello Molecular Dynamics Simulations. *J. Chem. Phys.* **2002**, *116*, 6941−6947.
(36) Fradelos, G.; Wesolowski, T. A. Importance of the Intermolecular Pauli Repulsion in Embedding Calculations for Molecular Properties: The Case of Excitation Energies for a Chromophore in Hydrogen-Bonded Environments. *J. Phys. Chem. A* **2011**, *115*, 10018−10026.
(37) Fradelos, G.; Wesolowski, T. A. The Importance of Going beyond Coulombic Potential in Embedding Calculations for Molecular Properties: The Case of Iso-G for Biliverdin in Protein-Like Environment. *J. Chem. Theory Comput.* **2011**, *7*, 213−222.
(38) Valderrama, E.; Wheatley, R. J. An Environmental Pseudopotential Approach to Molecular Interactions: Implementation in MOLPRO. *J. Comput. Chem.* **2003**, *24*, 2075−2082.
(39) Vaidehi, N.; Wesolowski, T. A.; Warshel, A. Quantum-Mechanical Calculations of Solvation Free-Energies. A Combined Ab Initio Pseudopotential Free-Energy Perturbation Approach. *J. Chem. Phys.* **1992**, *97*, 4264−4271.
(40) Zheng, H. One-Electron Approach and the Theory of the Self-Consistent Cluster-Embedding Calculation Method. *Phys. Lett. A* **1997**, *226*, 223−230.
(41) Zheng, H. Self-Consistent Cluster-Embedding Calculation Method and the Calculated Electronic Structure of NiO. *Phys. Rev. B* **1993**, *48*, 14868−14883.
(42) Zheng, H. Electronic Structures of *Ascaris* Trypsin Inhibitor in Solution. *Phys. Rev. E* **2003**, *68*, 051908.
(43) Day, P. N.; Jensen, J. H.; Gordon, M. S.; Webb, S. P.; Stevens, W. J.; Krauss, M.; Garmer, D.; Basch, H.; Cohen, D. An Effective Fragment Method for Modeling Solvent Effects in Quantum Mechanical Calculations. *J. Chem. Phys.* **1996**, *105*, 1968−1986.
(44) Wesolowski, T. A.; Warshel, A. Frozen Density Functional Approach for Ab Initio Calculations of Solvated Molecules. *J. Phys. Chem.* **1993**, *97*, 8050−8053.
(45) Wesolowski, T. A. Embedding a Multideterminantal Wave Function in an Orbital-Free Environment. *Phys. Rev. A* **2008**, *77*, 012504.
(46) Pernal, K.; Wesolowski, T. A. Orbital-Free Effective Embedding Potential: Density-Matrix Functional Theory Case. *Int. J. Quantum Chem.* **2009**, *109*, 2520−2525.
(47) Savin, A.; Wesolowski, T. A. Orbital-Free Embedding Effective Potential in Analytically Solvable Cases. *Prog. Theor. Chem. Phys.* **2009**, *19*, 327−339.
(48) Wesolowski, T. A., Savin, A. Recent Progress in Computational Chemistry. In *Recent Progress in Orbital-Free Density Functional Theory*; Wesolowski, T., Wang, Y., Eds.; World Scientific: Singapore, 2013; Vol. 6, pp 277−295.
(49) Kohn, W.; Sham, L. J. Self-Consistent Equations Including Exchange and Correlation Effects. *Phys. Rev.* **1965**, *140*, A1133−A1138.
(50) Levy, M. Electron-Densities in Search of Hamiltonians. *Phys. Rev. A* **1982**, *26*, 1200−1208.
(51) Hohenberg, P.; Kohn, W. Inhomogeneous Electron Gas. *Phys. Rev. B* **1964**, *136*, B864−B871.
(52) Cortona, P. Self-Consistently Determined Properties of Solids Without Band-Structure Calculations. *Phys. Rev. B* **1991**, *44*, 8454−8458.
(53) Elliott, P.; Cohen, M. H.; Wasserman, A.; Burke, K. Density Functional Partition Theory with Fractional Occupations. *J. Chem. Theory Comput.* **2009**, *5*, 827−833.

DOI: 10.1021/cr500502v
Chem. Rev. 2015, 115, 5891−5928

(54) Elliott, P.; Burke, K.; Cohen, M. H.; Wasserman, A. Partition Density-Functional Theory. *Phys. Rev. A* **2010**, *82*, 024501.
(55) Wesolowski, T. A.; Weber, J. Kohn-Sham Equations with Constrained Electron Density: An Iterative Evaluation of the Ground-State Electron Density of Interacting Molecules. *Chem. Phys. Lett.* **1996**, *248*, 71−76.
(56) Svensson, M.; Humbel, S.; Froese, R. D. J.; Matsubara, T.; Sieber, S.; Morokuma, K. NIOM: A Multilayered Integrated MO+MM Method for Geometry Optimizations and Single Point Energy Predictions. A Test for Diels-Alder Reactions and $Pt(P(t\text{−}Bu)_3)_2+H_2$ Oxidative Addition. *J. Phys. Chem.* **1996**, *100*, 19357−19363.
(57) Govind, N.; Wang, Y.; da Silva, A.; Carter, E. Accurate Ab Initio Energetics of Extended Systems via Explicit Correlation Embedded in a Density Functional Environment. *Chem. Phys. Lett.* **1998**, *295*, 129−134.
(58) Govind, N.; Wang, Y. A.; Carter, E. A. Electronic-Structure Calculations By First-Principles Density- Based Embedding of Explicitly Correlated Systems. *J. Chem. Phys.* **1999**, *110*, 7677−7688.
(59) Libisch, F.; Huang, C.; Carter, E. A. Embedded Correlated Wavefunction Schemes: Theory and Applications. *Acc. Chem. Res.* **2014**, *47*, 2768−2775.
(60) Wesolowski, T. A. One-Electron Equations for Embedded Electron Density: Challenge for Theory and Practical Payoffs in Multi-Level Modelling of Soft Condensed Matter. In *Computational Chemistry: Reviews of Current Trends*; Leszczynski, J., Ed.; World Scientific: Singapore, 2006; Vol. *X*, pp 1−82.
(61) Neugebauer, J. Chromophore-Specific Theoretical Spectroscopy: From Subsystem Density Functional Theory to Mode-Specific Vibrational Spectroscopy. *Phys. Rep.* **2010**, *489*, 1−87.
(62) Gomes, A. S. P.; Jacob, C. R. Quantum-Chemical Embedding Methods for Treating Local Electronic Excitations in Complex Chemical Systems. *Ann. Rep. Prog. Chem., Sect. C: Phys. Chem.* **2012**, *108*, 222−277.
(63) Jacob, C. R.; Neugebauer, J. Subsystem Density-Functional Theory. *Wiley Interdiscip. Rev. Comput. Mol. Sci.* **2014**, *4*, 325−362.
(64) Bendavid, L. I.; Carter, E. A. *Status in Calculating Electronic Excited States in Transition Metal Oxides from First Principles*; Springer: New York, 2014; pp 1−52.
(65) Yang, W. Direct Calculation of Electron Density in Density-Functional Theory. *Phys. Rev. Lett.* **1991**, *66*, 1438.
(66) Knizia, G.; Chan, G. K.-L. Density Matrix Embedding: A Simple Alternative to Dynamical Mean-Field Theory. *Phys. Rev. Lett.* **2012**, *109*, 186404.
(67) Knizia, G.; Chan, G. K.-L. Density Matrix Embedding: A Strong-Coupling Quantum Embedding Theory. *J. Chem. Theory Comput.* **2013**, *9*, 1428−1432.
(68) Goodpaster, J. D.; Barnes, T. A.; Manby, F. R.; Miller, T. F. Accurate and Systematically Improvable Density Functional Theory Embedding for Correlated Wavefunctions. *J. Chem. Phys.* **2014**, *140*, 18A507.
(69) Pruitt, S. R.; Bertoni, C.; Brorsen, K. R.; Gordon, M. S. Efficient and Accurate Fragmentation Methods. *Acc. Chem. Res.* **2014**, *47*, 2786−2794.
(70) Thomas, L. The Calculation of Atomic Fields. *Proc. Cambridge Philos. Soc.* **1927**, *23*, 542−548.
(71) Fermi, E. A. Statistical Method for Determining Some Properties of the Atoms and its Application to the Theory of the Periodic Table of Elements. *Z. Phys.* **1928**, *48*, 73−79.
(72) Wang, Y. A., Carter, E. A. Orbital-Free Kinetic Energy Functional Theory. In Theoretical Methods in Condensed Phase Chemistry; Kluwer: Amsterdam, 2000; pp 117−184.
(73) Wesolowski, T., Wang, Y., Eds.; Recent Progress in Orbital-Free Density Functional Theory. In *Recent Progress in Computational Chemistry*; World Scientific: Singapore, 2013; Vol. *6*.
(74) Harris, J. Adiabatic-Connection Approach to Kohn-Sham Theory. *Phys. Rev. A* **1984**, *29*, 1648−1659.
(75) Gunnarsson, O.; Lundqvist, B. I. Exchange and Correlation in Atoms, Molecules, and Solids by Spin-Density Functional Formalism. *Phys. Rev. B* **1976**, *13*, 4274−4298.
(76) Langreth, D.; Perdew, J. Exchange-Correlation Energy of a Metallic Surface-Wave-Vector Analysis. *Phys. Rev. B* **1977**, *15*, 2884−2901.
(77) Savin, A. In *Recent Advances in Computational Chemistry*; Chong, D., Ed.; World Scientific: Singapore, 1995; Vol. *I*, Part 1, pp 123−153.
(78) Roos, B. O.; Linse, P.; Siegbahn, P. E.; Blomberg, M. R. A. A Simple Method for the Evaluation of the Second-Order-Perturbation Energy from External Double-Excitations with a CASSCF Reference Wavefunction. *Chem. Phys.* **1982**, *66*, 197−207.
(79) Roos, B. O. In *Lecture Notes in Quantum Chemistry*; Roos, B. O., Ed.; Springer-Verlag: Berlin, 1992; pp 177−254.
(80) Jacob, C. R.; Beyhan, S. M.; Visscher, L. Exact Functional Derivative of the Nonadditive Kinetic-Energy Bifunctional in the Long-Distance Limit. *J. Chem. Phys.* **2007**, *126*, 234116.
(81) Goodpaster, J. D.; Ananth, N.; Manby, F. R.; Miller, T. F., III Exact Nonadditive Kinetic Potentials for Embedded Density Functional Theory. *J. Chem. Phys.* **2010**, *133*, 084103.
(82) Laricchia, S.; Fabiano, E.; Della Sala, F. Frozen Density Embedding Calculations with the Orbital-Dependent Localized Hartree-Fock Kohn-Sham Potential. *Chem. Phys. Lett.* **2011**, *518*, 114−118.
(83) Tamukong, P. K.; Khait, Y. G.; Hoffmann, M. R. Density Differences in Embedding Theory with External Orbital Orthogonality. *J. Phys. Chem. A* **2014**, DOI: 10.1021/jp5062495.
(84) Senatore, G.; Subbaswamy, K. R. Density Dependence of the Dielectric-Constant of Rare-Gas Crystals. *Phys. Rev. B* **1986**, *34*, 5754−5757.
(85) Kaduk, B.; Kowalczyk, T.; Van Voorhis, T. Constrained Density Functional Theory. *Chem. Rev.* **2011**, *112*, 321−370.
(86) Wu, Q.; Van Voorhis, T. Direct Optimization Method to Study Constrained Systems Within Density-Functional Theory. *Phys. Rev. A* **2005**, *72*, 024502.
(87) Lieb, E. Density Functionals for Coulomb-Systems. *Int. J. Quantum Chem.* **1983**, *24*, 243−277.
(88) Baroni, S.; Tuncel, E. Exact-Exchange Extension of the Local-Spin-Density Approximation in Atoms - Calculation of Total Energies and Electron-Affinities. *J. Chem. Phys.* **1983**, *79*, 6140−6144.
(89) Aquilante, F.; Wesolowski, T. A. Self-Consistency in Frozen-Density Embedding Theory Based Calculations. *J. Chem. Phys.* **2011**, *135*, 084120.
(90) Savin, A. Towards a Systematic Way to Correct Density Functional Approximations. *J. Chem. Phys.* **2014**, *140*, 18A509.
(91) Toulouse, J.; Colonna, F.; Savin, A. Long-Range-Short-Range Separation of the Electron-Electron Interaction in Density-Functional Theory. *Phys. Rev. A* **2004**, *70*, 062505.
(92) Wesolowski, T. A. Exact Inequality Involving the Kinetic Energy Functional $Ts[\rho]$ and Pairs of Electron Densities. *J. Phys. A: Math. Gen* **2003**, *36*, 10607−10613.
(93) Heine, V. The Pseudopotential Concept. In *Solid State Physics*; Ehrenreich, H. F. S., Turnbull, D., Eds.; Academic Press: New York, 1970; Vol. *24*, pp 1−36.
(94) Schwerdtfeger, P. The Pseudopotential Approximation in Electronic Structure Theory. *ChemPhysChem* **2011**, *12*, 3143−3155.
(95) Rajchel, Ł; Żuchowski, P. S.; Szcześniak, M. M.; Chałasiński, G. Derivation of the Supermolecular Interaction Energy from the Monomer Densities in the Density Functional Theory. *Chem. Phys. Lett.* **2010**, *486*, 160−165.
(96) Manby, F. R.; Stella, M.; Goodpaster, J. D.; Miller, T. F., III A Simple, Exact Density-Functional-Theory Embedding Scheme. *J. Chem. Theory Comput.* **2012**, *8*, 2564−2568.
(97) Khait, Y. G.; Hoffmann, M. R.; Wheeler, R. On the Orthogonality of Orbitals in Subsystem Kohn-Sham Density Functional Theory. *Annu. Rep. Comput. Chem.* **2012**, *8*, 53.
(98) Wang, B.; Stott, M. J. First-Principles Local Pseudopotentials for Group-IV Elements. *Phys. Rev. B* **2003**, *68*, 195102.
(99) Stefanovich, E. V.; Truong, T. N. Embedded Density Functional Approach for Calculations of Adsorption on Ionic Crystals. *J. Chem. Phys.* **1996**, *104*, 2946−2955.

DOI: 10.1021/cr500502v
Chem. Rev. 2015, 115, 5891−5928

(100) Dulak, M.; Wesolowski, T. A. On the Electron Leak Problem in Orbital-Free Embedding Calculationss. *J. Chem. Phys.* **2006**, *124*, 164101.
(101) Zhou, B.; Wang, Y.; Carter, E. Transferable Local Pseudopotentials Derived via Inversion of the Kohn-Sham Equations in a Bulk Environment. *Phys. Rev. B* **2004**, *69*, 125109.
(102) Stone, A. The Theory of Intermolecular Forces. In *The International Series of Monographs on Chemistry*; Oxford University Press: Oxford, U.K., 1997.
(103) Engkvist, O.; Åstrand, P.-O.; Karlström, G. Accurate Intermolecular Potentials Obtained from Molecular Wave Functions:-Bridging the Gap between Quantum Chemistry and Molecular Simulations. *Chem. Rev.* **2000**, *100*, 4087−4108.
(104) Gresh, N.; Cisneros, G. A.; Darden, T. A.; Piquemal, J.-P. Anisotropic, Polarizable Molecular Mechanics Studies of Inter- and Intramoecular Interactions and Ligand-Macromolecule Complexes. A Bottom-Up Strategy. *J. Chem. Theory Comput.* **2007**, *3*, 1960−1986.
(105) Poulsen, T. D.; Ogilby, P. R.; Mikkelsen, K. V. Linear Response Properties for Solvated Molecules Described by a Combined Multi-configurational Self-Consistent-Field/Molecular Mechanics Model. *J. Chem. Phys.* **2002**, *116*, 3730−3738.
(106) Gritsenko, O. Recent Progress in Orbital-Free Density Functional Theory. In *Recent Progress in Computational Chemistry*; Wesolowski, T., Wang, Y., Eds.; World Scientific: Singapore, 2013; Vol. 6, pp 355−365.
(107) Humbert-Droz, M.; Zhou, X.; Shedge, S. V.; Wesolowski, T. A. How to Choose the Frozen Density in Frozen-Density Embedding Theory-Based Numerical Simulations of Local Excitations? *Theor. Chem. Acc.* **2014**, *133*, 1−20.
(108) Wesolowski, T. A. Density Functional Theory with Approximate Kinetic Energy Functionals Applied to Hydrogen Bonds. *J. Chem. Phys.* **1997**, *106*, 8516−8526.
(109) Neugebauer, J.; Jacob, C. R.; Wesolowski, T. A.; Baerends, E. J. An Explicit Quantum Chemical Method for Modeling Large Solvation Shells Applied to Aminocoumarin C151. *J. Phys. Chem. A* **2005**, *109*, 7805−7814.
(110) Gotz, A. W.; Beyhan, S. M.; Visscher, L. Performance of Kinetic Energy Functionals for Interaction Energies in a Subsystem Formulation of Density Functional Theory. *J. Chem. Theory Comput.* **2009**, *5*, 3161−3174.
(111) Jacob, C. R.; Wesolowski, T. A.; Visscher, L. Orbital-Free Embedding Applied to the Calculation of Induced Dipole Moments in CO_2···X (X=He, Ne, Ar, Kr, Xe, Hg) van der Waals Complexes. *J. Chem. Phys.* **2005**, *123*, 174104.
(112) Dulak, M.; Wesolowski, T. A. Interaction Energies in Non-Covalently Bound Intermolecular Complexes Derived Using the Subsystem Formulation of Density Functional Theory. *J. Mol. Model.* **2007**, *13*, 631−642 International Conference and Workshop on Modeling and Design of Molecular Materials, Wroclaw, Poland, Sep 10−15, 2006.
(113) Neugebauer, J. On the Calculation of General Response Properties in Subsystem Density Functional Theory. *J. Chem. Phys.* **2009**, *131*, 084104.
(114) Jacob, C. J.; Neugebauer, J.; Jensen, L.; Visscher, L. Comparison of Frozen-Density Embedding and Discrete Reaction Field Solvent Models for Molecular Properties. *Phys. Chem. Chem. Phys.* **2006**, *8*, 2349−2359.
(115) Jacob, C. R.; Visscher, L. Calculation of Nuclear Magnetic Resonance Shieldings Using Frozen-Density Embedding. *J. Chem. Phys.* **2006**, *125*, 194104.
(116) Fux, S.; Jacob, C. R.; Neugebauer, J.; Visscher, L.; Reiher, M. Accurate Frozen-Density Embedding Potentials as a First Step Towards a Subsystem Description of Covalent Bonds. *J. Chem. Phys.* **2010**, *132*, 164101.
(117) Neugebauer, J.; Louwerse, M. J.; Belanzoni, P.; Wesolowski, T. A.; Baerends, E. J. Modeling Solvent Effects on Electron-Spin-Resonance Hyperfine Couplings by Frozen-Density Embedding. *J. Chem. Phys.* **2005**, *123*, 114101.
(118) Neugebauer, J.; Veldstra, J.; Buda, F. Theoretical Spectroscopy of Astaxanthin in Crustacyanin Proteins: Absorption, Circular Dichroism, and Nuclear Magnetic Resonance. *J. Phys. Chem. B* **2011**, *115*, 3216−3225.
(119) Götz, A. W.; Autschbach, J.; Visscher, L. Calculation of Nuclear Spin-Spin Coupling Constants Using Frozen Density Embedding. *J. Chem. Phys.* **2014**, *140*, 104107.
(120) Bulo, R. E.; Jacob, C. R.; Visscher, L. NMR Solvent Shifts of Acetonitrile from Frozen Density Embedding Calculations. *J. Phys. Chem. A* **2008**, *112*, 2640−2647.
(121) Fux, S.; Kiewisch, K.; Jacob, C. R.; Neugebauer, J.; Reiher, M. Analysis of Electron Density Distributions from Subsystem Density Functional Theory Applied to Coordination Bonds. *Chem. Phys. Lett.* **2008**, *461*, 353−359.
(122) Kiewisch, K.; Eickerling, G.; Reiher, M.; Neugebauer, J. Topological Analysis of Electron Densities from Kohn-Sham and Subsystem Density Functional Theory. *J. Chem. Phys.* **2008**, *128*, 044114.
(123) Neugebauer, J.; Baerends, E. J. Exploring the Ability of Frozen-Density Embedding to Model Induced Circular Dichroism. *J. Phys. Chem. A* **2006**, *110*, 8786−8796.
(124) Kevorkyants, R.; Dulak, M.; Wesolowski, T. A. Interaction Energies in Hydrogen-Bonded Systems: A Testing Ground for Subsystem Formulation of Density-Functional Theory. *J. Chem. Phys.* **2006**, *124*, 024104.
(125) Wesolowski, T. A.; Morgantini, P. Y.; Weber, J. Intermolecular Interaction Energies from the Total Energy Bifunctional: A Case Study of Carbazole Complexes. *J. Chem. Phys.* **2002**, *116*, 6411−6421.
(126) Laricchia, S.; Constantin, L. A.; Fabiano, E.; Della Sala, F. Laplacian-Level Kinetic Energy Approximations Based on the Fourth-Order Gradient Expansion: Global Assessment and Application to the Subsystem Formulation of Density Functional Theory. *J. Chem. Theory Comput.* **2014**, *10*, 164−179.
(127) Dułak, M., Wesołowski, T. A. In *Lecture Series on Computer and Computational Sciences*; Simos, T., Maroulis, G., Eds.; VSP/Brill: Leiden, The Netherlands, 2005; Vol. 3, pp 282−288.
(128) Wesolowski, T. A.; Chermette, H.; Weber, J. Accuracy of Approximate Kinetic Energy Functionals in the Model of Kohn-Sham Equations with Constrained Electron Density: The FH ··· NCH Complex as a Test Case. *J. Chem. Phys.* **1996**, *105*, 9182−9190.
(129) Wesolowski, T. A.; Weber, J. Kohn-Sham Equations with Constrained Electron Density: The Effect of Various Kinetic Energy Functional Parametrizations on the Ground-State Molecular Properties. *Int. J. Quantum Chem.* **1997**, *61*, 303−311.
(130) Bernard, Y. A.; Dulak, M.; Kaminski, J. W.; Wesolowski, T. A. The Energy-Differences Based Exact Criterion for Testing Approximations to the Functional for the Kinetic Energy of Non-Interacting Electrons. *J. Phys. A: Math. Theor.* **2008**, *41*, 055302.
(131) Lastra, J. M. G.; Kaminski, J. W.; Wesolowski, T. A. Orbital-Free Effective Embedding Potential at Nuclear Cusps. *J. Chem. Phys.* **2008**, *129*, 074107.
(132) Laricchia, S.; Fabiano, E.; Della Sala, F. On the Accuracy of Frozen Density Embedding Calculations with Hybrid and Orbital-Dependent Functionals for Non-Bonded Interaction Energies. *J. Chem. Phys.* **2012**, *137*, 014102.
(133) Laricchia, S.; Fabiano, E.; Della Sala, F. Semilocal and Hybrid Density Embedding Calculations of Ground-State Charge-Transfer Complexes. *J. Chem. Phys.* **2013**, *138*, 124112.
(134) Dulak, M.; Wesolowski, T. A. The Basis Set Effect on the Results of the Minimization of the Total Energy Bifunctional E[P-A,P-B]. *Int. J. Quantum Chem.* **2005**, *101*, 543−549.
(135) Gilbert, T. L. Hohenberg-Kohn Theorem for Nonlocal External Potentials. *Phys. Rev. B* **1975**, *12*, 2111.
(136) Parr, R. G.; Yang, W. *Density-Functional Theory of Atoms and Molecules*; Oxford: New York, 1989.
(137) de Silva, P.; Wesolowski, T. A. Pure-State Noninteracting *v*-Representability of Electron Densities from Kohn-Sham Calculations with Finite Basis Sets. *Phys. Rev. A* **2012**, *85*, 032518.

DOI: 10.1021/cr500502v
Chem. Rev. 2015, 115, 5891−5928

(138) Dirac, P. A. M. Note on Exchange Phenomena in the Thomas Atom. *Proc. Cambridge Philos. Soc.* **1930**, *26*, 376−385.
(139) Lundqvist, B. I.; Andersson, Y.; Shao, H.; Chan, S.; Langreth, D. C. Density-Functional Theory Including van-der-Waals Forces. *Int. J. Quantum Chem.* **1995**, *56*, 247−255.
(140) Andersson, Y.; Langreth, D. C.; Lundqvist, B. I. van der Waals Interactions in Density-Functional Theory. *Phys. Rev. Lett.* **1996**, *76*, 102−105.
(141) Rydberg, H.; Dion, M.; Jacobson, N.; Schroder, E.; Hyldgaard, P.; Simak, S. I.; Langreth, D. C.; Lundqvist, B. I. van der Waals Density Functional for Layered Structures. *Phys. Rev. Lett.* **2003**, *91*, 126402.
(142) Wesolowski, T. A. Approximating the Kinetic Energy Functional Ts[ρ]: Lessons from Four-Electron Systems. *Mol. Phys.* **2005**, *103*, 1165−1167.
(143) Borgoo, A.; Tozer, D. J. Density Scaling of Noninteracting Kinetic Energy Functionals. *J. Chem. Theory Comput.* **2013**, *9*, 2250−2255.
(144) Zhao, Q.; Morrison, R. C.; Parr, R. G. From Electron Densities to Kohn-Sham Kinetic Energies, Orbital Energies, Exchange-Correlation Potentials, and Exchange-Correlation Energies. *Phys. Rev. A* **1994**, *50*, 2138−2142.
(145) Boyer, L. L.; Mehl, M. J. A Self Consistent Atomic Deformation Model for Total Energy Calculations: Application to Ferroelectrics. *Ferroelectrics* **1993**, *150*, 13−24.
(146) Mehl, M. J.; Stokes, H. T.; Boyer, L. L. Development of a Kohn-Sham Like Potential in the Self-Consistent Atomic Deformation Model. *J. Phys. Chem. Solids* **1996**, *57*, 1405−1407.
(147) Mei, W. N.; Boyer, L. L.; Mehl, M. J.; Ossowski, M. M.; Stokes, H. T. Calculation of Electronic, Structural, and Vibrational Properties in Alkali Halides Using a Density-Functional Method with Localized Densities. *Phys. Rev. B* **2000**, *61*, 11425−11431.
(148) Kim, Y. S.; Gordon, R. G. Unified Theory for Intermolecular Forces Between Closed Shell Atoms and Ions. *J. Chem. Phys.* **1974**, *61*, 1−16.
(149) Ivanov, O. V.; Maksimov, E. G. Microscopic Calculations of Phonons in Polarizable-Ion Approach. *Phys. Rev. Lett.* **1992**, *69*, 108−111.
(150) Wesolowski, T. A.; Tran, F. Gradient-Free and Gradient-Dependent Approximations in the Total Energy Bifunctional for Weakly Overlapping Electron Densities. *J. Chem. Phys.* **2003**, *118*, 2072−2080.
(151) Dulak, M.; Kaminski, J. W.; Wesolowski, T. A. Equilibrium Geometries of Noncovalently Bound Intermolecular Complexes Derived from Subsystem Formulation of Density Functional Theory. *J. Chem. Theory Comput.* **2007**, *3*, 735−745.
(152) Casida, M. E.; Wesolowski, T. A. Generalization of the Kohn-Sham Equations with Constrained Electron Density Formalism and its Time-Dependent Response Theory Formulation. *Int. J. Quantum Chem.* **2004**, *96*, 577−588.
(153) Neugebauer, J. Couplings Between Electronic Transitions in a Subsystem Formulation of Time Dependent Density Functional Theory. *J. Chem. Phys.* **2007**, *97*, 134116.
(154) Pavanello, M. On the Subsystem Formulation of Linear-Response Time-Dependent DFT. *J. Chem. Phys.* **2013**, *138*, 204118.
(155) Neugebauer, J.; Curutchet, C.; Munoz-Losa, A.; Mennucci, B. A Subsystem TDDFT Approach for Solvent Screening Effects on Excitation Energy Transfer Couplings. *J. Chem. Theory Comput.* **2010**, *6*, 1843−1851.
(156) Pavanello, M.; Neugebauer, J. Modelling Charge Transfer Reactions with the Frozen Density Embedding Formalism. *J. Chem. Phys.* **2011**, *135*, 234103.
(157) Pavanello, M.; Van Voorhis, T.; Visscher, L.; Neugebauer, J. An Accurate and Linear-Scaling Method for Calculating Charge-Transfer Excitation Energies and Diabatic Couplings. *J. Chem. Phys.* **2013**, *138*, 054101.
(158) Warshel, A.; Weiss, R. An Empirical Valence Bond Approach for Comparing Reactions in Solutions and in Enzymes. *J. Am. Chem. Soc.* **1980**, *102*, 6218−6226.
(159) Warshel, A.; Florian, J. *Encyclopedia of Computational Chemistry*; John Wiley & Sons, Ltd.: New York, 2002.
(160) Wesolowski, T.; Muller, R. P.; Warshel, A. Ab Initio Frozen Density Functional Calculations of Proton Transfer Reactions in Solution. *J. Phys. Chem.* **1996**, *100*, 15444−15449.
(161) Štrajbl, M.; Hong, G.; Warshel, A. Ab Initio QM/MM Simulation with Proper Sampling:First Principle Calculations of The Free Energy of The Autodissociation of Water in Aqueous Solution. *J. Phys. Chem. B* **2002**, *106*, 13333−13343.
(162) Kevorkyants, R.; Eshuis, H.; Pavanello, M. DE-vdW: A van der Waals Inclusive Subsystem Density-Functional Theory. *J. Chem. Phys.* **2014**, *141*, 044127.
(163) Nafziger, J.; Wasserman, A. Density-Based Partitioning Methods for Ground-State Molecular Calculations. *J. Phys. Chem. A* **2014**, *118*, 7623−7639.
(164) Huang, C.; Carter, E. A. Potential-Functional Embedding Theory for Molecules and Materials. *J. Chem. Phys.* **2011**, *135*, 194104.
(165) Huang, C.; Pavone, M.; Carter, E. A. Quantum Mechanical Embedding Theory Based on a Unique Embedding Potential. *J. Chem. Phys.* **2011**, *134*, 154110.
(166) Fabiano, E.; Laricchia, S.; Sala, F. D. Frozen Density Embedding with Non-Integer Subsystems Particle Numbers. *J. Chem. Phys.* **2014**, *140*, 114101.
(167) Gritsenko, O. V.; Visscher, L. Density-Orbital Embedding Theory. *Phys. Rev. A* **2010**, *82*, 032519.
(168) Von Barth, U. Local-Density Theory of Multiplet Structure. *Phys. Rev. A* **1979**, *20*, 1693−1703.
(169) Englisch, H.; Englisch, R. Hohenberg-Kohn Theorem and Non-v-Representable Densities. *Physica A* **1983**, *121*, 253−268.
(170) Kutzler, F. W.; Painter, G. S. Energies of Atoms with Nonspherical Charge-Densities Calculated with Nonlocal Density-Functional Theory. *Phys. Rev. Lett.* **1987**, *59*, 1285−1288.
(171) Zbiri, M.; Atanasov, M.; Daul, C.; Garcia-Lastra, J. M.; Wesolowski, T. A. Application of the Density Orbital-Free Embedding Potential Functional Theory Derived to Calculate the Splitting Energies of Lanthanide Cations in Chloroelpasolite Crystals. *Chem. Phys. Lett.* **2004**, *397*, 441−446.
(172) Zbiri, M.; Daul, C. A.; Wesolowski, T. A. Effect of the f-Orbital Delocalization on the Ligand-Field Splitting Energies in Lanthanide-Containing Elpasolites. *J. Chem. Theory Comput.* **2006**, *2*, 1106−1111.
(173) Perdew, J. P.; Levy, M. Extrema of the Density Functional for the Energy - Excited-States from the Ground-State Theory. *Phys. Rev. B* **1985**, *31*, 6264−6272.
(174) Khait, Y. G.; Hoffmann, M. R. Embedding Theory for Excited States. *J. Chem. Phys.* **2010**, *133*, 044107.
(175) Daday, C.; König, C.; Valsson, O.; Neugebauer, J.; Filippi, C. State-Specific Embedding Potentials for Excitation-Energy Calculations. *J. Chem. Theory Comput.* **2013**, *9*, 2355−2367.
(176) Daday, C.; König, C.; Neugebauer, J.; Filippi, C. Wavefunction in Density Functional Theory Embedding for Excited States: Which Wavefunctions, which Densities? *ChemPhysChem* **2014**, *15*, 3205−3217.
(177) Wesolowski, T. A. Embedding Potentials for Excited States of Embedded Species. *J. Chem. Phys.* **2014**, *140*, 18A530.
(178) Perdew, J. P.; Ruzsinszky, A.; Constantin, L. A.; Sun, J.; Csonka, G. I. Some Fundamental Issues in Ground-State Density Functional Theory: A Guide for the Perplexed. *J. Chem. Theory Comput.* **2009**, *5*, 902−908.
(179) Klüner, T.; Govind, N.; Wang, Y. A.; Carter, E. A. Prediction of Electronic Excited States of Adsorbates on Metal Surfaces from First Principles. *Phys. Rev. Lett.* **2001**, *86*, 5954−5957.
(180) Höfener, S.; Gomes, A. S. P.; Visscher, L. Solvatochromic Shifts from Coupled-Cluster Theory Embedded in Density Functional Theory. *J. Chem. Phys.* **2013**, *139*, 104106.
(181) Casida, M. E. In *Recent Advances in Computational Chemistry*; Chong, D. P., Ed.; World Scientific: Singapore, 1995; Vol. *I*, Part 1, p 155.
(182) Wesolowski, T. A. Hydrogen-Bonding-Induced Shifts of the Excitation Energies in Nucleic Acid Bases: An Interplay Between Electrostatic and Electron Density Overlap Effects. *J. Am. Chem. Soc.* **2004**, *126*, 11444−11445.

DOI: 10.1021/cr500502v
Chem. Rev. 2015, 115, 5891−5928

(183) Fehrer, F.; Reinhard, P.; Suraud, E.; Giglio, E.; Gervais, B.; Ipatov, A. Linear and Non-Linear Response of Embedded Na Clusters. *Appl. Phys. A* **2006**, *82*, 151−159.
(184) Förster, T. Zwischenmolekulare Energiewanderung und Fluoreszenz. *Ann. Phys.* **1948**, *437*, 55−75.
(185) Dexter, D. L. A. Theory of Sensitized Luminescence in Solids. *J. Chem. Phys.* **1953**, *21*, 836−850.
(186) Marcus, R. A.; Sutin, N. Electron-Transfer Reactions with Unusual Activation Parameters - Treatment of Reactions Accompanied By Large Entropy Decreases. *Inorg. Chem.* **1975**, *14*, 213−216.
(187) Tran, F., Wesolowski, T. Recent Progress in Orbital-Free Density Functional Theory. In *Recent Progress in Computational Chemistry*; Wesolowski, T., Wang, Y., Eds.; World Scientific: Singapore, 2013; Vol. *6*, pp 429−442.
(188) Lee, H.; Lee, C. T.; Parr, R. G. Conjoint Gradient Correction to the Hartree-Fock Kinetic-Energy and Exchange-Energy Density Functionals. *Phys. Rev. A* **1991**, *44*, 768−771.
(189) March, N. H.; Santamaria, R. Nonlocal Relation Between Kinetic and Exchange Energy Densities in Hartree-Fock Theory. *Int. J. Quantum Chem.* **1991**, *39*, 585−592.
(190) Becke, A. D. Density-Functional Exchange-Energy Approximation with Correct Asymptotic-Behavior. *Phys. Rev. A* **1988**, *38*, 3098−3100.
(191) Fuentealba, P.; Reyes, O. Further Evidence of the Conjoint Correction to the Local Kinetic and Exchange Energy Density Functionals. *Chem. Phys. Lett.* **1995**, *232*, 31−34.
(192) Perdew, J. P.; Yue, W. Accurate and Simple Density Functional for the Electronic Exchange Energy - Generalized Gradient Approximation. *Phys. Rev. B* **1986**, *33*, 8800−8802.
(193) Lembarki, A.; Chermette, H. Obtaining a Gradient-Corrected Kinetic-Energy Functional from the Perdew-Wang Exchange Functional. *Phys. Rev. A* **1994**, *50*, 5328−5331.
(194) Perdew, J. P. In *Electronic Structure of Solids*; Ziesche, P., Eschrig, H., Eds.; Akademie Verlag: Berlin, 1991.
(195) Tran, F.; Wesolowski, T. A. Link Between the Kinetic- and Exchange-Energy Functionals in the Generalized Gradient Approximation. *Int. J. Quantum Chem.* **2002**, *89*, 441−446.
(196) Perdew, J. P.; Burke, K.; Ernzerhof, M. Generalized Gradient Approximation Made Simple. *Phys. Rev. Lett.* **1996**, *77*, 3865−3868.
(197) Karasiev, V. V.; Trickey, S. B.; Harris, F. E. Born-Oppenheimer Interatomic Forces from Simple, Local Kinetic Energy Density Functionals. *J. Comput.-Aided Mater. Des.* **2006**, *13*, 111−129.
(198) Adamo, C.; Barone, V. Physically Motivated Density Functionals with Improved Performances: The Modified Perdew-Burke-Ernzerhof Model. *J. Chem. Phys.* **2002**, *116*, 5933−5940.
(199) Constantin, L. A.; Fabiano, E.; Laricchia, S.; Della Sala, F. Semiclassical Neutral Atom as a Reference System in Density Functional Theory. *Phys. Rev. Lett.* **2011**, *106*, 186406.
(200) Laricchia, S.; Fabiano, E.; Constantin, L. A.; Della Sala, F. Generalized Gradient Approximations of the Noninteracting Kinetic Energy from the Semiclassical Atom Theory: Rationalization of the Accuracy of the Frozen Density Embedding Theory for Nonbonded Interactions. *J. Chem. Theory Comput.* **2011**, *7*, 2439−2451.
(201) Kirzhnits, D. A. Quantum Corrections to the Thomas-Fermi Equation. *Sov. Phys. JETP* **1957**, *5*, 64.
(202) von Weizsäcker, C. F. Regarding Theory of Nuclear Masses. *Z. Phys.* **1935**, *96*, 431.
(203) García-Lastra, J.; Wesolowski, T.; Barriuso, M.; Aramburu, J.; Moreno, M. Optical and Vibrational Properties of MnF_4^{-6} Complexes in Cubic Fluoroperovskites: Insight Through Embedding Calculations Using Kohn-Sham Equations with Constrained Electron Density. *J. Phys.: Condens. Matter* **2006**, *18*, 1519.
(204) König, C.; Neugebauer, J. Protein Effects on the Optical Spectrum of the Fenna-Matthews-Olson Complex from Fully Quantum Chemical Calculations. *J. Chem. Theory Comput.* **2013**, *9*, 1808−1820.
(205) Fradelos, G.; Kaminski, J. W.; Wesolowski, T. A.; Leutwyler, S. Cooperative Effect of Hydrogen-Bonded Chains in the Environment of a $\pi\pi^*$ Chromophore. *J. Phys. Chem. A* **2009**, *113*, 9766−9771.
(206) Fradelos, G.; Lutz, J. J.; Wesołowski, T. A.; Piecuch, P.; Włoch, M. Embedding vs Supermolecular Strategies in Evaluating the Hydrogen-Bonding-Induced Shifts of Excitation Energies. *J. Chem. Theory Comput.* **2011**, *7*, 1647−1666.
(207) Wesolowski, T. A. Application of the DFT-Based Embedding Scheme Using qn Explicit Functional of the Kinetic Energy to Determine the Spin Density of Mg^+ Embedded in Ne and Ar Matrices. *Chem. Phys. Lett.* **1999**, *311*, 87−92.
(208) Neugebauer, J.; Louwerse, M. J.; Baerends, E. J.; Wesolowski, T. A. The Merits of the Frozen-Density Embedding Scheme to Model Solvatochromic Shifts. *J. Chem. Phys.* **2005**, *122*, 094115.
(209) Gomes, A. S. P.; Jacob, C. R.; Visscher, L. Calculation of Local Excitations in Large Systems By Embedding Wave-Function Theory in Density-Functional Theory. *Phys. Chem. Chem. Phys.* **2008**, *10*, 5353−5362.
(210) Gomes, A. S. P.; Jacob, C. R.; Réal, F.; Visscher, L.; Vallet, V. Towards Systematically Improvable Models for Actinides in Condensed Phase: The Electronic Spectrum of Uranyl in $Cs_2UO_2Cl_4$ as a Test Case. *Phys. Chem. Chem. Phys.* **2013**, *15*, 15153−15162.
(211) Höfener, S. Coupled-Cluster Frozen-Density Embedding Using Resolution of the Identity Methods. *J. Comput. Chem.* **2014**, *35*, 1716−1724.
(212) Genova, A.; Ceresoli, D.; Pavanello, M. Periodic Subsystem Density-Functional Theory. *J. Chem. Phys.* **2014**, *141*, 174101.
(213) Tecmer, P.; Van Lingen, H.; Gomes, A. S. P.; Visscher, L. The Electronic Spectrum of $CuONg_4$ (Ng= Ne, Ar, Kr, Xe): New Insights in the Interaction of the CuO Molecule with Noble Gas Matrices. *J. Chem. Phys.* **2012**, *137*, 084308.
(214) Ludena, E. V., Karasiev, V. Kinetic Energy Functionals: History, Challeneges and Prospects in"Reviews of Modern Qunatum Chemistry. In *Reviews of Modern Quantum Chemistry*; World Scientific: Singapore, 2002; Vol. *1*, pp 612−665.
(215) de Silva, P.; Wesolowski, T. A. Exact Non-Additive Kinetic Potentials in Realistic Chemical Systems. *J. Chem. Phys.* **2012**, *137*, 094110.
(216) Beyhan, S. M.; Götz, A. W.; Jacob, C. R.; Visscher, L. The Weak Covalent Bond in NgAuF (Ng=Ar, Kr, Xe): A Challenge for Subsystem Density Functional Theory. *J. Chem. Phys.* **2010**, *132*, 044114.
(217) Seidl, A.; Görling, A.; Vogl, P.; Majewski, J. A.; Levy, M. Generalized Kohn-Sham Schemes and the Band-Gap Problem. *Phys. Rev. B* **1996**, *53*, 3764−3774.
(218) Laricchia, S.; Fabiano, E.; Della Sala, F. Frozen Density Embedding with Hybrid Functionals. *J. Chem. Phys.* **2010**, *133*, 164111.
(219) Schipper, P.; Gritsenko, S.; van Gisbergen, O. V.; Baerends, E. J. Molecular Calculations of Excitation Energies and (hyper)-Polarizabilities with a Statistical Average of Orbital Model Exchange-Correlation Potentials. *J. Chem. Phys.* **2000**, *112*, 1344−1352.
(220) Gritsenko, O.; Schipper, P.; Baerends, E. Approximation of the Exchange-Correlation Kohn-Sham Potential with a Statistical Average of Different Orbital Model Potentials. *Chem. Phys. Lett.* **1999**, *302*, 199−207.
(221) Jacob, C. R.; Visscher, L. A Subsystem Density-Functional Theory Approach for the Quantum Chemical Treatment of Proteins. *J. Chem. Phys.* **2008**, *128*, 155102.
(222) Oliver, G. L.; Perdew, J. P. Spin-Density Gradient Expansion for the Kinetic-Energy. *Phys. Rev. A* **1979**, *20*, 397−403.
(223) Kevorkyants, R.; Wang, X.; Close, D. M.; Pavanello, M. Calculating Hyperfine Couplings in Large Ionic Crystals Containing Hundreds of QM Atoms: Subsystem DFT Is the Key. *J. Phys. Chem. B* **2013**, *117*, 13967−13974.
(224) Solovyeva, A.; Pavanello, M.; Neugebauer, J. Spin Densities from Subsystem Density-Functional Theory: Assessment and Application to a Photosynthetic Reaction Center Complex Model. *J. Chem. Phys.* **2012**, *136*, 194104.
(225) Dulak, M.; Wesolowski, T. A. Nonlinearity of the Bifunctional of the Nonadditive Kinetic Energy: Numerical Consequences in Orbital-Free Embedding Calculations. *J. Chem. Theory Comput.* **2006**, *2*, 1538−1543.

DOI: 10.1021/cr500502v
Chem. Rev. 2015, 115, 5891−5928

(226) Dulak, M.; Kaminski, J. W.; Wesolowski, T. A. Linearized Orbital-Free Embedding Potential in Self-Consistent Calculations. *Int. J. Quantum Chem.* **2009**, *109*, 1886−1897.
(227) Staroverov, V.; Scuseria, G.; Davidson, E. Optimized Effective Potentials Yielding Hartree-Fock Energies and Densities. *J. Chem. Phys.* **2006**, *124*, 141103.
(228) Gritsenko, O. V.; van Leeuwen, R.; Baerends, E. J. Molecular Kohn-Sham Exchange-Correlation Potential from the Correlated Ab-Initio Electron-Density. *Phys. Rev. A* **1995**, *52*, 1870−1874.
(229) Wu, Q.; Yang, W. A Direct Optimization Method for Calculating Density Functionals and Exchange-Correlation Potentials from Electron Densities. *J. Chem. Phys.* **2003**, *118*, 2498−2509.
(230) Jacob, C. R. Unambiguous Optimization of Effective Potentials in Finite Basis Sets. *J. Chem. Phys.* **2011**, *135*, 244102.
(231) Roncero, O.; de Lara-Castells, M. P.; Villarreal, P.; Flores, F.; Ortega, J.; Paniagua, M.; Aguado, A. An Inversion Technique for the Calculation of Embedding Potentials. *J. Chem. Phys.* **2008**, *129*, 184104.
(232) Chai, J.-D.; Weeks, J. D. Orbital-Free Density Functional Theory: Kinetic Potentials and Ab Initio Local Pseudopotentials. *Phys. Rev. B* **2007**, *75*, 205122.
(233) Zhou, X.; Wesolowski, T. A.; Tabacchi, G.; Fois, E.; Calzaferri, G.; Devaux, A. First-Principles Simulation of the Absorption Bands of Fluorenone in Zeolite L. *Phys. Chem. Chem. Phys.* **2013**, *15*, 159−167.
(234) Neugebauer, J. Photophysical Properties of Natural Light-Harvesting Complexes Studied by Subsystem Density Functional Theory. *J. Phys. Chem. B* **2008**, *112*, 2207−2217.
(235) Wesolowski, T.; Warshel, A. Ab-Initio Free-Energy Perturbation Calculations of Solvation Free-Energy Using the Frozen Density-Functional Approach. *J. Phys. Chem.* **1994**, *98*, 5183−5187.
(236) Hong, G. Y.; Strajbl, M.; Wesolowski, T. A.; Warshel, A. Constraining the Electron Densities in DFT Method as an Effective Way for Ab Initio Studies of Metal-Catalyzed Reactions. *J. Comput. Chem.* **2000**, *21*, 1554−1561.
(237) Jacob, C. R.; Neugebauer, J.; Visscher, L. A Flexible Implementation of Frozen-Density Embedding for Use in Multilevel Simulations. *J. Comput. Chem.* **2008**, *29*, 1011−1018.
(238) Fradelos, G.; Kaminski, J. W.; Wesolowski, T. A.; Leutwyler, S. The Cooperative Effect of Hydrogen-Bonded Chains in the Environment of a $\pi \rightarrow \pi^*$ Chromophore. *J. Phys. Chem. A* **2009**, *113*, 9766.
(239) Gregory, J.; Clary, D.; Liu, K.; Brown, M.; Saykally, R. The Water Dipole Moment in Water Clusters. *Science* **1997**, *275*, 814−817.
(240) Kaminski, J. W.; Gusarov, S.; Wesolowski, T. A.; Kovalenko, A. Modeling Solvatochromic Shifts Using the Orbital-Free Embedding Potential at Statistically Mechanically Averaged Solvent Density. *J. Phys. Chem. A* **2010**, *114*, 6082.
(241) Hodak, M.; Lu, W.; Bernholc, J. Hybrid Ab Initio Kohn-Sham Density Functional Theory/Frozen-Density Orbital-Free Density Functional Theory Simulation Method Suitable for Biological Systems. *J. Chem. Phys.* **2008**, *128*, 014101.
(242) Coutinho, K.; Georg, H.; Fonseca, T.; Ludwig, V.; Canuto, S. An Efficient Statistically Converged Average Configuration for Solvent Effects. *Chem. Phys. Lett.* **2007**, *437*, 148−152.
(243) Fdez Galván, I.; Snchez, M.; Martin, M.; Olivares del Valle, F.; Aguilar, M. ASEP/MD: A Program for the Calculation of Solvent Effects Combining QM/MM Methods and the Mean Field Approximation. *Comput. Phys. Commun.* **2003**, *155*, 244−259.
(244) Zhou, X.; Kaminski, J. W.; Wesolowski, T. A. Multi-Scale Modelling of Solvatochromic Shifts from Frozen-Density Embedding Theory with Non-Uniform Continuum Model of the Solvent: The Coumarin 153 Case. *Phys. Chem. Chem. Phys.* **2011**, *13*, 10565−10576.
(245) Kovalenko, A. In *Molecular theory of solvation*; Hirata, F., Ed.; Springer: Amsterdam, The Netherlands, 2003; Vol. *24*, pp 169−275.
(246) Kovalenko, A.; Hirata, F. Self-Consistent Description of a Metal-Water Interface By the Kohn-Sham Density Functional Theory and the Three-Dimensional Reference Interaction Site Model. *J. Chem. Phys.* **1999**, *110*, 10095−10112.
(247) Shedge, S. V.; Wesolowski, T. A. Nonuniform Continuum Model for Solvatochromism Based on Frozen-Density Embedding Theory. *ChemPhysChem* **2014**, *15*, 3291−3300.
(248) Kiewisch, K.; Jacob, C. R.; Visscher, L. Quantum-Chemical Electron Densities of Proteins and of Selected Protein Sites from Subsystem Density Functional Theory. *J. Chem. Theory Comput.* **2013**, *9*, 2425−2440.
(249) Car, R.; Parrinello, M. Unified Approach for Molecular Dynamics and Density-Functional Theory. *Phys. Rev. Lett.* **1985**, *55*, 2471−2474.
(250) Jensen, L.; van Duijnen, P. T.; Snijders, J. G. A Discrete Solvent Reaction Field Model Within Density Functional Theory. *J. Chem. Phys.* **2003**, *118*, 514−521.
(251) Kongsted, J.; Osted, A.; Mikkelsen, K. V.; Christiansen, O. Linear Response Functions for Coupled Cluster/Molecular Mechanics Including Polarization Interactions. *J. Chem. Phys.* **2003**, *118*, 1620−1633.
(252) Höfener, S.; Visscher, L. Calculation of Electronic Excitations Using Wave-Function in Wave-Function Frozen-Density Embedding. *J. Chem. Phys.* **2012**, *137*, 204120.
(253) Goez, A.; Jacob, C. R.; Neugebauer, J. Modeling Environment Effects on Pigment Site Energies: Frozen Density Embedding with Fully Quantum-Chemical Protein Densits. *Comput. Theor. C* **2014**, *1040−1041*, 347−359.
(254) Zhou, X.; Sundholm, D.; Wesołowski, T. A.; Kaila, V. R. Spectral Tuning of Rhodopsin and Visual Cone Pigments. *J. Am. Chem. Soc.* **2014**, *136*, 2723−2726.
(255) Klüner, T.; Govind, N.; Wang, Y. A.; Carter, E. A. Periodic Density Functional Embedding Theory for Complete Active Space Self-Consistent Field and Configuration Interaction Calculations: Ground and Excited States. *J. Chem. Phys.* **2002**, *116*, 42−54.
(256) Huang, P.; Carter, E. A. Local Electronic Structure Around a Single Kondo Impurity. *Nano Lett.* **2006**, *6*, 1146−1150.
(257) Huang, P.; Carter, E. A. Self-Consistent Embedding Theory for Locally Correlated Configuration Interaction Wave Functions in Condensed Matter. *J. Chem. Phys.* **2006**, *125*, 084102.
(258) Kanan, D. K.; Sharifzadeh, S.; Carter, E. A. Quantum Mechanical Modeling of Electronic Excitations in Metal Oxides: Magnesia as a Prototype. *Chem. Phys. Lett.* **2012**, *519*, 18−24.
(259) Libisch, F.; Cheng, J.; Carter, E. A. Electron-Transfer-Induced Dissociation of H_2 on Gold Nanoparticles: Excited-State Potential Energy Surfaces via Embedded Correlated Wavefunction Theory. *Z. Phys. Chem.* **2013**, *227*, 1455−1466.
(260) Mukherjee, S.; Libisch, F.; Large, N.; Neumann, O.; Brown, L. V.; Cheng, J.; Lassiter, J. B.; Carter, E. A.; Nordlander, P.; Halas, N. J. Hot Electrons Do the Impossible: Plasmon-Induced Dissociation of H_2 on Au. *Nano Lett.* **2013**, *13*, 240−247.
(261) Zbiri, M.; Atanasov, M.; Daul, C.; Garcia-Lastra, J. M.; Wesolowski, T. A. Application of the Density Orbital-Free Embedding Potential Functional Theory Derived to Calculate the Splitting Energies of Lanthanide Cations in Chloroelpasolite Crystals. *Chem. Phys. Lett.* **2004**, *397*, 441−446.
(262) Landau, A.; Eliav, E.; Ishikawa, Y.; Kaldor, U. Intermediate Hamiltonian Fock-Space Coupled-Cluster Method: Excitation Energies of Barium and Radium. *J. Chem. Phys.* **2000**, *113*, 9905−9910.
(263) Landau, A.; Eliav, E.; Ishikawa, Y.; Kaldor, U. Intermediate Hamiltonian Fock-Space Coupled Cluster Method in the One-Hole One-Particle Sector: Excitation Energies of Xenon and Radon. *J. Chem. Phys.* **2001**, *115*, 6862−6865.
(264) Visscher, L.; Eliav, E.; Kaldor, U. Formulation and Implementation of the Relativistic Fock-Space Coupled Cluster Method for Molecules. *J. Chem. Phys.* **2001**, *115*, 9720−9726.
(265) Solovyeva, A., Pavanello, M., Neugebauer, J. Describing Long-Range Charge-Separation Processes with Subsystem Density-Functional Theory *J. Chem. Phys.* **2014**, *140*, 164103.
(266) McConnell, H. M. Vector Model for Indirect Proton Hyperfine Interactions in π-Electron Radicals. *Proc. Natl. Acad. Sci. U.S.A.* **1957**, *43*, 721.
(267) Eriksson, L. A.; Wang, J.; Boyd, R. J.; Lunell, S. A Comparative Study of the Hyperfine Structures of Neutral Nitrogen Oxides: DFT vs CISD Results. *J. Phys. Chem.* **1994**, *98*, 792−799.

DOI: 10.1021/cr500502v
Chem. Rev. 2015, 115, 5891−5928

(268) Lund, A., Shiotani, M., Shimada, S. *Principles and Applications of ESR Spectroscopy*; Springer: New York, 2011; Vol. *76*.
(269) Karasiev, V.; Trickey, S.; Harris, F. E. Born-Oppenheimer Interatomic Forces from Simple, Local Kinetic Energy Density Functionals. *J. Comput.-Aided Mater. Des.* **2006**, *13*, 111−129.
(270) Fux, S., Reiher, M. *Electron Density and Chemical Bonding II*; Springer: New York, 2012; pp 99−142.
(271) Geerlings, P.; De Proft, F.; Langenaeker, W. Conceptual Density Functional Theory. *Chem. Rev.* **2003**, *103*, 1793−1874.
(272) Lee, C.; Yang, W.; Parr, R. G. Development of the Colle-Salvetti Correlation-Energy Formula into a Functional of the Electron Density. *Phys. Rev. B* **1988**, *37*, 785−789.
(273) Becke, A. D. Density Functional Thermochemistry. III. The Role of Exact Exchange. *J. Chem. Phys.* **1993**, *98*, 5648−5652.
(274) Becke, A. D. A. New Mixing of Hartree-Fock and Local Density Functional Theories. *J. Chem. Phys.* **1993**, *98*, 1372−1377.
(275) Burke, K.; Ernzerhof, M.; Perdew, J. P. The Adiabatic Connection Method: A Non-Empirical Hybrid. *Chem. Phys. Lett.* **1997**, *265*, 115−120.
(276) Adamo, C.; Barone, V. Toward Reliable Density Functional Methods Without Adjustable Parameters: The PBE0Model. *J. Chem. Phys.* **1999**, *110*, 6158−6170.
(277) Trail, J. R.; Bird, D. M. Density-Functional Embedding Using a Plane-Wave Basis. *Phys. Rev. B* **2000**, *62*, 16402−16411.
(278) Xiang, Y.; Warshel, A. Quantifying Free Energy Profiles of Proton Transfer Reactions in Solution and Proteins By Using a Diabatic FDFT Mapping. *J. Phys. Chem. B* **2008**, *112*, 1007−1015.
(279) Hong, G.; Rosta, E.; Warshel, A. Using the Constrained DFT Approach in Generating Diabatic Surfaces and Off Diagonal Empirical Valence Bond Terms for Modeling Reactions in Condensed Phases. *J. Phys. Chem. B* **2006**, *110*, 19570−19574.
(280) Rosta, E.; Warshel, A. Origin of Linear Free Energy Relationships: Exploring the Nature of the Off-Diagonal Coupling Elements in S_N2 Reactions. *J. Chem. Theory Comput.* **2012**, *8*, 3574−3585.
(281) Olsson, M. H.; Hong, G.; Warshel, A. Frozen Density Functional Free Energy Simulations of Redox Proteins: Computational Studies of the Reduction Potential of Plastocyanin and Rusticyanin. *J. Am. Chem. Soc.* **2003**, *125*, 5025−5039.
(282) Lee, F. S.; Chu, Z. T.; Warshel, A. Microscopic and Semimicroscopic Calculations of Electrostatic Energies in Proteins by the Polaris and ENZYMIX Programs. *J. Comput. Chem.* **1993**, *14*, 161−185.
(283) Leopoldini, M.; Russo, N.; Toscano, M.; Dulak, M.; Wesolowski, T. A. Mechanism of Nitrate Reduction by Desulfovibrio Desulfuricans Nitrate Reductase - A Theoretical Investigation. *Chem.—Eur. J.* **2006**, *12*, 2532−2541.
(284) Wesolowski, T. A.; Ellinger, Y.; Weber, J. Density Functional Theory with an Approximate Kinetic Energy Functional Applied to Study Structure and Stability of Weak van der Waals Complexes. *J. Chem. Phys.* **1998**, *108*, 6078−6083.
(285) Tran, F.; Weber, J.; Wesolowski, T. A. Theoretical Study of the Benzene Dimer By the Density- Functional-Theory Formalism Based on Electron-Density Partitioning. *Helv. Chim. Acta* **2001**, *84*, 1489−1503.
(286) Schluns, D.; Klahr, K.; Muck-Lichtenfeld, C.; Visscher, L.; Neugebauer, J. Subsystem-DFT Potential-Energy Curves for Weakly Interacting Systems. *Phys. Chem. Chem. Phys.* **2015**, DOI: 10.1039/C4CP04936E.
(287) Jurečka, P.; Sponer, J.; Černy, J.; Hobza, P. Benchmark Database of Accurate (MP2 and CCSD(T) Complete Basis Set Limit) Interaction Energies of Small Model Complexes, DNA Base Pairs, and Amino Acid Pairs. *Phys. Chem. Chem. Phys.* **2006**, *8*, 1985−1993.
(288) Řezáč, J.; Riley, K. E.; Hobza, P. S66: A Well-balanced Database of Benchmark Interaction Energies Relevant to Biomolecular Structures. *J. Chem. Theory Comput.* **2011**, *7*, 2427−2438.
(289) Tran, F.; Alameddine, B.; Jenny, T. A.; Wesolowski, T. A. π-Stacking Behavior of Selected Nitrogen-Containing PAHs. *J. Phys. Chem. A* **2004**, *108*, 9155−9160.
(290) Tran, F.; Weber, J.; Wesolowski, T. A.; Cheikh, F.; Ellinger, Y.; Pauzat, F. Physisorption of Molecular Hydrogen on Polycyclic Aromatic Hydrocarbons: A Theoretical Study. *J. Phys. Chem. B* **2002**, *106*, 8689−8696.
(291) Sharifzadeh, S.; Huang, P.; Carter, E. A. All-Electron Embedded Correlated Wavefunction Theory for Condensed Matter Electronic Structure. *Chem. Phys. Lett.* **2009**, *470*, 347−352.
(292) Sharifzadeh, S.; Huang, P.; Carter, E. Embedded Configuration Interaction Description of CO on Cu (111): Resolution of the Site Preference Conundrum. *J. Phys. Chem. C* **2008**, *112*, 4649−4657.
(293) Lahav, D.; Kluner, T. A Self-Consistent Density Based Embedding Scheme Applied to the Adsorption of CO on Pd(111). *J. Phys.: Condens. Matter* **2007**, *19*, 226001.
(294) Wesolowski, T. A.; Vulliermet, N.; Weber, J. Study of the Physisorption of CO on the MgO(100) Surface Using the Approach of Kohn-Sham Equations with Constrained Electron Density. *J. Mol. Struct. (THEOCHEM)* **1999**, *458*, 151−160.
(295) Vulliermet, N.; Wesolowski, T. A.; Weber, J. Theoretical Study of the Physisorption of CO on Metal Oxide Surfaces Using the KSCED-DFT Approach. *Collect. Czech. Chem. Commun.* **1998**, *63*, 1447−1459.
(296) Wesolowski, T. A.; Goursot, A.; Weber, J. Properties of CO Adsorbed in ZSM5 Zeolite: Density Functional Theory Study Using the Embedding Scheme Based on Electron Density Partitioning. *J. Chem. Phys.* **2001**, *115*, 4791−4797.
(297) Iannuzzi, M.; Kirchner, B.; Hutter, J. Density Functional Embedding for Molecular Systems. *Chem. Phys. Lett.* **2006**, *421*, 16−20.
(298) Shimojo, F.; Kalia, R. K.; Nakano, A.; Vashishta, P. Embedded Divide-and-Conquer Algorithm on Hierarchical Real-Space Grids: Parallel Molecular Dynamics Simulation Based on Linear-Scaling Density Functional Theory. *Comput. Phys. Commun.* **2005**, *167*, 151−164.
(299) White, S. R. Density Matrix Formulation for Quantum Renormalization Groups. *Phys. Rev. Lett.* **1992**, *69*, 2863−2866.
(300) White, S. R. Density-Matrix Algorithms for Quantum Renormalization Groups. *Phys. Rev. B* **1993**, *48*, 10345−10356.
(301) Marti, K. H.; Reiher, M. The Density Matrix Renormalization Group Algorithm in Quantum Chemistry. *Z. Phys. Chem.* **2010**, *224*, 583−599.
(302) Chan, G. K.-L.; Sharma, S. The Density Matrix Renormalization Group in Quantum Chemistry. *Annu. Rev. Phys. Chem.* **2011**, *62*, 465−481.
(303) Dresselhaus, T.; Neugebauer, J.; Knecht, S.; Keller, S.; Ma, Y.; Reiher, M. Self-Consistent Embedding of Density-Matrix Renormalization Group Wavefunctions in a Density Functional Environment. *J. Chem. Phys.* **2014**, *142*, 044111.
(304) Georges, A.; Kotliar, G.; Krauth, W.; Rozenberg, M. Dynamical Mean-Field Theory of Strongly Correlated Fermion Systems and the Limit of Infinite Dimensions. *Rev. Mod. Phys.* **1996**, *68*, 13−125.
(305) Andersson, K.; Malmqvist, P.-Å; Roos, B. O. Second-Order Perturbation Theory with a Complete Active Space Self-Consistent Field Reference Function. *J. Chem. Phys.* **1992**, *96*, 1218−1226.
(306) Roos, B. O.; Andersson, K.; Fülscher, M. P.; Malmqvist, P.-Å.; Serrano-Andrés, L.; Pierloot, K.; Merchán, M. *Advances in Chemical Physics*; John Wiley & Sons, Inc.: New York, 2007; pp 219−331.
(307) Roca-Sanjuán, D.; Aquilante, F.; Lindh, R. Multiconfiguration Second-Order Perturbation Theory Approach to Strong Electron Correlation in Chemistry and Photochemistry. *Wiley. Interdiscip. Rev. Comput. Mol. Sci.* **2012**, *2*, 585−603.
(308) Perdew, J. P.; Yue, W. Accurate and Simple Density Functional for the Electronic Exchange Energy - Generalized Gradient Approximation. *Phys. Rev. B* **1986**, *33*, 8800−8802.
(309) Perdew, J. P. Density-Functional Approximation for the Correlation Energy of the Inhomogeneous Electron Gas. *Phys. Rev. B* **1986**, *33*, 8822−8824.
(310) Møller, C.; Plesset, M. S. Note on an Approximation Treatment for Many-Electron Systems. *Phys. Rev.* **1934**, *46*, 618−622.
(311) Sigbahn, P. E. M. In *Lecture Notes in Quantum Chemistry*; Roos, B. O., Ed.; Springer-Verlag: Berlin, 1992; Vol. *58*, pp 177−254.

DOI: 10.1021/cr500502v
Chem. Rev. 2015, 115, 5891−5928